The role of ATF2 in insulin action

The role of ATF2 in insulin action

Proefschrift

ter verkrijging van

de graad van Doctor aan de Universiteit Leiden,
op gezag van Rector Magnificus prof. mr. P.F. van der Heijden,
volgens besluit van het College voor Promoties
te verdedigen op dinsdag 23 juni 2009
klokke 11.15 uur

door

Bart Baan

geboren te Leiden

in 1977

Promotiecommissie

Promotores:	Prof. dr. J.A. Maassen Prof. dr. P. ten Dijke
Co-promoter:	Dr. D.M. Ouwens
Overige leden:	Prof. dr. B. van de Water Prof. dr. A.K. Raap Dr. E. Kalkhoven (Universiteit Utrecht)

ISBN: 978-94-901-2235-5

The research described in this thesis was performed at the department of Molecular Cell Biology, Leiden University Medical Centre, the Netherlands. This work was supported by a grant of the Dutch Diabetes Research Foundation.

Printing of this thesis was financially supported by the Dutch Diabetes Research Foundation and the J.E. Jurriaanse Stichting.

This thesis was printed by Gildeprint Drukkerijen, Enschede.

Table of contents

1

Introduction and
Outline of the thesis

Chapter 1

Chapter 1

Introduction and Outline of the thesis

Regulation of glucose homeostasis

Glucose is the primary, and in the case of the brain, the essential source of energy for the cells in the body. The blood glucose level in the body is tightly regulated and maintained at approximately 5 mmol/l. Failure to maintain blood glucose in the normal range leads to chronically high (hyperglycemia) or low (hypoglycemia) glucose levels. In the absence of adequate treatment, hypoglycemia may result in lethargy, loss of consciousness and, in extreme cases, can lead to coma, brain damage and death. In case of persistent hyperglycemia, such as untreated diabetes mellitus, the high glucose level in the blood represents the main risk factor for development of diabetes-related complications, including retinopathy, nephropathy, diabetic neuropathy, and erectile dysfunction (1).

The blood glucose level is tightly controlled by the reciprocal actions of two hormones, insulin and glucagon. The peptide hormone insulin is produced in the pancreas in the β-cells of the islets of Langerhans. In response to high blood glucose levels, glucose enters the β-cells via the glucose transporter GLUT2. Within the β-cells, glucose is metabolized by glycolysis and citric acid cycle and converted into ATP via oxidative phosphorylation. The resulting increase in ATP-levels leads to closure of the ATP-dependent potassium channel at the cell surface and membrane depolarization. Upon membrane depolarization, the voltage-dependent calcium channel opens, calcium flows into the β-cell and triggers the secretion of insulin directly into the bloodstream. In the body, insulin exerts a pleiotropic and anabolic response, the most important effects being the suppression of endogenous glucose production by the liver, the stimulation of glucose uptake by skeletal muscle and white adipose tissue, the storage of glucose in the form of glycogen in liver and skeletal muscle, the stimulation of triglyceride synthesis and suppression of lipolysis in white adipose tissue and stimulation of amino acid uptake and protein synthesis. Glucagon, which is produced by the α-cells in the islets of Langerhans, counteracts the effects of insulin on glucose metabolism by stimulating the release of glucose from the liver via stimulation of hepatic gluconeogenesis and glycogenolysis.

Diabetes mellitus

Diabetes mellitus is a disease characterized by the inability to regulate blood glucose levels, resulting in chronically increased blood glucose levels, or 'hyperglycemia' (2). Multiple types of diabetes mellitus can be distinguished on the basis of the cause of the hyperglycemia, which either results from insufficient or even absence of insulin secretion by the β-cells, in combination with a suboptimal response of peripheral target tissues to insulin, a phenomenon referred to as insulin resistance.

In case of type 1 diabetes, dysregulation of the immune system results in immunological intolerance towards the insulin-producing β-cells. This leads to inflammation of the islets of Langerhans and selective destruction of the β-cells (3) Insulin synthesis and secretion are also affected in Maturity-onset diabetes of the young (MODY) (4) and Maternally inherited Diabetes and Deafness (MIDD), due to genetic factors impacting on β-cell development and mitochondrial function (5).

Insulin resistance characterizes type 2 diabetes, the most prevalent type of diabetes, but is also found in gestational diabetes and steroid diabetes. In insulin resistance, the production of insulin is (initially) normal, but the response induced by insulin in peripheral tissues is blunted. When the production of insulin by the pancreas can no longer compensate for the peripheral insulin resistance due to β-cell dysfunction, the type 2 diabetes mellitus and hyperglycemia become overt.

Type 2 diabetes is often found as component of the metabolic syndrome, which is characterized by hypertension, central obesity, hyperlipidemia and insulin resistance that result in increased mortality due to cardiovascular incidents. The prevalence of both type 2 diabetes and the metabolic syndrome is reaching epidemic proportions, as the average age of onset of both diseases has markedly decreased over the past decades. In order to improve insulin action in patients with type 2 diabetes, a detailed understanding of the molecular mechanisms of insulin action and how this process is dysregulated under conditions of insulin resistance is required.

Mechanism of insulin action

When reaching its target tissues, the extra-cellular insulin signal is relayed via the insulin receptor at the cell surface and the associated post-receptor insulin signal transduction pathways. Figure 1 summarizes the key events in the transduction of the insulin signal into the cells.

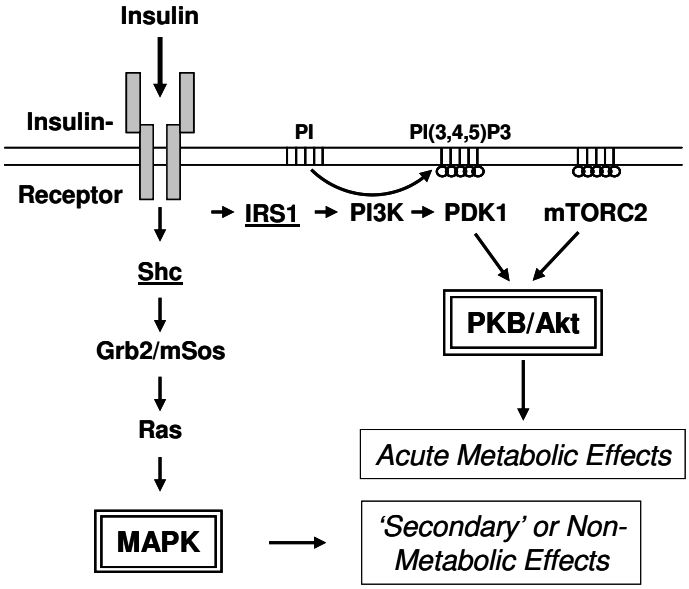

Figure 1. The two major insulin signaling pathways. For a detailed description see text.

The insulin receptor (IR) is a heterodimeric transmembrane protein, consisting of two extracellular α-chains responsible for insulin binding and two membrane spanning β-chains that contain intracellular tyrosine kinase domains. Insulin binds to the two α-chains of the IR on the outer surface of the plasma membrane. This interaction leads to a conformational change that induces activation of the intracellular kinase domains. These kinase domains subsequently trans-phosphorylate a number of tyrosine residues on the opposite β-chain (6). A subset of these phosphorylations stabilize the active conformation and further enhance the IR tyrosine kinase activity (amino acids (aa) 1146, 1150 and 1151), while other phospho-tyrosine (pY) residues (most notably aa 953, 960 and 972), function as docking sites for a number of IR substrates (7). Currently, over ten substrates of the IR have been identified, including isoforms of Src-homology-2-containing (Shc (8)), Grb2-associated binder 1 (Gab1 (9)), Cas-Br-M (murine) ecotropic retroviral transforming sequence homologue (Cbl (10)), the adaptor protein APS (11), and six members of the insulin receptor substrate (IRS1-6) family ((12-16), reviewed in (17)). The predominant substrates, however, are IRS1 and Shc. They define the two major insulin effector pathways: IRS1 and its downstream signaling pathway is responsible for most of the metabolic responses of insulin (18-20), while Shc regulates mostly non-metabolic processes induced by insulin, such as cell growth, survival and cellular differentiation (21). Both pathways will be discussed below.

IRS1 mediated signaling

The activated IR phosphorylates IRS1 on multiple tyrosine residues, which subsequently serve as docking sites for proteins containing Src-homology-2 (SH2) domains, the most important being the regulatory p85α subunit of class 1A phosphatidylinositol 3-kinase (PI-3K (18), reviewed in (22)). PI-3K consists of a p110 catalytic subunit and a p85 regulatory subunit. The binding of the p85 subunit via its two SH2-domains to pY residues on IRS1 leads to activation of the catalytic p110 subunit and recruitment of PI-3K to the plasma membrane. There, the p110 subunit catalyses the phosphorylation of specific phospholipids, phosphoinositides, on the 3-position to produce phosphatidylinositol-3-phosphates (PIP3), especially PI(3,4,5)P3. Signaling molecules that contain pleckstrin homology (PH) domains bind this type of lipid second messenger. The local insulin-induced increase in PIP3 results in the recruitment of the PH-domain containing kinases phosphoinositide-dependent kinase 1 (PDK1 (23)) and protein kinase B (PKB; also called Akt (24)) to the plasma membrane. PDK1 regulates the activity of members of the AGC family of protein kinases, which include protein kinase C (PKC), p70 ribosomal S6 kinase (p70S6K), serum glucocorticoid-induced kinase (SGK) and PKB/Akt, the latter being one of the most important signaling intermediates in metabolic insulin signaling. In case of PKB/Akt, binding to PIP3 facilitates the PDK1-mediated phosphorylation of Thr308, one of the sites critical for activation of the protein kinase (25). PIP3 is also required for phosphorylation of Ser473 on PKB/Akt by the mTORC2 complex, consisting of the protein kinase mammalian target of rapamycin (mTOR) bound to a regulatory subunit, known as rapamycin-insensitive companion of mTOR (rictor (26;27)).

PKB/Akt, when phosphorylated on Thr308 and Ser473 is active and directly regulates a number of multiple intracellular substrates important for glucose, protein and fat metabolism (see Figure 2, reviewed in (28) and (29)). For example, PKB/Akt regulates the activity of AS160 involved in translocation of glucose transporters (GLUT4) to the plasma membrane. In addition, PKB inhibits the enzyme glycogen synthase kinase 3 (GSK3),

thereby alleviating the repression of glycogen synthase (GS) and stimulating glycogen synthesis. PKB affects protein synthesis via phosphorylation of tuberous sclerosis complex 2 (TSC2; reviewed in (30)). This phosphorylation inhibits TSC2 activity. In complex with TSC1, TSC2 negatively regulates mTOR. Thus, the inhibition of TSC2 by PKB efficiently activates mTOR. As part of a larger protein complex activated mTOR then regulates protein synthesis by phosphorylating p70 S6K and eukaryotic translation initiation factor 4E binding protein-1 (4EBP1). PKB also regulates the expression of gluconeogenic and lipogenic enzymes by controlling the activity of several members of the forkhead box (FOXO) family of transcription factors (31;32). Hepatic gluconeogenesis is regulated via forkhead box other-1 (FOXO1), which activates gluconeogenic genes. FOXO1 is phosphorylated by PKB/Akt and subsequently exported from the nucleus, whereby transcription of gluconeogenic genes is terminated (33). The same principle applies to another forkhead box transcription factor, FOXA2, which is a crucial regulator of fasting lipid metabolism. PKB-mediated phosphorylation of FOXA2 prevents its nuclear localization and transcriptional activity (34).

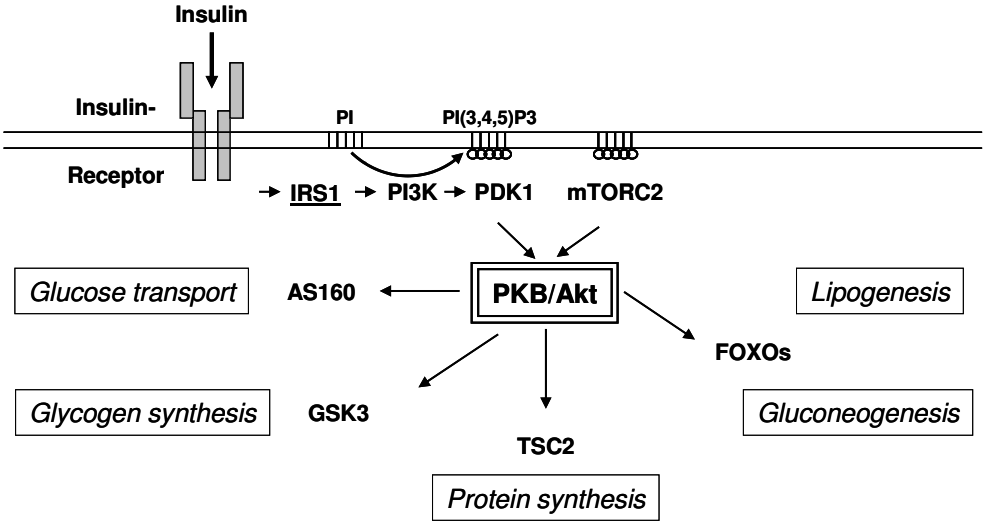

Figure 2. The IRS-dependent insulin signaling pathway. For a detailed description see text.

Shc-mediated signaling

The other major IR-pathway signals via Shc ((17); Figure 3). The activated IR phosphorylates Shc on tyrosines, which facilitates the binding of the adaptor protein growth factor receptor bound 2 (Grb2) via its SH2-domain. Via its SH3 domain, Grb2 is bound to the nucleotide exchange factor mammalian son-of sevenless (mSos). The recruitment of Grb-2-mSos to receptor-associated Shc brings mSos in the vicinity of the small GTP-binding protein Ras that is localized at the plasma membrane. mSos activates Ras by exchanging Ras-bound GDP for GTP. Ras then functions as a molecular switch triggering activation of multiple effectors, including PI-3K, Raf and RalGDS.

The p110 subunit of PI-3K has been shown to interact with active Ras (35) and this interaction modestly increases the PI-3K activity (36). However, in cells expressing

normal untransformed Ras, the contribution of mitogen-induced Ras-dependent PI-3K activity to the total PI-3K activity is only minor (24;37). Raf-activation is complex (for a detailed review see (38)), but Ras-dependent recruitment of Raf to the plasma-membrane seems sufficient for its activation. The active Raf kinase then triggers a kinase cascade that results in the phosphorylation and activation of MAPK and ERK kinase (MEK1/2). Subsequently, MEK1/2 activates the mitogen activated protein kinase (MAPK) family member extracellular signal regulated kinase (ERK1/2) via phosphorylation. ERK1/2 targets include p90 ribosomal protein S6 kinase (p90RSK) and transcription factors such as c-Myc, TCF and Elk1, thereby promoting gene expression (39;40). It has been shown that ERK does not play a role in mediating the acute metabolic effects of insulin (41;42). However its role in the regulation of insulin-induced gene expression has not been thoroughly investigated.

Insulin-induced Ras activation also leads to the activation of Ras-like small GTPase Ral via the Ral-guanine exchange factor Ral-GDS. Via still unknown mechanisms, presumably involving Src kinase, Ral then induces activation of the stress-activated protein kinases (SAPKs) p38 and JNK (43;44). Targets of these kinases include ATF2 and the members of the Jun transcription factor family, in addition to SAP-1, Elk1 and MAPKAPK-2 and -3 (40;45;46). The insulin-induced activation of p38 has further been described to play a role in insulin-induced glucose transport in a number of differentiated cell types (47;48). The role of JNK-activation in insulin-induced responses is still largely unknown.

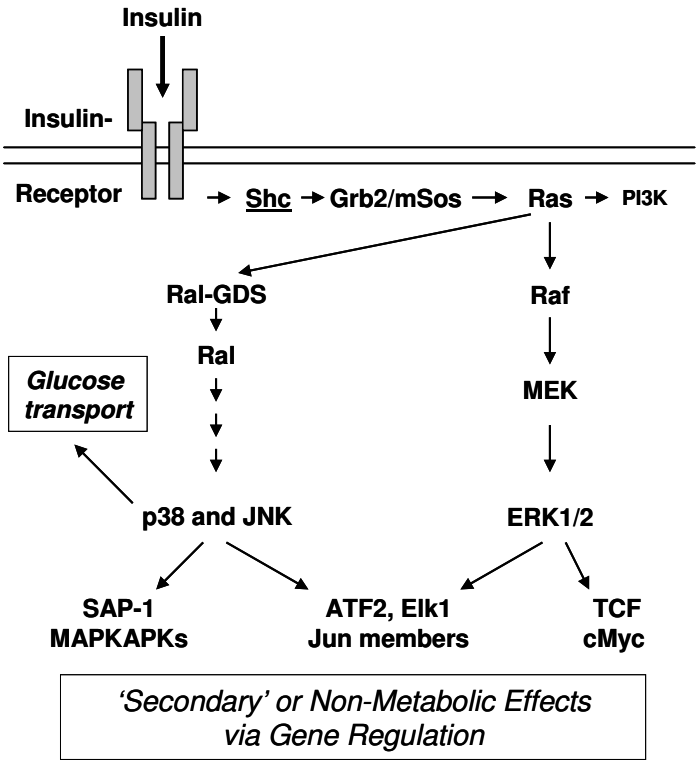

Figure 3. The Shc-dependent insulin signaling pathway. For a detailed description see text.

Previous studies performed in our research group identified ATF2 as a novel component of the insulin signaling system in cultured cells (44). The ATF2-phosphorylation in response to insulin was found to be dependent on a two-step mechanism which required cooperation of the ERK1/2-pathway with one of the SAPK-pathways ((44) and this thesis).

The SAPKs p38 and JNK, which are both capable of activating ATF2 on their own (e.g. not in cooperation with other kinases) are known to be activated by insulin stimulation (47;49). However, increasing evidence suggests that JNK, but also p38, play a key role in the development of insulin resistance in a number of tissues (50-53). Therefore, ATF2 can function as a potential regulator of insulin-induced gene expression, but can also be involved in development of insulin resistance and possible, it can do both.

Outline of this thesis

The research described in this thesis is aimed at further characterization of the role of ATF2 in insulin action. Chapter 2 is an introduction to the ATF2 protein, with particular focus on its possible functions in metabolic control and insulin action. Chapters 3 and 4 address the mechanism of insulin-induced ATF2 phosphorylation in JNK-deficient and JNK-containing cultured cells, respectively. In chapter 5, data on the identification of insulin-induced ATF2-dependent genes in cultured cells is presented. Chapter 6 describes our findings on the *in vivo* ATF2 regulation by insulin and the effects of high fat diet-induced insulin resistance thereon. In chapter 7 these results are summarized and discussed.

References

1. Brownlee, M. and Cerami, A. (1981) *Annu. Rev. Biochem.* **50,** 385-432
2. Saltiel, A. R. and Kahn, C. R. (2001) *Nature* **414,** 799-806
3. Atkinson, M. A. and Eisenbarth, G. S. (2001) *Lancet* **358,** 221-229
4. Vaxillaire, M. and Froguel, P. (2006) *Endocrinol. Metab Clin. North Am.* **35,** 371-84, x
5. Maassen, J. A., 'T Hart, L. M., Van Essen, E., Heine, R. J., Nijpels, G., Jahangir Tafrechi, R. S., Raap, A. K., Janssen, G. M., and Lemkes, H. H. (2004) *Diabetes* **53 Suppl 1,** S103-S109
6. Hubbard, S. R., Wei, L., Ellis, L., and Hendrickson, W. A. (1994) *Nature* **372,** 746-754
7. Schlessinger, J. (2000) *Cell* **103,** 211-225
8. Gustafson, T. A., He, W., Craparo, A., Schaub, C. D., and O'Neill, T. J. (1995) *Mol. Cell Biol.* **15,** 2500-2508
9. Lehr, S., Kotzka, J., Herkner, A., Sikmann, A., Meyer, H. E., Krone, W., and Muller-Wieland, D. (2000) *Biochemistry* **39,** 10898-10907
10. Baumann, C. A., Ribon, V., Kanzaki, M., Thurmond, D. C., Mora, S., Shigematsu, S., Bickel, P. E., Pessin, J. E., and Saltiel, A. R. (2000) *Nature* **407,** 202-207
11. Moodie, S. A., leman-Sposeto, J., and Gustafson, T. A. (1999) *J Biol. Chem.* **274,** 11186-11193
12. Sun, X. J., Rothenberg, P., Kahn, C. R., Backer, J. M., Araki, E., Wilden, P. A., Cahill, D. A., Goldstein, B. J., and White, M. F. (1991) *Nature* **352,** 73-77
13. Sun, X. J., Wang, L. M., Zhang, Y., Yenush, L., Myers, M. G., Jr., Glasheen, E., Lane, W. S., Pierce, J. H., and White, M. F. (1995) *Nature* **377,** 173-177
14. Lavan, B. E., Lane, W. S., and Lienhard, G. E. (1997) *J Biol. Chem.* **272,** 11439-11443
15. Fantin, V. R., Sparling, J. D., Slot, J. W., Keller, S. R., Lienhard, G. E., and Lavan, B. E. (1998) *J Biol. Chem.* **273,** 10726-10732

16. Cai, D., Dhe-Paganon, S., Melendez, P. A., Lee, J., and Shoelson, S. E. (2003) *J Biol. Chem.* **278,** 25323-25330
17. Virkamaki, A., Ueki, K., and Kahn, C. R. (1999) *J Clin. Invest* **103,** 931-943
18. Cheatham, B., Vlahos, C. J., Cheatham, L., Wang, L., Blenis, J., and Kahn, C. R. (1994) *Mol. Cell Biol.* **14,** 4902-4911
19. Clarke, J. F., Young, P. W., Yonezawa, K., Kasuga, M., and Holman, G. D. (1994) *Biochem. J* **300 (Pt 3),** 631-635
20. Kanai, F., Ito, K., Todaka, M., Hayashi, H., Kamohara, S., Ishii, K., Okada, T., Hazeki, O., Ui, M., and Ebina, Y. (1993) *Biochem. Biophys. Res. Commun.* **195,** 762-768
21. Sasaoka, T. and Kobayashi, M. (2000) *Endocr. J* **47,** 373-381
22. Shepherd, P. R., Withers, D. J., and Siddle, K. (1998) *Biochem. J* **333 (Pt 3),** 471-490
23. Alessi, D. R., James, S. R., Downes, C. P., Holmes, A. B., Gaffney, P. R., Reese, C. B., and Cohen, P. (1997) *Curr. Biol.* **7,** 261-269
24. Burgering, B. M. and Coffer, P. J. (1995) *Nature* **376,** 599-602
25. Alessi, D. R., Andjelkovic, M., Caudwell, B., Cron, P., Morrice, N., Cohen, P., and Hemmings, B. A. (1996) *EMBO J* **15,** 6541-6551
26. Sarbassov, D. D., Guertin, D. A., Ali, S. M., and Sabatini, D. M. (2005) *Science* **307,** 1098-1101
27. Hresko, R. C. and Mueckler, M. (2005) *J Biol. Chem.* **280,** 40406-40416
28. Taniguchi, C. M., Emanuelli, B., and Kahn, C. R. (2006) *Nat. Rev. Mol. Cell Biol.* **7,** 85-96
29. Whiteman, E. L., Cho, H., and Birnbaum, M. J. (2002) *Trends Endocrinol. Metab* **13,** 444-451
30. Harris, T. E. and Lawrence, J. C., Jr. (2003) *Sci STKE.* **2003,** re15
31. Tran, H., Brunet, A., Griffith, E. C., and Greenberg, M. E. (2003) *Sci STKE.* **2003,** RE5
32. Burgering, B. M. (2008) *Oncogene* **27,** 2258-2262
33. Puigserver, P., Rhee, J., Donovan, J., Walkey, C. J., Yoon, J. C., Oriente, F., Kitamura, Y., Altomonte, J., Dong, H., Accili, D., and Spiegelman, B. M. (2003) *Nature* **423,** 550-555
34. Wolfrum, C., Asilmaz, E., Luca, E., Friedman, J. M., and Stoffel, M. (2004) *Nature* **432,** 1027-1032
35. Rodriguez-Viciana, P., Warne, P. H., Dhand, R., Vanhaesebroeck, B., Gout, I., Fry, M. J., Waterfield, M. D., and Downward, J. (1994) *Nature* **370,** 527-532
36. Rodriguez-Viciana, P., Warne, P. H., Khwaja, A., Marte, B. M., Pappin, D., Das, P., Waterfield, M. D., Ridley, A., and Downward, J. (1997) *Cell* **89,** 457-467
37. van Weering, D. H., Medema, J. P., van Puijenbroek, A., Burgering, B. M., Baas, P.D., and Bos, J. L. (1995) *Oncogene* **11,** 2207-2214
38. Morrison, D. K. and Cutler, R. E. (1997) *Curr. Opin. Cell Biol.* **9,** 174-179
39. Pouyssegur, J., Volmat, V., and Lenormand, P. (2002) *Biochem. Pharmacol.* **64,** 755-763
40. Turjanski, A. G., Vaque, J. P., and Gutkind, J. S. (2007) *Oncogene* **26,** 3240-3253
41. van den Berghe, N., Ouwens, D. M., Maassen, J. A., van Mackelenbergh, M. G., Sips, H. C., and Krans, H. M. (1994) *Mol. Cell Biol.* **14,** 2372-2377
42. Sakaue, M., Bowtell, D., and Kasuga, M. (1995) *Mol. Cell Biol.* **15,** 379-388
43. de Ruiter, N. D., Wolthuis, R. M., van Dam, H., Burgering, B. M., and Bos, J.L. (2000) *Mol. Cell Biol.* **20,** 8480-8488

44. Ouwens, D. M., de Ruiter, N. D., van der Zon, G. C., Carter, A. P., Schouten, J., van der Burgt. C., Kooistra, K., Bos, J. L., Maassen, J. A., and van Dam, H. (2002) *EMBO J* **21,** 3782-3793
45. Bogoyevitch, M. A. and Kobe, B. (2006) *Microbiol. Mol. Biol. Rev.* **70,** 1061-1095
46. Shi, Y. and Gaestel, M. (2002) *Biol. Chem.* **383,** 1519-1536
47. Somwar, R., Perreault, M., Kapur, S., Taha, C., Sweeney, G., Ramlal, T., Kim, D. Y., Keen, J., Cote, C. H., Klip, A., and Marette, A. (2000) *Diabetes* **49,** 1794-1800
48. Sweeney, G., Somwar, R., Ramlal, T., Volchuk, A., Ueyama, A., and Klip, A. (1999) *J Biol. Chem.* **274,** 10071-10078
49. Miller, B. S., Shankavaram, U. T., Horney, M. J., Gore, A. C., Kurtz, D. T., and Rosenzweig, S. A. (1996) *Biochemistry* **35,** 8769-8775
50. Wellen, K. E. and Hotamisligil, G. S. (2005) *J Clin. Invest* **115,** 1111-1119
51. Yang, R. and Trevillyan, J. M. (2008) *Int. J Biochem. Cell Biol.* **40,** 2702-2706
52. Tilg, H. and Moschen, A. R. (2008) *Mol. Med.* **14,** 222-231
53. Wang, X. L., Zhang, L., Youker, K., Zhang, M. X., Wang, J., LeMaire, S. A., Coselli, J. S., and Shen, Y. H. (2006) *Diabetes* **55,** 2301-2310

2

ATF2, a novel player in insulin action and insulin resistance?

Manuscript in preparation

Chapter 2

Chapter 2

ATF2, a novel player in insulin action and insulin resistance?

Bart Baan and D. Margriet Ouwens

Department of Molecular Cell Biology, Leiden University Medical Centre, Leiden, the Netherlands

Activating transcription factor 2 (ATF2) is strongly associated with the cellular response to stress stimuli, such as viral infection, pro-inflammatory cytokines, osmotic stress and DNA damaging agents. However, ATF2 has also been identified as a component of the insulin signaling system, both *in vitro* and *in vivo*. Studies in rodents and *D. melanogaster* have implicated ATF2 in the regulation of glucose and lipid metabolism via induction of PPARγ coactivator 1α (PGC1α) and phosphoenolpyruvate-carboxykinase (PEPCK) expression, suggesting that ATF2 contributes to metabolic control. Conversely, ATF2 also regulates the expression of genes implicated in the development of insulin resistance, β-cell dysfunction and complications associated with type 2 diabetes. This suggests that ATF2 not only participates in insulin action, but that deregulation of ATF2 activity may contribute to the pathogenesis of type 2 diabetes mellitus. This review sheds light on this dual role of ATF2 in metabolic control, insulin action and insulin resistance.

The ATF/CREB family of transcription factors. Activating transcription factor 2 (ATF2; also referred to as cAMP-Responsive Element (CRE) Binding Protein 2 (CREB2) or CRE-Binding Protein-1 (CREBP-1)) is part of the mammalian ATF/CREB family of transcription factors ((1;2) and Figure 1). All members of the ATF/CREB family share the ability to bind to the ATF/CRE consensus site 5'-TG/TACNTCA-3' and contain a basic leucine zipper (bZIP) domain, which is responsible for DNA-binding and dimerization (1;2). Whereas the CREB-subfamily members ATF1, CREM and CREB respond primarily to cAMP/PKA activation, most of the other members of the ATF/CREB family are associated with cellular stress-responses. For example, ATF2-transactivation and ATF3-expression are predominantly induced by stress stimuli (3;4), whereas ATF4 and ATF6 are critical elements of the unfolded protein response induced by endoplasmic reticulum (ER) stress (5).

Structure of ATF2. The human ATF2 gene is located on chromosome 2q32 and encodes a 505 amino acid protein (6). Figure 2 shows a schematic representation of the ATF2 protein, which consists of an amino-terminal transactivation domain (TAD) and a carboxyterminal bZIP-domain, interconnected by a proline-enriched stretch and a histone acetylase (HAT) domain (7;8). ATF2 also contains two nuclear localization signals, a nuclear export signal and multiple sites that can be modified by phosphorylation, ubiquitination and glycosylation (7;8).

ATF2 is highly conserved among species. For example, the mouse ATF2 protein is highly similar to the human counterpart, in that it lacks the first 18 amino acids and differs in only 2 amino acids in the remaining part of the protein. The ATF2 homolog from *D. melanogaster*, dATF2, displays ~50% sequence similarity with mammalian ATF2 and shows conservation of the entire bZIP-domain and part of the TAD-domain (9).

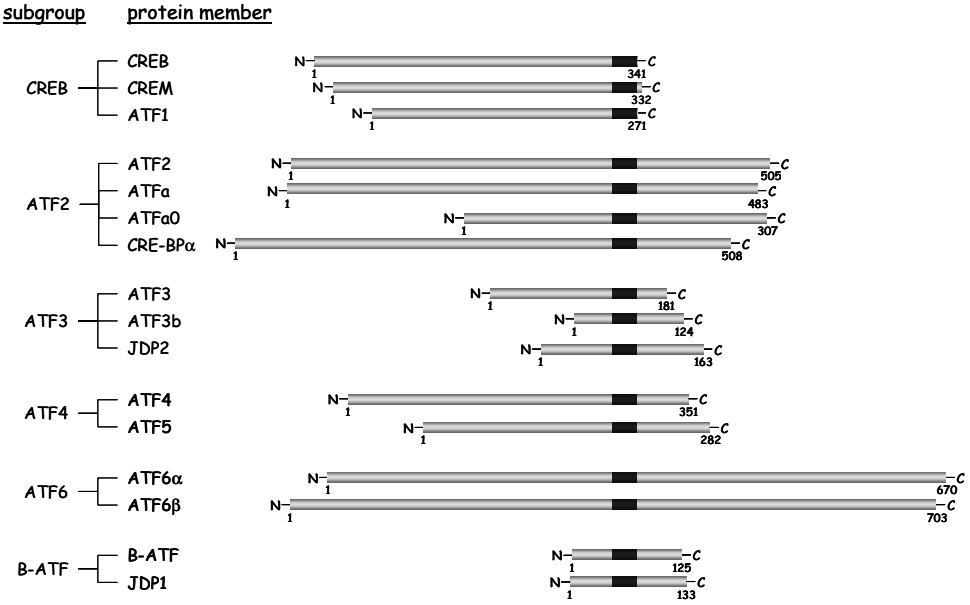

Figure 1. The ATF/CREB family of transcription factors. The protein members can be divided into six subgroups, according to their sequence similarity. The box indicates the bZIP domain. Adapted from (7).

The transactivation domain. Deletion studies using fusion proteins of the DNA-binding domain of the yeast transcription factor GAL4 and ATF2 have delineated the minimal TAD to amino acids 19-96 ((3), see Figure 2). Structural analysis of amino acids 1-105 divides the ATF2-TAD into two subdomains (10). The aminoterminal subdomain (Met19-Gly56) contains a Zn-finger motif with a structure very similar to the Zn-fingers found in the DNA-binding domains of many transcription factors. In contrast to the amino acids responsible for interaction with the phosphate backbone of DNA, the two Cys- (Cys27 and Cys32) and two His-residues (His45 and His49) that coordinate the binding of the Zn-ion, as well as the amino acids that form the hydrophobic core, are well conserved between ATF2 and Zn-finger motifs of other transcription factors. Although point-mutations of the crucial Zn-binding residues or complete deletion of the Zn-finger decreased both basal and serum-induced transcriptional activity of GAL4-ATF2 (11;12), some transcriptionally active mammalian isoforms (see Figure 3 and below) and dATF2 lack the Zn-finger motif (9;13-15). Therefore, the role of the Zn-finger domain in the regulation of ATF2 transactivation *in vivo* remains to be established.

The structure of the carboxyterminal TAD subdomain (Pro57-Lys105) is highly flexible (10). Phosphorylation of several residues within this region, most notably Thr69 and Thr71 (Figure 2), increases the transcriptional activity of ATF2 (3;16-21), suggesting that this subdomain is likely to undergo conformational changes in response to stimuli that promote ATF2 activation. Furthermore, the carboxyterminal part of the TAD, including the regulatory phosphorylation sites, is well conserved in dATF2 (9).

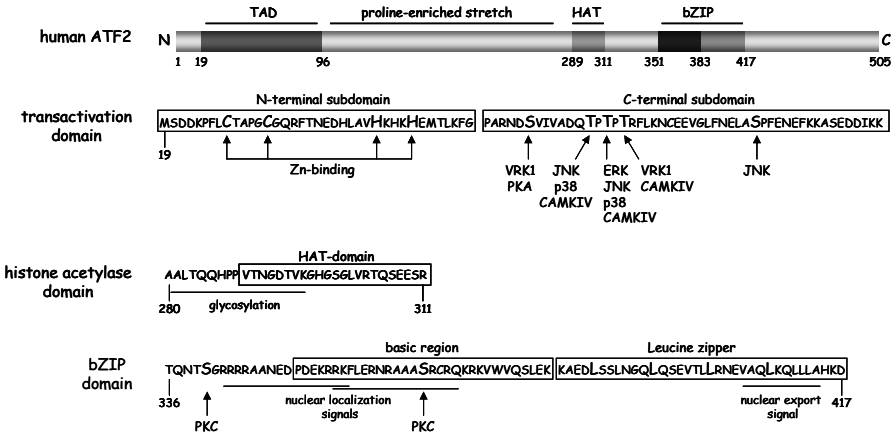

Figure 2. Structure of the human ATF2 protein and its subdomains. ATF2 consists of an amino-terminal transactivation domain (TAD) and a carboxyterminal bZIP-domain, interconnected by a proline-enriched stretch and a histone acetylase domain (HAT). ATF2 also contains two nuclear localization signals, a nuclear export signal and multiple sites that can be modified by phosphorylation and glycosylation. The arrows indicate the residues critical for zinc binding or residues that can be phosphorylated by protein kinase A (PKA), protein kinase C (PKC), extracellular signal regulated kinase (ERK), cJun N-terminal kinase (JNK), p38, or vaccinia-related kinase (VRK).

The histone acetylase domain. ATF2 has been found to acetylate histones H2B and H4 *in vitro* (22). The putative HAT domain of ATF2 is located between amino acids 289-311 (22). Ectopic expression of mutant ATF2 proteins, in which the amino acids critical for *in vitro* HAT activity were replaced by alanines, destroyed the ultraviolet (UV) irradiation-induced activation of a CRE-dependent luciferase reporter gene (22;23). A role for the HAT region in *in vivo* ATF2 function, however, has not yet been demonstrated. It should be noted in this respect that the HAT domain is not conserved in the highly-related ATFa protein (also known as ATF7), which can partially compensate for the loss of ATF2 in ATF2-/- mice (24).

The bZIP domain. The bZIP domain is located between Pro351 and Asp417 (Figure 2). The basic region (Pro351-Lys382) and leucine zipper (Lys383-Asp417) in the bZIP-domain direct DNA-binding and dimer formation, respectively (1;2). Overlapping with the bZIP domain, two nuclear localization signals (Arg342-Lys357 and Arg356-Gln371) and a leucine-rich nuclear export signal (Val405-Ala414) have been identified (25).

Based on sequence similarities, the bZIP proteins identified in the human genome have been arranged in 12 families, that form 3 subgroups on the basis of their dimerization properties (26). Within this classification, ATF2 forms a small family with ATFa and CRE-BPa. The ATF2-family belongs to the subgroup of bZIP transcription factors that can form both homo- and heterodimers (26). ATF2 itself can form heterodimers with several members of the CREB/ATF and Jun/Fos families, such as ATF3, cJun and JunD (7). Furthermore, several other types of transcription factors, including C/EBP and Smad-proteins have been found to bind to DNA in association with ATF2 (27-29).

In 'in gel-retardation' assays, the various ATF2-containing dimers all bind the ATF/CRE consensus site: 5'-TG/TACNTCA-3' (13;30;31), but cause a different degree of DNA

bending, which may contribute to regulatory specificity (32). Compared to the ATF2/ATF2 homodimer, the ATF2/cJun dimer combination is reported to be a more potent transcriptional activator on minimal promoters (13;30;31). However, the relative activities of the various dimers on more complex promoters, such as the c-jun promoter (33) or the proximal element of the interferon γ (IFNγ) promoter (34) is less clear.

Isoforms. In all mammalian species examined, distinct ATF2 isoforms exist due to differential splicing or alternate promoter usage of the ATF2 gene (9;13-15;35;36). As shown for the human and mouse variants in Figure 3, most isoforms contain the bZIP domain, but differ in the length of the TAD, the presence of the Zn-finger and the presence of the proline-enriched stretch linking the TAD- and HAT-domain (13-15;35). Only one described variant of ATF2, termed ATF2sm, lacks most of the bZIP domain. It contains the first part of the aminoterminal TAD, including the regulatory residues Thr69 and Thr71 and the complete carboxyterminus from the last portion of the bZIP domain (36). Currently, only a few isoforms have been analyzed for biological activity (13-15;35;36). However, the presence of the bZIP domain in almost all variants suggests normal dimerization and DNA-binding properties.

Post-translational modification. ATF2 contains multiple sites that can be modified by posttranslational modification, including phosphorylation, ubiquitination and glycosylation. Table 1 lists the various phosphorylation sites in ATF2 as well the kinases responsible for inducing phosphorylation on these sites.

Table 1. Modification of ATF2 by phosphorylation

Residue	*Function*	*Kinase*	*Reference*
Ser62	transactivation	Protein kinase A VRK1	(37) (38)
Thr69	transactivation	CAMKIV JNK p38	(39) (3;16;17;19) (17;18;21)
Thr71	transactivation	CAMKIV ERK JNK p38	(39) (18;20) (3;16;17;19) (17;18;21)
Thr73	transactivation	CAMKIV VRK1	(39) (38)
Ser90	unknown	JNK	(3;19;20)
Ser121	transactivation	Protein kinase Cα	(40)
Ser340	unknown	Protein kinase C	(37)
Ser367	unknown	Protein kinase C	(2)
Ser490	DNA damage	ATM	(41)
Ser498	DNA damage	ATM	(41)

A. Human ATF2 isoforms

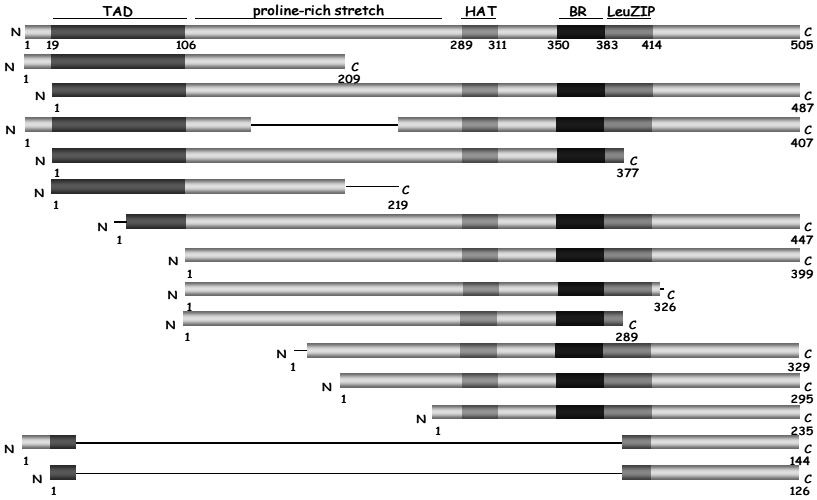

B. Mouse ATF2 isoforms

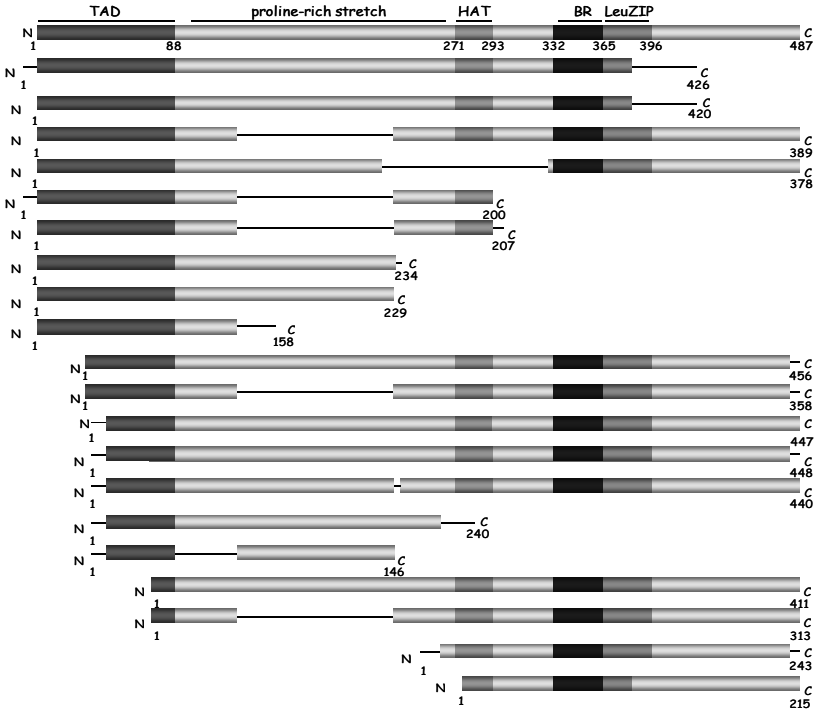

Figure 3. ATF2 isoforms. Alignment of the ATF2 variants in the human (A) and mouse (B) genome.

As will be discussed in more detail under "Regulation of ATF2 activity", phosphorylation of Thr69 and Thr71 by mitogen-activated protein kinases (MAPK) (see Figure 4 (3;16-21)) or Ca2+/calmodulin-dependent kinase IV (CaMKIV (39)) and phosphorylation of Ser62 and Thr73 by vaccinia-related kinase 1 (VRK1 (38)) enhances the transcriptional activity of ATF2. Ser490 and Ser498 are phosphorylated by ataxia telangiectasia mutated (ATM) kinase (41). However, these phosphorylations do not affect ATF2 transcriptional activity, but link ATF2 to the DNA damage response. The function of Ser90, Ser121, Ser340 and Ser367 phosphorylation is less well defined (Table 1).

In addition to phosphorylation, ATF2 might also be regulated by glycosylation. ATF2 was among the proteins identified in a high-throughput analysis of O-linked β-N-acetylglucosamine glycosylated proteins from the brain (42). The region of ATF2-glycosylation (Ala280-Lys296) overlaps in part with the HAT domain, but it remains to be determined whether glycosylation affects ATF2 function. Finally, ubiquitination of ATF2 targets the protein for degradation (43).

Regulation of ATF2 activity. The transcriptional activation capacity of ATF2 is promoted by a large number of distinct stimuli associated with cellular stress, such as viral protein products, oncogenes, pro-inflammatory cytokines, amino acid starvation, heat shock, osmotic stress and DNA damaging agents (3;44), but also mitogenic stimulation with epidermal growth factor (EGF), insulin or serum induces ATF2 transactivation (18;45).
Regulation of ATF2 activity by phosphorylation. The predominant mechanism causing ATF2 transactivation involves the phosphorylation of Thr69 and Thr71 (3;19), but phosphorylation of other residues may also result in activation of ATF2 (Table 1). The MAPK members cJun N-terminal kinase (JNK) or p38 are responsible for the cellular stress-induced phosphorylation of both Thr69 and Thr71 (3;16;17;19;20;46). In response to growth factors, ATF2-Thr69 and Thr71-phosphorylation is induced via a two-step mechanism that requires cooperation of two Ras-dependent MAPK-pathways (18). The ERK1/2-pathway induces phosphorylation of Thr71, whereas subsequent Thr69 phosphorylation is mediated by either p38 or JNK, in a cell type-dependent manner ((18;45) see Figure 4). ATF2 knock-in mice that express an ATF2 mutant in which Thr69 and Thr71 were replaced by alanines ($ATF2^{AA}$), have a phenotype strikingly similar to that of the complete ATF2 knock-out mouse (24;47). Also, in *D. melanogaster*, the p38-mediated phosphorylation of Thr59 and Thr61, the equivalents of mammalian Thr69 and Thr71, was found to be required for transcriptional activation of dATF2 (9;48). These studies highlight the importance of Thr69 and Thr71 for ATF2 function.

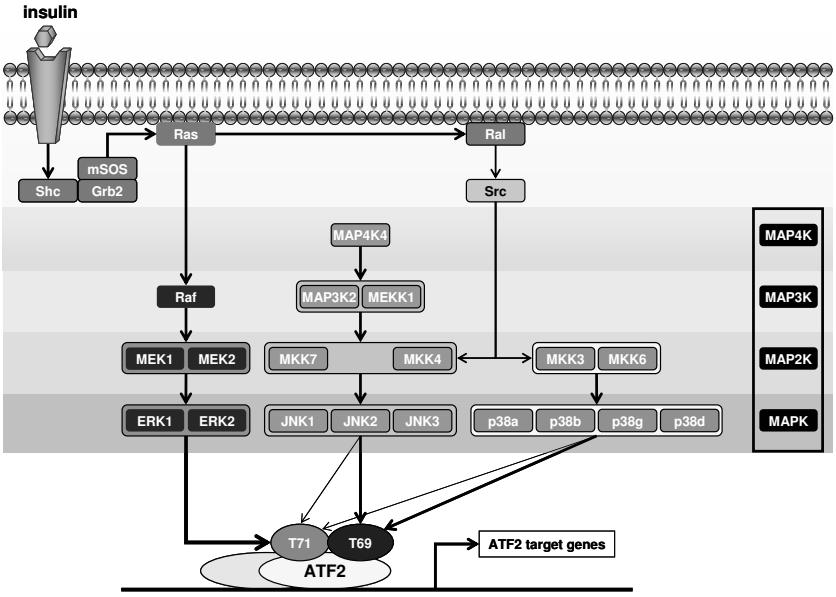

Figure 4. Regulation of ATF2 activation by insulin and MAPkinases. Activation of the Ras–Raf–MEK–ERK1/2 pathway by insulin induces phosphorylation of Thr71, whereas subsequent Thr69 phosphorylation requires the Ral–RalGDS–Src–p38 pathway (18;45).

How phosphorylation of the TAD leads to initiation of ATF2-dependent transcription is still unclear. Reporter-assays with GAL4-ATF2 fusion proteins have suggested that ATF2 is held in an inactive conformation by a direct interaction of the Zn-finger in the TAD with the bZIP domain (49;50). Consequently, transactivation of ATF2 in response to extracellular stimuli has been proposed to involve disruption of this inhibitory interaction through phosphorylation or by association with viral or cellular proteins (44;49). Also other mechanisms have been suggested via which phosphorylation of Thr69 and Thr71 leads to initiation of ATF2-dependent transcription. For example, in response to amino acid starvation ATF2-Thr69+71-phosphorylation has been found to precede *in vivo* acetylation of histone H2B and H4 (51). Histone acetylation is thought to facilitate transcription by altering the accessibility of DNA to transcriptional activators or chromatin remodelling enzymes (52). Future studies should clarify whether the acetylation of H2B and H4 can be ascribed to the putative intrinsic HAT activity of ATF2 (22) or results from ATF2-dependent recruitment of histone acetyltransferases, such as p300/CBP (40;53). Finally, phosphorylation of Thr69 and Thr71 has been implicated in ATF2-dimerization and has been reported to prevent, but also to promote ubiquitin-dependent degradation of ATF2 in different experimental systems (43;54;55).

Regulation of ATF2 activity by protein-protein interactions. Association of ATF2 with transcriptional co-activators or repressors may also affect the transcriptional activity. Proteins that activate ATF2 via protein-protein interactions include, in addition to the p300/CBP-protein mentioned previously (40;53), the adenoviral E1A protein (12;56), the hepatitis B pX protein (57), the nuclear chaperones bZIP enhancer factor and Tax (58) and

the co-activator undifferentiated embryonic cell transcription factor 1 (59). In contrast, ATF2-dependent recruitment of the repressive histone-variant macroH2A has been reported to prevent transcriptional activation of the IL8 gene in a cell-specific manner (60). In addition, ATF2-interaction with TBP-interacting protein 49b (61), Jun dimerization protein 2 (62) and interferon regulatory factor-2-binding protein-1 (63) have been found to suppress ATF2 transcriptional activity.

Subcellular localization. One report suggests that the nuclear transport signals in ATF2 direct the trafficking of the protein between the nucleus and the cytosol. In certain cell lines, heterodimerization with cJun serves to sequester ATF2 in the nucleus (25). Also, although ATF2 itself is not sumoylated, sumoylation of ATF2 dimer partners may have an impact on ATF2 subcellular localization. Sumoylated cJun and ATFa are transcriptionally inactive and at least sumoylated ATFa is primarily localized in the cytosol (64;65). Studies in other cell types, however, do not confirm a cytoplasmic localization of ATF2 (45).

ATF2-dependent gene expression. The various stimuli and protein-protein interactions regulating ATF2-activity as well as the multiple DNA sequences that can bind the different ATF2-containing dimers provide numerous levels on which ATF2-dependent target gene transcription can be regulated. Accordingly, studies aimed at characterizing ATF2-regulated genes using knock-out mouse models, gel-retardation assays, as well as 'ChIP-on-chip' analysis using (phosphospecific) ATF2 antibodies in cisplatin-treated cells, have generated an enormous list of potential target genes (7;8;24;44;66;67). It should, however, be noted that ATF2-dependence has not been validated for all of the identified genes.

Previous reports addressing the function of ATF2 in oncogenesis and DNA repair (7;8;44) have divided the (potential) ATF2 target genes into functional groups, including (i) transcription factors (ATF3, c-jun, CHOP, CREB1, Egr1, fosB, FOXO3a, HIF1α, PPARα, SREBP1c and TCF7L2), (ii) cell cycle intermediates (CDKN1B, CDKN2A cyclin A and cyclin D1), (iii) chemokines and pro-inflammatory cytokines (FasL, IFNβ, IFNγ, IGF2, IGFBP6, IL1β, IL4, IL6, IL8, MT3, TGFβ and TNFα), (iv) signaling proteins (AKT1, APS, MAP4K4, MKP1, PTEN and SHC1), (v)proteins engaged in the response to cellular stress (ATF3, CHOP and Grp78/BiP) and (vi) proteins involved in the DNA damage response (ERCC1, ERCC3, XPA, ATM, RAD23B, FOXD1 and GADD45), (vii) regulators of apoptosis (Bcl2, TBcl2-like 11 and TRAF3), (viii) adhesion (E-selectin, P-selectin, VCAM-1 and collagen), (ix) invasion (MMP2, uPA and iNOS) and (x) metabolism (apolipoproteins A1 and C3, insulin, PEPCK and PCG1α)(24;34;39;48;66-93).

As shown in Table 2, a large number of these (potential) ATF2 target genes also play regulatory roles in insulin action, β-cell (dys)function and/or glucose- and lipid metabolism. Other potential ATF2-regulated genes have been linked to the pathogenesis of type 2 diabetes (T2D) and diabetes-related complications. Intriguingly, phosphorylation of ATF2 is not only increased by insulin *in vitro and in vivo*, but also in rodent models of high-fat diet induced insulin resistance. Below, we will discuss the possible functions of ATF2 in relation to normal metabolic control and the pathogenesis of T2D.

Table 2. Functional classification of (potential) ATF2-target genes involved in insulin action, β-cell function and type 2 diabetes

Function	*Genes*	*References*
Adipocyte dysfunction	HIF1α, IGF2, IL1β, IL6, MMP2, MT3, TNFα	(66;67;83;84)
Candidate genes for T2D	CDKN2A, MAP4K4, TCF7L2	(66;88)
ER stress	ATF3, CHOP, Grp78/BiP	(68;71;78)
Glucose metabolism	PEPCK, PCG1α, SREBP1c	(48;69;70;72;73)
Inhibition of insulin signaling	IL1β, IL6, PTEN, TNFα	(67;83;84;92;93)
Insulin signaling	AKT1, APS, FOXO3a, MKP1, SHC1	(24;66)
Lipid metabolism	apolipoprotein A1, apolipoprotein C3, PPARα, SREBP1c	(66;91)
Vascular complications and fibrosis	collagen, Egr1, E-selectin, HIF1α, iNOS, P-selectin, TGFβ, VCAM-1	(66;67;77;80;81)
β-cell (dys)function	ATF3, IL1β, insulin	(39;67;68;90)

ATF2 and metabolic regulation.

Lessons from animal models. Various mouse models with deletions in the ATF2 gene have been generated. The first mouse described, ATF2m/m, expresses low levels of an ATF2-variant lacking amino acids 277-329 (47;94). These mice were born, displayed lower viability and growth in addition to bone abnormalities and reduced numbers of Purkinje cells in the brain (94). Mice completely lacking ATF2 die shortly after birth due to respiratory problems (47), while knock-out mice lacking both ATF2 and its closest homologue ATFa (also known as ATF7), or mice expressing ATF2 mutated at Thr69 and Thr71 on an ATFa-/- background, are not born due to developmental abnormalities in heart and liver, both in hepatocytes and the hematopoietic cells, already apparent at E12.5 (24). Unfortunately, experiments performed with these mouse models do not provide information on the role of ATF2 in metabolic control.

Selective ablation of dATF2 in the fat body of *D. melanogaster*, however, does identify a metabolic function for dATF2 (48). The fat body serves to sense energy and nutrient availability and coordinates the appropriate metabolic response. Knockdown of dATF2 in the fat body severely reduced phosphoenolpyruvate carboxykinase (PEPCK) expression. PEPCK is a crucial enzyme in hepatic glucose production and in lipid homeostasis in adipose tissue (95;96). In the *D. melanogaster* fat body, the ATF2/PEPCK pathway was found to regulate lipid metabolism and more specifically the synthesis of triglycerides from glycerol-3-phosphate (48).

Lessons from in vivo and in vitro studies. Studies in rat hepatoma cells have confirmed the regulation of PEPCK expression through the p38/ATF2 pathway in response to arsenite and retinoic acid (72;73). Furthermore, the ATF2 target gene and potential dimer-partner ATF3 has been linked to suppression of PEPCK expression *in vivo* (97). Insulin is known to decrease PEPCK levels in the liver (95), but an involvement of the ATF2/ATF3 pathway in this process remains to be determined. ATF2 has further been implicated in the regulation of PPARγ co-activator 1α (PGC1α). This transcriptional co-activator is activated by signals that control energy and nutrient homeostasis (98;99). In brown adipose tissue and skeletal muscle, the p38/ATF2 pathway contributes to PGC1α induction in response to a β-adrenergic stimulus and exercise, respectively (69;70;100).

A gene profiling study on chromatin immunoprecipitated from cisplatin-treated breast cancer cells with a phosphospecific ATF2 antibody identified more enzymes involved in the regulation of glucose and lipid metabolism, such as sterol regulatory element binding protein 1c (SREBP1c), peroxisome proliferator activated receptor α (PPARα) and the apolipoproteins A1 and C3, as well as components of the insulin signaling system, including Akt1, adaptor protein containing PH and SH2 domains (APS), FOXO3a, Map kinase phosphatase 1 (MKP1) and Src homologous collagen-1 (SHC1) (66). Except for apolipoprotein C3 and MKP1, a role for ATF2 in the regulation of these genes has not been validated yet. Apolipoprotein C3 is a very low density lipoprotein (VLDL) protein and inhibits lipoprotein lipase and hepatic lipase, thereby delaying the breakdown of triglyceride-rich particles. DNAseI footprinting analysis and gel retardation studies have demonstrated ATF2 binding to the apolipoprotein C3 promoter (91). Also, ATF2 stimulates apolipoprotein C3 promoter activity in reporter assays in HepG2 cells (91).

In cultured cell lines, the expression of MKP1 is induced by insulin and blunted by shRNA-mediated silencing of ATF2 ((101); BB and DMO, unpublished results: see *Chapter 5*). Also studies in embryonic livers from mice lacking both ATF2 and ATFa (also known as ATF7) confirm MKP1 as an ATF2-regulated gene (24). MKP1 is a negative regulator of the upstream activators of ATF2, i.e. the MAP kinases p38, JNK and ERK1/2 (24;102). In adipocytes, MKP1 has an inhibitory effect on the production of monocyte chemoattractant protein 1 (MCP1), a chemokine highly associated with the development of adipocyte dysfunction in insulin resistance (103). Conversely, mice lacking the MKP1 gene are resistant for diet-induced obesity (104). Therefore, further studies are clearly required to clarify the role of MKP1 in *in vivo* insulin action.

ATF2 has also been implicated in the regulation of β-cell function and proliferation. In isolated rat islets, Ca^{2+}-induced activation of CAMKIV leads to phosphorylation of ATF2 and induction of ATF2-dependent insulin expression (39). Transfection studies in rat insulinomas confirm ATF2 as crucial regulator of glucose-induced insulin transcription by demonstrating ATF2 binding to a CRE-binding element in the human insulin promoter (90). ATF2 further regulates the induction of the cyclin D1 gene in response to regenerating gene product stimulation of β-cells (105). Finally, gene variants in two other cell cycle regulators, i.e. cyclin-dependent kinase inhibitor 2A (CDKN2A) and transcription factor 7 like 2 (TCF7L2, also known as TCF4), that associate with type 2 diabetes and reduced insulin secretion (106;107), were also identified as potential ATF2-regulated genes in a ChIP-on-chip analysis using (phosphospecific) ATF2 antibodies in cisplatin-treated cells (66).

ATF2 and insulin resistance. Insulin resistance in combination with insufficient compensatory insulin secretion due to β-cell dysfunction characterizes type 2 diabetes (T2D) (108). One of the features of insulin resistance is elevated activity of the stress kinase JNK in several insulin target tissues including liver, fat and adipose tissue ((109;110) reviewed in (111)). High fat diet (HFD)-induced insulin resistance in rodent models is mitigated by pharmacological or shRNA-mediated inhibition of JNK activity (112-114). Furthermore, it was found that JNK1-, but not JNK2-knockout mice are resistant to the development of insulin resistance induced by HFD (109;115). JNK activation has been described to inhibit insulin signaling directly via serine phosphorylation of IRS proteins, thereby interfering with tyrosine phosphorylation of the proteins and subsequent activation of downstream signaling pathways (116). Alternatively, JNK may affect insulin

sensitivity indirectly via expression of pro-inflammatory cytokines (116;117). In the insulin resistant state, macrophages infiltrate major insulin target tissues, such as liver and adipose tissue, and various cytokines, including IL6 and TNFα, are released by both macrophages and adipose tissue (118). In hepatocytes, IL6 has been linked to the induction of suppressor of cytokine signaling 3 (SOCS3) (119), a protein that binds to and inhibits the insulin receptor, but also targets the IRS proteins for proteasomal degradation (120;121). In 3T3L1 adipocytes, TNFα increases the expression of MAP4K4 (88). MAP4K4 is an upstream activator of JNK (Figure 4), has been identified as T2D candidate gene (122) and is reported to inhibit adipocyte differentiation and glucose uptake in adipocytes (123). In primary muscle cells isolated from human subjects with T2D, silencing of MAP4K4 restored insulin sensitivity and prevented TNFα-induced insulin resistance (124).

ATF2 has been implicated in induction of IL6, TNFα and MAPK4K4. Silencing ATF2 in 3T3L1 adipocytes abrogates the induction of MAP4K4 (88) and expression of wildtype ATF2 is required for maximal induction of IL6 and TNFα in mouse models (67). Also, studies in *D. melanogaster* support the role of ATF2 in the immune response (9). Interestingly, ATF2-phosphorylation is elevated in both the liver and white adipose tissue from HFD-fed mice (125), suggesting that ATF2 may participate in the pathogenesis of insulin resistance, in addition to and possibly as a downstream effector of JNK.

Furthermore, increased JNK activity was also found in the hypothalamus of HFD-induced insulin resistant mice (126). As ATF2 is highly expressed in the brain (2), amongst others in the arcuate nucleus (127), a region of the hypothalamus that is associated with the control of food intake (128;129), this finding potentially links neuronal ATF2 with the metabolic disturbances found in the insulin resistant state.

An important question is whether activation of the JNK/ATF2-axis within a specific organ might be responsible for the development of insulin resistance. In contrast to ATF2, mice with tissue-specific alterations in JNK1 activity have been generated and analyzed for alterations in insulin sensitivity following high-fat feeding. Whereas overexpression or ablation of JNK in skeletal muscle does not affect glycogen metabolism, or protein levels of key molecules regulating glucose metabolism (130;131), liver-specific knockdown of JNK1 led to a significant reduction in plasma glucose and insulin levels and enhanced insulin-mediated phosphorylation of PKB/Akt (132). In line with these data, mice with antisense oligonucleotide-mediated JNK1-silencing in liver failed to develop insulin resistance and steatohepatitis in response to high-fat feeding (114). Mice with specific ablation of JNK1 in adipose tissue show a greatly reduced susceptibility to insulin resistance induced by high-fat feeding (119). In addition, the HFD-induced expression and secretion of IL6 in adipose tissue was abrogated in adipose-specific JNK1 knock-out mice (119). As described above, IL6-induced expression of hepatic SOCS3 may contribute to insulin resistance. In support of this model, mice with a fat-specific deletion of JNK1 are protected against HFD-induced increase in SOCS3 expression and abrogation of insulin-mediated PKB/Akt-phosphorylation in the liver (119). As the accumulation of macrophages in adipose tissue may also trigger the inflammatory changes seen in insulin resistance and T2D, various groups have generated mice with JNK1 deficiency in myeloid and hematopoietic cells. One report shows that ablation of JNK1 in myeloid cells ameliorates obesity-induced insulin resistance, but subsequent studies did not confirm this finding (119;133-135). Interestingly, all reports found a reduction in the expression of the ATF2 target genes TNFα and IL6 in adipose and hepatic tissue of macrophage-specific JNK-deficient mice.

Despite these suggestive data, the involvement of ATF2 in JNK-dependent processes associated with insulin resistance has not been thoroughly examined. Future studies on mice with a tissue-specific ablation of ATF2 are required to detail the contribution of ATF2 to these JNK-dependent processes.

ATF2 and β-cell dysfunction. Islet cells from patients with T2D show increased inflammation characterized by the presence of immune cell infiltration, amyloid deposits, cytokines and apoptotic cells (136). Various studies implicate ATF2 and ATF2-regulated genes in β-cell dysfunction and apoptosis. Exposure of β-cells to amylin induces a p38-dependent increase in ATF2-phosphorylation (137). Furthermore, amylin-induced apoptosis is prevented by silencing of ATF2 (137). The increase in ATF2 phosphorylation induced by IL1β is mediated by JNK and inhibition of JNK prevents IL1β-induced apoptosis (138;139). Future studies should detail whether the induction of ATF2-regulated genes, IL1β, ATF3, CHOP and BiP/Grp78 (66;68;71) also contributes to β-cell dysfunction and apoptosis. Increased expression of ATF3 in β-cells has been found to lower the levels of IRS2, a key regulator of β-cell survival (140). The induction of IL1β by ATF2 may cause a vicious cycle resulting in progressive β-cell loss. Furthermore, IL1β exposure of β-cells results in endoplasmic reticulum stress, amongst others via the induction of ATF3, CHOP and BiP/Grp78 (141).

ATF2 and T2D-associated complications. Endothelial dysfunction is a co-morbidity in T2D and insulin resistance. Insulin regulates vasodilation by increasing endothelial nitric-oxide synthase (eNOS) activity through the PI3K-PKB/Akt-pathway (142). In insulin resistance, defects in insulin-induced endothelium-dependent vasodilation have been reported (143). ATF2 has been found in complex with the promoter of phosphatase and tensin homolog (PTEN). Furthermore, two potential inducers of endothelial dysfunction in T2D, resistin and free fatty acids, have been found to increase PTEN levels in endothelial cells via activation of the p38/ATF2-pathway (92;93). PTEN acts as a phosphatase to dephosphorylate the product of PI3K, phosphatidylinositol (3,4,5)-triphosphate (PIP3). Thus, activation of ATF2 can contribute to endothelial dysfunction by inhibiting the PI3K-PKB/Akt- dependent phosphorylation of eNOS (142).

The characterization of ATF2-target genes in cisplatin-treated breast cancer cells also identified several genes (66) including collagen, early growth response 1 (Egr1), E-selectin, IGF2, inducible nitric oxide synthase (iNOS), P-selectin, transforming growth factor β (TGFβ) and vascular cell adhesion molecule 1 (VCAM-1), that are associated with endothelial dysfunction as well as other T2D-associated complications, like tissue fibrosis and diabetic nephropathy (144-147). However, further clarification of the involvement of ATF2 in these processes is still needed.

Conclusions and perspectives. ATF2 has been identified as component of the insulin signaling system *in vitro* and *in vivo* (18;45;125). The nature of the ATF2-regulated genes suggests a function for ATF2 in the regulation of glucose and lipid metabolism, as well as β-cell function. Genetic evidence from *D. melanogaster* supports a function for ATF2 in lipid metabolism. Intriguingly, in obesity and insulin resistance, a sustained increase in the activity of the p38/ATF2- and JNK/ATF2-signalling pathways is observed, which may contribute to the development of T2D and associated complications. Future studies should elucidate whether insulin or conditions associated with insulin resistance and obesity induce distinct sets of ATF2-target genes.

Acknowledgements
The authors acknowledge the financial support of the Dutch Diabetes Research Foundation (grant 2001.00.46) and COST-action BM602 for their studies.

References

1. Hai, T. W., Liu, F., Coukos, W. J., and Green, M. R. (1989) *Genes Dev.* **3,** 2083-2090
2. Maekawa, T., Sakura, H., Kanei-Ishii, C., Sudo, T., Yoshimura, T., Fujisawa, J., Yoshida, M., and Ishii, S. (1989) *EMBO J.* **8,** 2023-2028
3. van Dam, H., Wilhelm, D., Herr, I., Steffen, A., Herrlich, P., and Angel, P. (1995) *EMBO J.* **14,** 1798-1811
4. Hai, T., Wolfgang, C. D., Marsee, D. K., Allen, A. E., and Sivaprasad, U. (1999) *Gene Expr.* **7,** 321-335
5. Kim, I., Xu, W., and Reed, J. C. (2008) *Nat. Rev. Drug Discov.* **7,** 1013-1030
6. Ozawa, K., Sudo, T., Soeda, E., Yoshida, M. C., and Ishii, S. (1991) *Genomics* **10,** 1103-1104
7. Vlahopoulos, S. A., Logotheti, S., Mikas, D., Giarika, A., Gorgoulis, V., and Zoumpourlis, V. (2008) *Bioessays* **30,** 314-327
8. Bhoumik, A., Lopez-Bergami, P., and Ronai, Z. (2007) *Pigment Cell Res.* **20,** 498-506
9. Sano, Y., Akimaru, H., Okamura, T., Nagao, T., Okada, M., and Ishii, S. (2005) *Mol. Biol. Cell* **16,** 2934-2946
10. Nagadoi, A., Nakazawa, K., Uda, H., Okuno, K., Maekawa, T., Ishii, S., and Nishimura, Y. (1999) *J. Mol. Biol.* **287,** 593-607
11. Matsuda, S., Maekawa, T., and Ishii, S. (1991) *J. Biol. Chem.* **266,** 18188-18193
12. Flint, K. J. and Jones, N. C. (1991) *Oncogene* **6,** 2019-2026
13. Ivashkiv, L. B., Liou, H. C., Kara, C. J., Lamph, W. W., Verma, I. M., and Glimcher, L. H. (1990) *Mol. Cell Biol.* **10,** 1609-1621
14. Kara, C. J., Liou, H. C., Ivashkiv, L. B., and Glimcher, L. H. (1990) *Mol. Cell Biol.* **10,** 1347-1357
15. Chyan, Y. J., Rawson, T. Y., and Wilson, S. H. (2003) *Gene* **312,** 117-124
16. Gupta, S., Campbell, D., Derijard, B., and Davis, R. J. (1995) *Science* **267,** 389-393
17. Raingeaud, J., Gupta, S., Rogers, J. S., Dickens, M., Han, J., Ulevitch, R. J., and Davis, R. J. (1995) *J. Biol. Chem.* **270,** 7420-7426
18. Ouwens, D. M., de Ruiter, N. D., van der Zon, G. C., Carter, A. P., Schouten, J., van der Burgt, C., Kooistra, K., Bos, J. L., Maassen, J. A., and van Dam, H. (2002) *EMBO J.* **21,** 3782-3793
19. Livingstone, C., Patel, G., and Jones, N. (1995) *EMBO J.* **14,** 1785-1797
20. Morton, S., Davis, R. J., and Cohen, P. (2004) *FEBS Lett.* **572,** 177-183
21. Zhu, T. and Lobie, P. E. (2000) *J. Biol. Chem.* **275,** 2103-2114
22. Kawasaki, H., Schiltz, L., Chiu, R., Itakura, K., Taira, K., Nakatani, Y., and Yokoyama, K. K. (2000) *Nature* **405,** 195-200
23. Kawasaki, H., Taira, K., and Yokoyama, K. (2000) *Nucleic Acids Symp. Ser.* 259-260
24. Breitwieser, W., Lyons, S., Flenniken, A. M., Ashton, G., Bruder, G., Willington, M., Lacaud, G., Kouskoff, V., and Jones, N. (2007) *Genes Dev.* **21,** 2069-2082
25. Liu, H., Deng, X., Shyu, Y. J., Li, J. J., Taparowsky, E. J., and Hu, C. D. (2006) *EMBO J.* **25,** 1058-1069
26. Vinson, C., Myakishev, M., Acharya, A., Mir, A. A., Moll, J. R., and Bonovich, M. (2002) *Mol. Cell Biol.* **22,** 6321-6335

27. Sano, Y., Harada, J., Tashiro, S., Gotoh-Mandeville, R., Maekawa, T., and Ishii, S. (1999) *J. Biol. Chem.* **274,** 8949-8957
28. Kageyama, R., Sasai, Y., and Nakanishi, S. (1991) *J. Biol. Chem.* **266,** 15525-15531
29. Shuman, J. D., Cheong, J., and Coligan, J. E. (1997) *J. Biol. Chem.* **272,** 12793-12800
30. Benbrook, D. M. and Jones, N. C. (1990) *Oncogene* **5,** 295-302
31. Hai, T. and Curran, T. (1991) *Proc. Natl. Acad. Sci. U. S. A* **88,** 3720-3724
32. Kerppola, T. K. and Curran, T. (1993) *Mol. Cell Biol.* **13,** 5479-5489
33. van Dam, H., Duyndam, M., Rottier, R., Bosch, A., de Vries-Smits, L., Herrlich, P., Zantema, A., Angel, P., and van der Eb, A. J. (1993) *EMBO J.* **12,** 479-487
34. Penix, L. A., Sweetser, M. T., Weaver, W. M., Hoeffler, J. P., Kerppola, T. K., and Wilson, C. B. (1996) *J. Biol. Chem.* **271,** 31964-31972
35. Georgopoulos, K., Morgan, B. A., and Moore, D. D. (1992) *Mol. Cell Biol.* **12,** 747-757
36. Bailey, J., Phillips, R. J., Pollard, A. J., Gilmore, K., Robson, S. C., and Europe-Finner, G. N. (2002) *J. Clin. Endocrinol. Metab* **87,** 1717-1728
37. Sakurai, A., Maekawa, T., Sudo, T., Ishii, S., and Kishimoto, A. (1991) *Biochem. Biophys. Res. Commun.* **181,** 629-635
38. Sevilla, A., Santos, C. R., Vega, F. M., and Lazo, P. A. (2004) *J. Biol. Chem.* **279,** 27458-27465
39. Ban, N., Yamada, Y., Someya, Y., Ihara, Y., Adachi, T., Kubota, A., Watanabe, R., Kuroe, A., Inada, A., Miyawaki, K., Sunaga, Y., Shen, Z. P., Iwakura, T., Tsukiyama, K., Toyokuni, S., Tsuda, K., and Seino, Y. (2000) *Diabetes* **49,** 1142-1148
40. Kawasaki, H., Song, J., Eckner, R., Ugai, H., Chiu, R., Taira, K., Shi, Y., Jones, N., and Yokoyama, K. K. (1998) *Genes Dev.* **12,** 233-245
41. Bhoumik, A., Takahashi, S., Breitweiser, W., Shiloh, Y., Jones, N., and Ronai, Z. (2005) *Mol. Cell* **18,** 577-587
42. Khidekel, N., Ficarro, S. B., Peters, E. C., and Hsieh-Wilson, L. C. (2004) *Proc. Natl. Acad. Sci. U. S. A* **101,** 13132-13137
43. Firestein, R. and Feuerstein, N. (1998) *J. Biol. Chem.* **273,** 5892-5902
44. van Dam, H. and Castellazzi, M. (2001) *Oncogene* **20,** 2453-2464
45. Baan, B., van Dam, H., van der Zon, G. C., Maassen, J. A., and Ouwens, D. M. (2006) *Mol. Endocrinol.* **20,** 1786-1795
46. Adamson, A. L., Darr, D., Holley-Guthrie, E., Johnson, R. A., Mauser, A., Swenson, J., and Kenney, S. (2000) *J. Virol.* **74,** 1224-1233
47. Maekawa, T., Bernier, F., Sato, M., Nomura, S., Singh, M., Inoue, Y., Tokunaga, T., Imai, H., Yokoyama, M., Reimold, A., Glimcher, L. H., and Ishii, S. (1999) *J. Biol. Chem.* **274,** 17813-17819
48. Okamura, T., Shimizu, H., Nagao, T., Ueda, R., and Ishii, S. (2007) *Mol. Biol. Cell.* **18,** 1519-1529
49. Li, X. Y. and Green, M. R. (1996) *Genes Dev.* **10,** 517-527
50. Abdel-Hafiz, H. A., Heasley, L. E., Kyriakis, J. M., Avruch, J., Kroll, D. J., Johnson, G. L., and Hoeffler, J. P. (1992) *Mol. Endocrinol.* **6,** 2079-2089
51. Bruhat, A., Cherasse, Y., Maurin, A. C., Breitwieser, W., Parry, L., Deval, C., Jones, N., Jousse, C., and Fafournoux, P. (2007) *Nucleic Acids Res.* **35,** 1312-1321
52. Kuo, M. H. and Allis, C. D. (1998) *Bioessays* **20,** 615-626
53. Duyndam, M. C., van Dam, H., Smits, P. H., Verlaan, M., van der Eb, A. J., and Zantema, A. (1999) *Oncogene* **18,** 2311-2321
54. Fuchs, S. Y. and Ronai, Z. (1999) *Mol. Cell Biol.* **19,** 3289-3298

55. Fuchs, S. Y., Tappin, I., and Ronai, Z. (2000) *J. Biol. Chem.* **275,** 12560-12564
56. Liu, F. and Green, M. R. (1990) *Cell* **61,** 1217-1224
57. Perini, G., Oetjen, E., and Green, M. R. (1999) *J. Biol. Chem.* **274,** 13970-13977
58. Virbasius, C. M., Wagner, S., and Green, M. R. (1999) *Mol. Cell* **4,** 219-228
59. Fukushima, A., Okuda, A., Nishimoto, M., Seki, N., Hori, T. A., and Muramatsu, M. (1998) *J. Biol. Chem.* **273,** 25840-25849
60. Agelopoulos, M. and Thanos, D. (2006) *EMBO J.* **25,** 4843-4853
61. Cho, S. G., Bhoumik, A., Broday, L., Ivanov, V., Rosenstein, B., and Ronai, Z. (2001) *Mol. Cell Biol.* **21,** 8398-8413
62. Jin, C., Ugai, H., Song, J., Murata, T., Nili, F., Sun, K., Horikoshi, M., and Yokoyama, K. K. (2001) *FEBS Lett.* **489,** 34-41
63. Kimura, M. (2008) *FEBS Lett.* **582,** 2833-2837
64. Bossis, G., Malnou, C. E., Farras, R., Andermarcher, E., Hipskind, R., Rodriguez, M., Schmidt, D., Muller, S., Jariel-Encontre, I., and Piechaczyk, M. (2005) *Mol. Cell Biol.* **25,** 6964-6979
65. Hamard, P. J., Boyer-Guittaut, M., Camuzeaux, B., Dujardin, D., Hauss, C., Oelgeschlager, T., Vigneron, M., Kedinger, C., and Chatton, B. (2007) *Nucleic Acids Res.* **35,** 1134-1144
66. Hayakawa, J., Mittal, S., Wang, Y., Korkmaz, K. S., Adamson, E., English, C., Ohmichi, M., McClelland, M., and Mercola, D. (2004) *Mol. Cell* **16,** 521-535
67. Reimold, A. M., Kim, J., Finberg, R., and Glimcher, L. H. (2001) *Int. Immunol.* **13,** 241-248
68. Liang, G., Wolfgang, C. D., Chen, B. P., Chen, T. H., and Hai, T. (1996) *J. Biol. Chem.* **271,** 1695-1701
69. Cao, W., Daniel, K. W., Robidoux, J., Puigserver, P., Medvedev, A. V., Bai, X., Floering, L. M., Spiegelman, B. M., and Collins, S. (2004) *Mol. Cell Biol.* **24,** 3057-3067
70. Yan, Z., Li, P., and Akimoto, T. (2007) *Exerc. Sport Sci. Rev.* **35,** 97-101
71. Bruhat, A., Jousse, C., Carraro, V., Reimold, A. M., Ferrara, M., and Fafournoux, P. (2000) *Mol. Cell Biol.* **20,** 7192-7204
72. Lee, M. Y., Jung, C. H., Lee, K., Choi, Y. H., Hong, S., and Cheong, J. (2002) *Diabetes* **51,** 3400-3407
73. Cheong, J., Coligan, J. E., and Shuman, J. D. (1998) *J. Biol. Chem.* **273,** 22714-22718
74. Shimizu, M., Nomura, Y., Suzuki, H., Ichikawa, E., Takeuchi, A., Suzuki, M., Nakamura, T., Nakajima, T., and Oda, K. (1998) *Exp. Cell Res.* **239,** 93-103
75. Beier, F., Taylor, A. C., and LuValle, P. (2000) *J. Biol. Chem.* **275,** 12948-12953
76. Beier, F., Lee, R. J., Taylor, A. C., Pestell, R. G., and LuValle, P. (1999) *Proc. Natl. Acad. Sci. U. S. A* **96,** 1433-1438
77. Matsuo, N., Tanaka, S., Gordon, M. K., Koch, M., Yoshioka, H., and Ramirez, F. (2006) *J. Biol. Chem.* **281,** 5445-5452
78. Chen, K. D., Hung, J. J., Huang, H. L., Chang, M. D., and Lai, Y. K. (1997) *Eur. J. Biochem.* **248,** 120-129
79. Bhat, N. R., Feinstein, D. L., Shen, Q., and Bhat, A. N. (2002) *J. Biol. Chem.* **277,** 29584-29592
80. Kim, E. S., Sohn, Y. W., and Moon, A. (2007) *Cancer Lett.* **252,** 147-156
81. Song, H., Ki, S. H., Kim, S. G., and Moon, A. (2006) *Cancer Res.* **66,** 10487-10496
82. De Cesare, D., Vallone, D., Caracciolo, A., Sassone-Corsi, P., Nerlov, C., and Verde, P. (1995) *Oncogene* **11,** 365-376

83. Steinmuller, L. and Thiel, G. (2003) *Biol. Chem.* **384,** 667-672
84. Tsai, E. Y., Jain, J., Pesavento, P. A., Rao, A., and Goldfeld, A. E. (1996) *Mol. Cell Biol.* **16,** 459-467
85. Du, W. and Maniatis, T. (1992) *Proc. Natl. Acad. Sci. U. S. A* **89,** 2150-2154
86. Li, H. and Wicks, W. D. (2001) *Arch. Biochem. Biophys.* **394,** 1-12
87. Samten, B., Townsend, J. C., Weis, S. E., Bhoumik, A., Klucar, P., Shams, H., and Barnes, P. F. (2008) *J. Immunol.* **181,** 2056-2064
88. Tesz, G. J., Guilherme, A., Guntur, K. V., Hubbard, A. C., Tang, X., Chawla, A., and Czech, M. P. (2007) *J. Biol. Chem.* **282,** 19302-19312
89. Falvo, J. V., Parekh, B. S., Lin, C. H., Fraenkel, E., and Maniatis, T. (2000) *Mol. Cell Biol.* **20,** 4814-4825
90. Hay, C. W., Ferguson, L. A., and Docherty, K. (2007) *Biochim. Biophys. Acta* **1769,** 79-91
91. Hadzopoulou-Cladaras, M., Lavrentiadou, S. N., Zannis, V. I., and Kardassis, D. (1998) *Biochemistry* **37,** 14078-14087
92. Wang, X. L., Zhang, L., Youker, K., Zhang, M. X., Wang, J., LeMaire, S. A., Coselli, J. S., and Shen, Y. H. (2006) *Diabetes* **55,** 2301-2310
93. Shen, Y. H., Zhang, L., Gan, Y., Wang, X., Wang, J., LeMaire, S. A., Coselli, J. S., and Wang, X. L. (2006) *J. Biol. Chem.* **281,** 7727-7736
94. Reimold, A. M., Grusby, M. J., Kosaras, B., Fries, J. W., Mori, R., Maniwa, S., Clauss, I. M., Collins, T., Sidman, R. L., Glimcher, M. J., and Glimcher, L. H. (1996) *Nature* **379,** 262-265
95. Barthel, A. and Schmoll, D. (2003) *Am. J. Physiol Endocrinol. Metab* **285,** E685-E692
96. Reshef, L., Olswang, Y., Cassuto, H., Blum, B., Croniger, C. M., Kalhan, S. C., Tilghman, S. M., and Hanson, R. W. (2003) *J. Biol. Chem.* **278,** 30413-30416
97. Allen-Jennings, A. E., Hartman, M. G., Kociba, G. J., and Hai, T. (2002) *J. Biol. Chem.* **277,** 20020-20025
98. Lin, J., Handschin, C., and Spiegelman, B. M. (2005) *Cell Metab* **1,** 361-370
99. Rodgers, J. T., Lerin, C., Gerhart-Hines, Z., and Puigserver, P. (2008) *FEBS Lett.* **582,** 46-53
100. Akimoto, T., Li, P., and Yan, Z. (2008) *Am. J. Physiol Cell Physiol* **295,** C288-C292
101. Byon, J. C., Dadke, S. S., Rulli, S., Kusari, A. B., and Kusari, J. (2001) *Mol. Cell Biochem.* **218,** 131-138
102. Owens, D. M. and Keyse, S. M. (2007) *Oncogene* **26,** 3203-3213
103. Ito, A., Suganami, T., Miyamoto, Y., Yoshimasa, Y., Takeya, M., Kamei, Y., and Ogawa, Y. (2007) *J. Biol. Chem.* **282,** 25445-25452
104. Wu, J. J., Roth, R. J., Anderson, E. J., Hong, E. G., Lee, M. K., Choi, C. S., Neufer, P. D., Shulman, G. I., Kim, J. K., and Bennett, A. M. (2006) *Cell Metab* **4,** 61-73
105. Takasawa, S., Ikeda, T., Akiyama, T., Nata, K., Nakagawa, K., Shervani, N. J., Noguchi, N., Murakami-Kawaguchi, S., Yamauchi, A., Takahashi, I., Tomioka-Kumagai, T., and Okamoto, H. (2006) *FEBS Lett.* **580,** 585-591
106. Perry, J. R. and Frayling, T. M. (2008) *Curr. Opin. Clin. Nutr. Metab Care* **11,** 371-377
107. Florez, J. C. (2008) *Diabetologia* **51,** 1100-1110
108. Saltiel, A. R. and Kahn, C. R. (2001) *Nature* **414,** 799-806
109. Hirosumi, J., Tuncman, G., Chang, L., Gorgun, C. Z., Uysal, K. T., Maeda, K., Karin, M., and Hotamisligil, G. S. (2002) *Nature* **420,** 333-336

110. Solinas, G., Naugler, W., Galimi, F., Lee, M. S., and Karin, M. (2006) *Proc. Natl. Acad. Sci. U. S. A.* **103,** 16454-16459
111. Yang, R. and Trevillyan, J. M. (2008) *Int. J. Biochem. Cell Biol.* **40,** 2702-2706
112. Kaneto, H., Nakatani, Y., Miyatsuka, T., Kawamori, D., Matsuoka, T. A., Matsuhisa, M., Kajimoto, Y., Ichijo, H., Yamasaki, Y., and Hori, M. (2004) *Nat. Med.* **10,** 1128-1132
113. Stebbins, J. L., De, S. K., Machleidt, T., Becattini, B., Vazquez, J., Kuntzen, C., Chen, L. H., Cellitti, J. F., Riel-Mehan, M., Emdadi, A., Solinas, G., Karin, M., and Pellecchia, M. (2008) *Proc. Natl. Acad. Sci. U. S. A* **105,** 16809-16813
114. Singh, R., Wang, Y., Xiang, Y., Tanaka, K. E., Gaarde, W. A., and Czaja, M. J. (2009) *Hepatology* **49,** 87-96
115. Tuncman, G., Hirosumi, J., Solinas, G., Chang, L., Karin, M., and Hotamisligil, G. S. (2006) *Proc. Natl. Acad. Sci. U. S. A* **103,** 10741-10746
116. Wellen, K. E. and Hotamisligil, G. S. (2005) *J. Clin. Invest* **115,** 1111-1119
117. Ogawa, W. and Kasuga, M. (2008) *Science* **322,** 1483-1484
118. Rasouli, N. and Kern, P. A. (2008) *J. Clin. Endocrinol. Metab* **93,** S64-S73
119. Sabio, G., Das, M., Mora, A., Zhang, Z., Jun, J. Y., Ko, H. J., Barrett, T., Kim, J. K., and Davis, R. J. (2008) *Science* **322,** 1539-1543
120. Emanuelli, B., Peraldi, P., Filloux, C., Chavey, C., Freidinger, K., Hilton, D. J., Hotamisligil, G. S., and van Obberghen, E. (2001) *J Biol. Chem.* **276,** 47944-47949
121. Rui, L., Yuan, M., Frantz, D., Shoelson, S., and White, M. F. (2002) *J Biol. Chem.* **277,** 42394-42398
122. Elbein, S. C., Das, S. K., Hallman, D. M., Hanis, C. L., and Hasstedt, S. J. (2009) *Diabetes* **58,** 268-274
123. Tang, X., Guilherme, A., Chakladar, A., Powelka, A. M., Konda, S., Virbasius, J. V., Nicoloro, S. M., Straubhaar, J., and Czech, M. P. (2006) *Proc. Natl. Acad. Sci. U. S. A* **103,** 2087-2092
124. Bouzakri, K. and Zierath, J. R. (2007) *J. Biol. Chem.* **282,** 7783-7789
125. Baan et al., *Manuscript in preparation* (Chapter 6)
126. Prada, P. O., Zecchin, H. G., Gasparetti, A. L., Torsoni, M. A., Ueno, M., Hirata, A. E., Corezola do Amaral, M. E., Hoer, N. F., Boschero, A. C., and Saad, M. J. (2005) *Endocrinology* **146,** 1576-1587
127. Pearson, A. G., Curtis, M. A., Waldvogel, H. J., Faull, R. L., and Dragunow, M. (2005) *Neuroscience* **133,** 437-451
128. Schwartz, M. W., Woods, S. C., Porte, D., Jr., Seeley, R. J., and Baskin, D. G. (2000) *Nature* **404,** 661-671
129. Plum, L., Belgardt, B. F., and Bruning, J. C. (2006) *J. Clin. Invest* **116,** 1761-1766
130. Fujii, N., Boppart, M. D., Dufresne, S. D., Crowley, P. F., Jozsi, A. C., Sakamoto, K., Yu, H., Aschenbach, W. G., Kim, S., Miyazaki, H., Rui, L., White, M. F., Hirshman, M. F., and Goodyear, L. J. (2004) *Am. J. Physiol Cell Physiol* **287,** C200-C208
131. Witczak, C. A., Hirshman, M. F., Jessen, N., Fujii, N., Seifert, M. M., Brandauer, J., Hotamisligil, G. S., and Goodyear, L. J. (2006) *Biochem. Biophys. Res. Commun.* **350,** 1063-1068
132. Yang, R., Wilcox, D. M., Haasch, D. L., Jung, P. M., Nguyen, P. T., Voorbach, M. J., Doktor, S., Brodjian, S., Bush, E. N., Lin, E., Jacobson, P. B., Collins, C. A., Landschulz, K. T., Trevillyan, J. M., Rondinone, C. M., and Surowy, T. K. (2007) *J. Biol. Chem.* **282,** 22765-22774

133. Solinas, G., Vilcu, C., Neels, J. G., Bandyopadhyay, G. K., Luo, J. L., Naugler, W., Grivennikov, S., Wynshaw-Boris, A., Scadeng, M., Olefsky, J. M., and Karin, M. (2007) *Cell Metab* **6,** 386-397
134. Vallerie, S. N., Furuhashi, M., Fucho, R., and Hotamisligil, G. S. (2008) *PLoS. ONE.* **3,** e3151
135. Das, M., Sabio, G., Jiang, F., Rincon, M., Flavell, R. A., and Davis, R. J. (2009) *Cell* **136,** 249-260
136. Ehses, J. A., Boni-Schnetzler, M., Faulenbach, M., and Donath, M. Y. (2008) *Biochem. Soc. Trans.* **36,** 340-342
137. Zhang, S., Liu, H., Liu, J., Tse, C. A., Dragunow, M., and Cooper, G. J. (2006) *FEBS J.* **273,** 3779-3791
138. Ammendrup, A., Maillard, A., Nielsen, K., Aabenhus, A. N., Serup, P., Dragsbaek, M. O., Mandrup-Poulsen, T., and Bonny, C. (2000) *Diabetes.* **49,** 1468-1476
139. Bonny, C., Oberson, A., Steinmann, M., Schorderet, D. F., Nicod, P., and Waeber, G. (2000) *J Biol. Chem.* **275,** 16466-16472
140. Li, D., Yin, X., Zmuda, E. J., Wolford, C. C., Dong, X., White, M. F., and Hai, T. (2008) *Diabetes* **57,** 635-644
141. Eizirik, D. L., Cardozo, A. K., and Cnop, M. (2008) *Endocr. Rev.* **29,** 42-61
142. Muniyappa, R., Iantorno, M., and Quon, M. J. (2008) *Endocrinol. Metab Clin. North Am.* **37,** 685-68x
143. Baron, A. D. (1999) *Am. J Cardiol.* **84,** 25J-27J
144. Wang, C. C., Sharma, G., and Draznin, B. (2006) *Am. J. Hypertens.* **19,** 366-372
145. Hasan, R. N., Phukan, S., and Harada, S. (2003) *Arterioscler. Thromb. Vasc. Biol.* **23,** 988-993
146. Petersen, M., Thorikay, M., Deckers, M., van Dinther, M., Grygielko, E. T., Gellibert, F., de Gouville, A. C., Huet, S., ten Dijke, P., and Laping, N. J. (2008) *Kidney Int.* **73,** 705-715
147. Ban, C. R. and Twigg, S. M. (2008) *Vasc. Health Risk Manag.* **4,** 575-596

3

The nuclear appearance of ERK and p38 determines the sequential induction of ATF2-Thr71 and ATF2-Thr69-phosphorylation by serum in JNK-deficient cells

Manuscript conditionally accepted for publication

Chapter 3

Chapter 3

The nuclear appearance of ERK and p38 determines the sequential induction of ATF2-Thr71 and ATF2-Thr69-phosphorylation by serum in JNK-deficient cells

Bart Baan, Gerard C.M. van der Zon, J. Antonie Maassen and D. Margriet Ouwens

From the Department of Molecular Cell Biology, Section Signal Transduction and Ageing, Leiden University Medical Centre, Leiden, the Netherlands

Growth factors activate ATF2 via sequential phosphorylation of Thr69 and Thr71, where the ATF2-Thr71-phosphorylation precedes the induction of ATF2-Thr69+71-phosphorylation. Here, we studied the mechanisms contributing to serum-induced two-step ATF2-phosphorylation in JNK1,2-deficient embryonic fibroblasts. Using anion exchange chromatography, ERK1/2 and p38 were identified as ATF2–kinases in vitro. Inhibitor studies as well as nuclear localization experiments show that the sequential nuclear appearance of ERK1/2 and p38 determines the induction of ATF-Thr71 and ATF2-Thr69+71-phosphorylation in response to serum.

ATF2 is a ubiquitously expressed member of the cAMP-responsive element (CRE)-binding protein family of basic region-leucine zipper (bZIP) transcription factors also including CREB (1) and ATF3, ATF4, ATF6 and B-ATF (2;3). ATF2 can form homo- and heterodimers with other ATF-family members (3), but also with the activating protein-1 (AP-1) family member cJun (4). The various dimer compositions confer an enormous repertoire of target genes on ATF2, which include cell cycle regulators, proteins involved in invasion or adhesion, growth factors and pro-inflammatory cytokines, DNA repair genes, transcriptional factors and molecules associated with metabolic control (5;6).

In the absence of a stimulus, ATF2 is held in an inactive conformation (7). Phosphorylation of residues within the activation domain leads to ATF2 transcriptional activation (8-10). In particular, phosphorylation of two threonine (Thr) residues, Thr69 and Thr71, is required and sufficient for transcriptional activation of ATF2 (11;12).

Inducers of cellular stress, like pro-inflammatory cytokines, oncogenes, viruses, heat shock, osmotic stress and DNA-damaging agents as well as growth factors, increase the transactivation capacity of ATF2 through phosphorylation of the Thr69 and Thr71 residues. The activation pattern induced by mitogens, however, differs from that mediated by inducers of cellular stress. Cellular stresses induce a prolonged phosphorylation of ATF2, whereas the activation induced by growth factors is much more transient and, importantly, is elicited via a two-step mechanism (13). Within minutes after the addition of growth factors, phosphorylation of ATF2-Thr71 is induced, whereas subsequent phosphorylation of ATF2-Thr69 occurs several minutes later. Notably, this mechanism involves cooperation of distinct Ras-effector pathways. The Ras-Raf-MEK-ERK1/2 pathway directs the phosphorylation of ATF2-Thr71, whereas the Ras-Ral pathway is required for subsequent ATF2-Thr69 phosphorylation.

Here, we studied the mechanisms contributing to serum-induced two-step ATF2-phosphorylation in JNK1,2-deficient embryonic fibroblasts. Therefore, ATF2 kinases were purified from serum-treated cells by anion exchange chromatography. Using pharmacological inhibitors and nuclear localization experiments, we further detailed the

role of the purified kinases in the serum-mediated induction of ATF2-Thr71 and ATF2-Thr69+71-phosphorylation, respectively.

Results

The main ATF2 N-terminal kinase activities co-purify with ERK1/2 and p38 in serum-treated JNK1,2 -/- cells. To identify ATF2-kinases in JNK1,2-/- cells, cell lysates prepared after 10 min of serum stimulation were fractionated by anion-exchange chromatography on monoQ columns. Analysis of the obtained fractions showed that the bulk of ATF2-directed kinase activity co-purified with fractions containing ERK1/2. A smaller peak of ATF2-directed kinase activity was recovered in a fraction co-purifying with p38 (Figure 1A, solid line).

Incubation of the cells with U0126, an inhibitor of the upstream activator of ERK1/2: MEK1/2 (14), strongly reduced the serum-induced ATF2 kinase activity in the fractions co-purifying with ERK1/2 (Figure 1A, dashed line). Furthermore, addition of the p38 inhibitor SB203580 (15) to the in vitro kinase assay completely blocked ATF2-kinase activity in the fraction co-purifying with p38 (Figure 1B). Similar results were obtained for JNK1,2-/- cells treated with epidermal growth factor (EGF) (data not shown). Thus, the major ATF2-directed kinase activities in growth factor stimulated JNK1,2-/- cells are represented by ERK1/2 and p38.

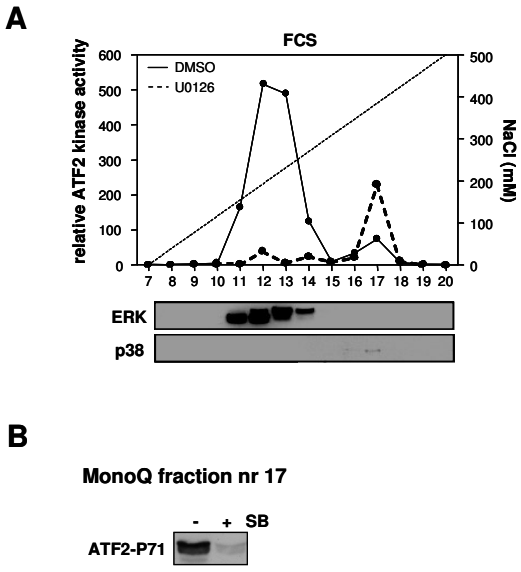

Figure 1. Identification of ERK1/2 and p38 as the major ATF2 kinases activities in JNK -/- cells. (A) JNK-/- cells, pretreated with vehicle (solid line) or U0126 (dashed line) for 15 minutes, were FCS stimulated for 10 minutes before lysis. MonoQ anion exchange-fractionation was performed on these lysates and the obtained fractions were used in an ATF2-directed *in vitro* kinase assay using GST-ATF2 as substrate. ATF2-Thr71 specific phosphorylation of GST-ATF2 was determined by Western blotting using the ATF2-Thr71 phospho-specific antibody. Relative ATF2-Thr71 reactivity was plotted against MonoQ fraction number. The presence of phospho-ERK1/2 and p38 MAPK in the different fractions was determined by western blotting. (B) The p38-containing MonoQ fraction (#17) was used in an *in vitro* kinase assay in the presence of vehicle or SB203850 with GST-ATF2 as the substrate. ATF2-Thr71 specific phosphorylation of GST-ATF2 was determined by Western blotting using a ATF2-Thr71 phospho-specific antibody.

*Inhibition of ERK1/2 and p38 differentially abrogates ATF2-Thr71 and ATF2-Thr69+71 phosphorylation in serum-stimulated JNK1,2 -/- cells.*As both ERK1/2 and p38 were identified as ATF2-directed kinases from JNK1,2-/- cells, we next analyzed the effects of U0126 and SB203580 on serum-induced ATF2-Thr71 and ATF2-Thr69+71 phosphorylation. Western blot analysis of lysates of JNK1,2-/- cells, showed that ATF2-Thr71 phosphorylation was induced after 2-4 min, whereas the onset of ATF2-Thr69+71 was detected at 4-6 min after serum addition (Figure 2A).

The presence of SB203580 lowered the absolute levels of Thr71-phosphorylated ATF2 both in the basal state as well as following incubation with serum (Figure 2B/C). However, the fold-induction (as compared to t=0 minutes) of ATF2 Thr71-phosphorylation by serum was slightly enhanced in the presence of SB203580 (Figure 2B/C). The complete inhibition of the serum-induced phosphorylation of MAPKAPK-2 (16), another downstream target of p38, confirmed effectiveness of SB203580 (Figure 2D). In contrast to SB203580, the presence of U0126 completely abrogated the induction of ATF2-Thr71 phosphorylation by serum (Figure 2B). These results suggest that, in these cells, ERK1/2 rather than p38 is responsible for the phosphorylation of ATF2 on Thr71 observed at 2-4 minutes after serum stimulation. In line with previous reports showing that ERK1/2 is not capable of phosphorylating ATF2 on Thr69 (13;17), the presence of SB203580, but not U0126, completely prevented serum-induced ATF2-Thr69+71-phosphorylation in JNK1,2-/- cells (Figure 2B).

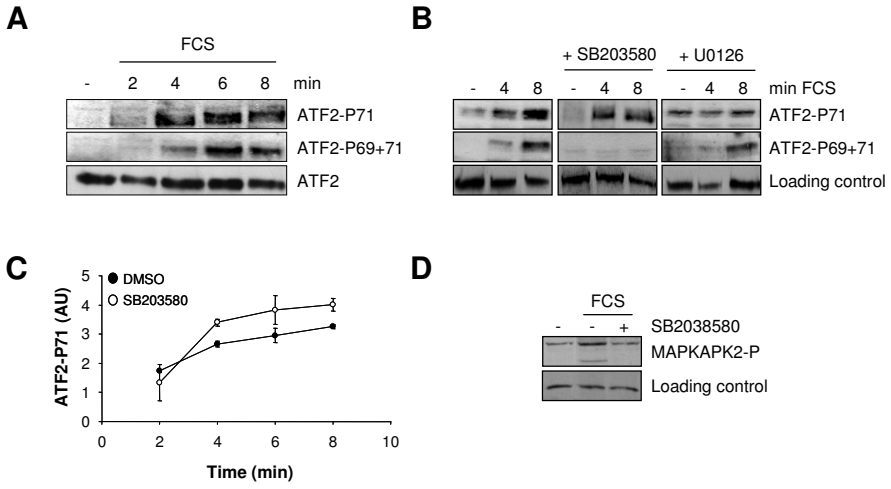

Figure 2. Inhibition of ERK1/2 and p38 differentially abrogates ATF2-Thr71 and ATF2-Thr69+71 phosphorylation in serum-stimulated JNK1,2 -/- cells. (A) Serum-starved JNK-/- cells were treated with 20% fetal calf serum (FCS). Total cell lysates were prepared at indicated time-points and analyzed by Western blotting using phospho-specific ATF2-Thr71 and ATF2-Thr69+71 antibodies. (B) Serum-starved JNK -/- cells were pre-incubated for 30 minutes with vehicle or inhibitors U0126 or SB203580 before serum-stimulation (FCS; 20%) for the times indicated. ATF2-Thr71- and Thr69+71-phosphorylation levels were determined by immunoblotting with specific antibodies. (C) The relative ATF2-Thr71 phosphorylation of the vehicle and SB203580-treated lysates were quantified and plotted against the time of stimulation. (D) Serum-starved JNK-/- cells were treated with carrier or SB, FCS-stimulated for 10 minutes and lysed as described above. MAPKAPK-2 phosphorylation was determined by immunoblotting.

The onset of ATF2-Thr71 and ATF2-Thr69+71-phosphorylation associates with nuclear translocation of ERK1/2 and p38. Immunofluorescence experiments showed that phosphorylated ATF2 is localized in the nucleus and confirmed that the p38 inhibitor SB203580 abolished serum-induced phosphorylation of ATF2-Thr69+71, but not of ATF2-Thr71 (Figure 3).

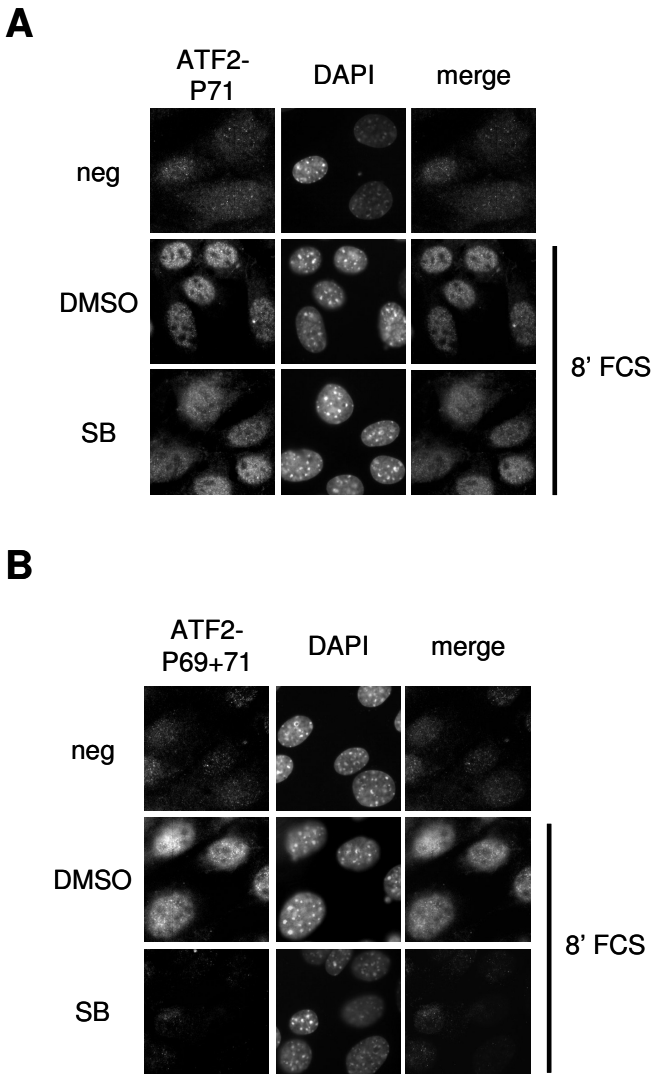

Figure 3. Serum-induced ATF2-Thr69+71, but not Thr71-phosphorylation is SB203580-sensitive in JNK-/- cells. Serum-starved JNK-/- cells were treated with SB203580 (SB) for 30 minutes prior to stimulation with 20% serum (FCS) for 8 minutes. Cells were fixed and stained with antibodies for (A) Thr71- or (B) Thr69+71-phosphorylated ATF2 followed by FITC-conjugated secondary antibodies (green). DNA was stained with DAPI (blue). Full-colour illustration can be found at page 122.

Serum stimulation of JNK1,2-/- cells induced the phosphorylation of both ERK1/2 and p38 within 2 minutes (Figure 4A). As the MAPkinases involved in ATF2-phosphorylation are simultaneously activated, their sequential role in ATF2-phosphorylation cannot simply be explained by sequential activation. Therefore, we determined if differences in nuclear appearance of ERK1/2 and p38 might determine the differential onset of ATF2-Thr71 and ATF2-Thr69+71 phosphorylation.

Using cell fractionation and immunofluorescence procedures, we found that within 2 minutes, serum induced the nuclear translocation of phosphorylated ERK1/2 (Figure 4B/5A) and that this was paralleled by the induction of ATF2-Thr71 phosphorylation (Figure 4B). Nuclear translocation of phosphorylated p38 was observed 4 minutes after serum addition and was paralleled by ATF2-Thr69+71 phosphorylation (Figure 4B/5A).

Purity of the cell fractions was checked by Western Blotting, using EF-1β and Lamin A antibodies as cytosolic and nuclear markers, respectively (Figure 4C).

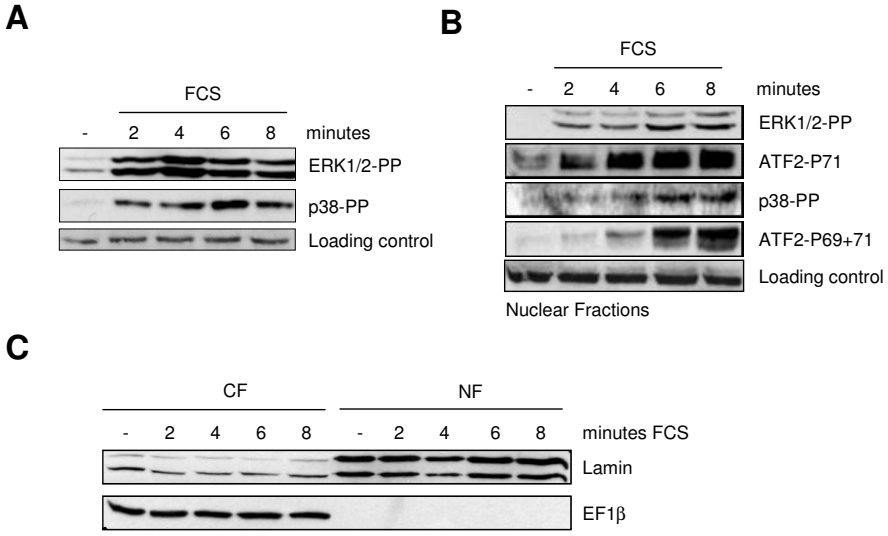

Figure 4. The onset of ATF2-Thr71 and ATF2-Thr69+71-phosphorylation coincides with the appearance of ERK1/2 and p38 in nuclear fractions (A) Lysates from serum-starved JNK-/- cells prepared at the indicated time points after FCS stimulation were examined for phosphorylation of ERK1/2 and p38 and ATF2-Thr71 and Thr69+71 by immunoblotting with phospho-specific antibodies as described. (B) Serum-starved JNK-/- cells were serum-stimulated as described, at the times indicated cellular fractions were prepared and the nuclear fractions examined for phosphorylation of ERK1/2 and p38 and ATF2-Thr71 and Thr69+71 by immunoblotting with phospho-specific antibodies as described. (C) Serum-starved JNK-/- cells were serum-stimulated as described, at the times indicated cellular fractions were prepared and the purity of both cytosolic (CF) and nuclear (NF) fractions was examined by immunoblotting with Elongation Factor (EF)-1 beta and Lamin A-specific antibodies.

Finally, the presence of SB203580 abrogated nuclear phospho-p38 immunoreactivity found in response to serum (Figure 5B) and severely reduced the serum-induced phospho-ATF2-Thr69+71 and phospho-p38 signals in nuclear extracts (Figure 5C).

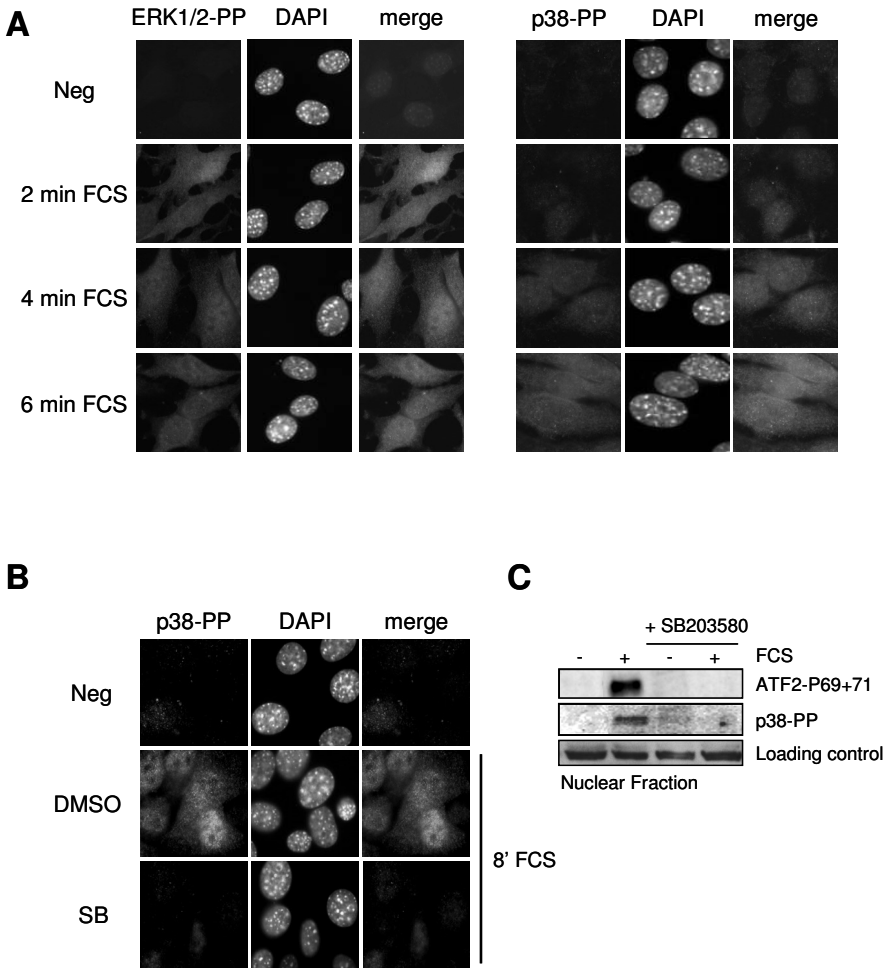

Figure 5. The onset of ATF2-Thr71 and ATF2-Thr69+71-phosphorylation associates with nuclear translocation of ERK1/2 and p38. (A) Serum-starved JNK-/- cells were stimulated with 20% serum (FCS) and fixed at the times indicated. The fixed cells were stained with antibodies for phospho-ERK1/2 (ERK1/2-PP) or phospho-p38 (p38-PP) followed by FITC-conjugated secondary antibodies (green). DNA was stained with DAPI (blue). (B) Serum-starved JNK-/- cells pre-treated with vehicle or SB203850 for 30 minutes prior to 8 minute FCS-stimulation were fixed and stained for phospho-p38 (p38-PP) as described above. (C) Serum-starved JNK-/- cells, pre-treated with vehicle or SB203850 were serum-stimulated for 8 minutes, after which cellular fractions were prepared and the nuclear fractions examined for p38- and ATF2-Thr69+71 phosphorylation by immunoblotting with phospho-specific antibodies as described. Full-colour illustration can be found at page 123.

Discussion

The present study identifies the MAP kinases ERK1/2 and p38 as the major growth factor-induced ATF2-directed kinases in JNK-/- cells and elucidates their role in two-step ATF2-phosphorylation mechanism in response to growth factors.

Using MonoQ anion exchange chromatography we found that, in JNK-/- cells, the major serum-induced ATF2-directed kinase activities co-purified with the ERK1/2 and p38 fractions (Figure 1A). MonoQ separation of EGF- or insulin-stimulated JNK-deficient cell lysates resulted in similar ATF2-kinase profiles (data not shown), suggesting that these kinases are involved in general mitogenic signaling towards ATF2.

The role of ERK1/2 and p38 in serum-stimulated ATF2 phosphorylation in JNK-deficient fibroblasts was further established by inhibitor studies: treatment of these cells with U0126 abolished the serum-induced ATF2-kinase activity in the ERK1/2-containing fraction and reduced the early ATF2 phosphorylation on Thr71 found in cell lysates (Figure 1 and 2) This suggests that ERK is the kinase responsible for the first phosphorylation of ATF2 on Thr71 in response to serum.

As ERK1/2 is incapable of phosphorylating ATF2 on Thr69 (13;17), cooperation with another kinase seems necessary for efficient ATF2-Thr69+71 phosphorylation. Our study identified p38 as the other ATF2-directed kinase in serum-treated JNK-/- cells. p38 is known to be capable of phosphorylating ATF2 on both Thr69 and 71 residues (13;17;18). In response to inducers of cellular stress the onset of ATF2-Thr69+71 coincides with the onset of ATF2-Thr71-phosphorylation and this process seems completely p38-dependent in JNK-deficient cells (13;17). This raises the question whether activation of p38 alone may be sufficient for the induction of ATF2-phosphorylation in response to serum. Our data suggest that ERK1/2 activation is biologically relevant for serum-induced two-step ATF2-phosphorylation. In contrast to ERK1/2, the activity of p38 is low in serum-stimulated fibroblasts and, therefore, insufficient to phosphorylate ATF2 Thr71 and/or Thr69 efficiently by itself. However, these low levels of active p38 are essential and appear to be sufficient to phosphorylate Thr69 when ATF2 is already mono-phosphorylated on Thr71 by ERK1/2. Furthermore, recombinant p38 was reported to phosphorylate GST-ATF2 via a double collision mechanism *in vitro* (19). After the first (random) phosphorylation event of ATF2 on Thr69 or Thr71, p38 dissociates from the mono-phosphorylated ATF2 substrate. It then re-associates with ATF2 for phosphorylation of the second threonine. Importantly, the efficiency of the second phosphorylation step is differentially affected by the two mono-phosphorylated forms of ATF2: whereas Thr71-phosphorylated ATF2 was readily phosphorylated on Thr69, ATF2 mono-phosphorylated on Thr69 was found to be an inefficient substrate for p38-mediated Thr71- phosphorylation. Thus, efficient phosphorylation of ATF2 by recombinant active p38 only occurs in the order Thr71 → Thr69+71. In our JNK-deficient system, phosphorylation of ATF2-Thr71 by ERK1/2 might prime ATF2 for subsequent efficient ATF2-Thr69-phosphorylation by p38. Accordingly, inhibiting p38 activity reduced the ATF2-directed activity present in p38-containing MonoQ fraction and abolished the serum-induced ATF2-Thr69 phosphorylation found in JNK-/- cell lysates (Figure 1, 2 and 3). These findings suggest that in these cells, ERK1/2 and p38 cooperate to efficiently phosphorylate ATF2 on Thr69 and Thr71.

Finally, localization studies using cell fractioning and immunofluorescence experiments showed that although ERK1/2 and p38 are activated simultaneously in response to serum in JNK-/- cells, the nuclear appearance of these kinases is different, with nuclear presence of ERK1/2 preceding p38. Notably, the nuclear appearance of ERK1/2 correlated with the ATF2-Thr71 phosphorylation, while nuclear translocation of p38

paralleled the detection of phospho-Thr69+71 ATF2. In addition, treatment of JNK-/- cells with SB203580, which abolished ATF2-Thr69+71 phosphorylation, also prevented nuclear appearance of phosphorylated p38. These results suggest that despite simultaneous activation of ERK1/2 and p38 by serum, their differential nuclear appearances can explain the differential kinetics of ATF2 phosphorylation.

The data presented in this study suggest that the serum-induced two-step mechanism of ATF2-phosphorylation in JNK-deficient cells is dependent on cooperation of ERK1/2 with p38. We propose that sequential nuclear appearance of these kinases is a determining factor driving this mechanism.

Materials and Methods

Cell culture and cell stimulation. JNK8 cells (JNK1 and 2 knockout embryonic fibroblasts) were cultured in Dulbecco's modified Eagle's medium (DMEM) containing 9% fetal bovine serum (FBS) and antibiotics. Before cell-stimulations, the cells were serum-starved (DMEM w/ 0.5% FBS) for 16h. When inhibitors were used, cells were pre-treated for 30 minutes with 2.5 μM SB203580 (Promega) or for 15 minutes with 10 μM U0126 (Promega), before addition of serum (FCS) to 20%.

Western blot analysis and antibodies. Whole cell lysates were prepared from 9 cm dishes that were rinsed twice with ice-cold phosphate-buffered saline (PBS) and lysed in 750 μl Laemmli sample buffer. Proteins were separated on polyacrylamide slab gels and transferred to Immobilon (Millipore). Blots were stained with Ponceau S before blocking to verify equal loading and appropriate protein transfer. Filters were incubated with antibodies as described previously (13). The antibodies used were: Lamin A and phospho-specific ATF2-Thr69+71, ATF2-Thr71, p38-Thr180/Tyr182, ERK1/2-Thr202/Tyr204 and MAPKAPK2-P (all polyclonal, Cell Signaling); p38 (N-20), ATF2 (C-19) and ERK1/21 (K-23) (Santa Cruz) and secondary antibodies: goat anti-rabbit and goat anti-mouse IgG–HRP conjugate (Promega). The Elongation Factor (EF)-1β antibody was described previously (20). The specificity of the phospho-specific ATF2 antibodies (P71 and P69+71) has been verified previously (13;17).

MonoQ/anion-exchange chromatography. Anion-exchange chromatography was performed essentially as described previously (13). Briefly, stimulated cells were scraped in MonoQ lysis buffer [20 mM Tris (pH 7.0), 0.27 M sucrose, 1 mM EDTA, 1 mM EGTA, 1% Triton X-100, 10 mM sodium β-glycerolphosphate, 50 mM NaF, 5 mM sodium pyrophosphate, 1 mM sodium orthovanadate, 0.1% (v/v) β-mercaptoethanol and Complete protease inhibitors (Roche Biochemicals)]. Lysates of six 9-cm dishes (~8000 mg protein) were diluted twofold with MonoQ buffer [50 mM Tris.Cl (pH 7.5), 1 mM EDTA, 1 mM EGTA, 5% (v/v) glycerol, 0.03% (w/v) Brij-35, 1 mM benzamidine, 0.3 mM sodium orthovanadate and 0.1% (v/v) β-mercaptoethanol] and applied to a MonoQ HR 5/5 column (Amersham Pharmacia Biotech) equilibrated in MonoQ buffer. After washing, the column was developed with a linear salt gradient to 700 mM NaCl in MonoQ buffer and fractions of 1 ml were collected. Aliquots of 10 μl from each fraction were used in *in vitro* ATF2 kinase assays.

Preparation of cellular fractions. For cell fractionation experiments, lysates were prepared from 9 cm dishes that were rinsed twice with ice-cold phosphate buffered saline (PBS) and scraped in 1 ml of cold RIPA buffer [30 mM Tris–HCl pH 7.5, 1mM EDTA, 150 mM NaCl, 0.5% Triton X-100, 0.5% Na-DOC, 1 mM sodium orthovanadate, 10 mM sodium fluoride and Complete protease inhibitors (Roche)]. Nuclei were pelleted by centrifugation

(10 min, 14000 rpm, 4°C). Supernatants were collected and stored as cytosolic fractions. Nuclear pellets were washed twice with RIPA and Laemmli buffer was added. Before western blotting nuclear samples were sonicated and boiled. Purity of the cell fractions was checked by Western Blotting, using EF-1β and Lamin A antibodies as cytosolic and nuclear markers, respectively (Figure 4C).

ATF2 kinase assays. For *in vitro* ATF2 kinase assays, equal volumes of MonoQ-fractions and equal amounts of protein from cytosolic or nuclear extracts were incubated at 30°C with 2 μg of purified GST-ATF2-N substrate (12) and 50 μM ATP in a total volume of 60 μl of kinase buffer [25 mM HEPES, pH 7.4, 25 mM MgCl2, 25 mM β-glycerolphosphate, 5 mM β-mercaptoethanol and 100 μM sodium orthovanadate]. When indicated, kinase assays were performed in the presence of vehicle (DMSO) or inhibitor SB203580 (2.5 μM). Reactions were terminated by the addition of 20 μl of 4x Laemmli buffer and subsequently analyzed by SDS–PAGE/immunoblotting with phospho-specific ATF2-Thr71 antibodies. Blots were quantitated using Scion Image software.

Immunofluorescence. Cells were grown on coverslips. After stimulation, cells were washed twice with ice-cold PBS and subsequently fixed in 3.7% formaldehyde in PBS for 15 minutes at room temperature. Coverslips were washed with Tris buffered saline [TBS; 25 mM Tris, 100 mM NaCl, 5 mM KCl, 0.7 mM $CaCl_2.2H_2O$, 0.5 $MgCl_2$.6H2O] and permeabilised for 5 minutes with 0.1% Triton X-100 in TBS, subsequently washed with 0.2% BSA/TBS, blocked for 30 minutes in 2% BSA/TBS at room temperature and then incubated overnight at 4°C with primary antibodies diluted 1:250 in 0.2% BSA/TBS. After 0.2% BSA/TBS washes, coverslips were incubated with appropriate secondary antibodies diluted 1:100 in 0.2% BSA/TBS for 2 hrs at room temperature. Thereafter coverslips were washed sequentially with 0.2% BSA/TBS and TBS, mounted in DAPI-containing Vectashield solution (Vector Laboratories) and fixed with nail polish. Fluorescence was detected using a Leica DM-RXA microscope. Pictures were acquired as color images (MERGE) and prepared using Photopaint and Coreldraw software.

References

1. Mayr, B. and Montminy, M. (2001) *Nat. Rev. Mol. Cell Biol.* **2,** 599-609
2. Hai, T. and Hartman, M. G. (2001) *Gene* **273,** 1-11
3. Hai, T. W., Liu, F., Coukos, W. J., and Green, M. R. (1989) *Genes Dev.* **3,** 2083-2090
4. Hai, T. and Curran, T. (1991) *Proc. Natl. Acad. Sci. U. S. A* **88,** 3720-3724
5. Bhoumik, A., Lopez-Bergami, P., and Ronai, Z. (2007) *Pigment Cell Res.* **20,** 498-506
6. Vlahopoulos, S. A., Logotheti, S., Mikas, D., Giarika, A., Gorgoulis, V., and Zoumpourlis, V. (2008) *Bioessays* **30,** 314-327
7. Li, X. Y. and Green, M. R. (1996) *Genes Dev.* **10,** 517-527
8. Sakurai, A., Maekawa, T., Sudo, T., Ishii, S., and Kishimoto, A. (1991) *Biochem. Biophys. Res. Commun.* **181,** 629-635
9. Sevilla, A., Santos, C. R., Vega, F. M., and Lazo, P. A. (2004) *J. Biol. Chem.* **279,** 27458-27465
10. Ban, N., Yamada, Y., Someya, Y., Ihara, Y., Adachi, T., Kubota, A., Watanabe, R., Kuroe, A., Inada, A., Miyawaki, K., Sunaga, Y., Shen, Z. P., Iwakura, T., Tsukiyama, K., Toyokuni, S., Tsuda, K., and Seino, Y. (2000) *Diabetes* **49,** 1142-1148
11. Livingstone, C., Patel, G., and Jones, N. (1995) *EMBO J.* **14,** 1785-1797
12. van Dam, H., Wilhelm, D., Herr, I., Steffen, A., Herrlich, P., and Angel, P. (1995) *EMBO J.* **14,** 1798-1811

13. Ouwens, D. M., De Ruiter, N. D., Van Der Zon, G. C., Carter, A. P., Schouten, J., Van Der Burgt, C., Kooistra, K., Bos, J. L., Maassen, J. A., and van Dam, H. (2002) *EMBO J.* **21,** 3782-3793
14. Favata, M. F., Horiuchi, K. Y., Manos, E. J., Daulerio, A. J., Stradley, D. A., Feeser, W. S., Van Dyk, D. E., Pitts, W. J., Earl, R. A., Hobbs, F., Copeland, R. A., Magolda, R. L., Scherle, P. A., and Trzaskos, J. M. (1998) *J. Biol. Chem.* **273,** 18623-18632
15. Cuenda, A., Rouse, J., Doza, Y. N., Meier, R., Cohen, P., Gallagher, T. F., Young, P. R., and Lee, J. C. (1995) *FEBS Lett.* **364,** 229-233
16. Rouse, J., Cohen, P., Trigon, S., Morange, M., Alonso-Llamazares, A., Zamanillo, D., Hunt, T., and Nebreda, A. R. (1994) *Cell* **78,** 1027-1037
17. Morton, S., Davis, R. J., and Cohen, P. (2004) *FEBS Lett.* **572,** 177-183
18. Raingeaud, J., Gupta, S., Rogers, J. S., Dickens, M., Han, J., Ulevitch, R. J., and Davis, R. J. (1995) *J. Biol. Chem.* **270,** 7420-7426
19. Waas, W. F., Lo, H. H., and Dalby, K. N. (2001) *J. Biol. Chem.* **276,** 5676-5684
20. Sanders, J., Brandsma, M., Janssen, G. M., Dijk, J., and Moller, W. (1996) *J. Cell Sci.* **109,** 1113-1117

4

The role of JNK, p38 and ERK MAP-kinases in insulin-induced Thr69 and Thr71-phosphorylation of transcription factor ATF2

Molecular Endocrinology (2006) 20(8): 1786-1795

Chapter 4

Chapter 4

The role of JNK, p38 and ERK MAP-kinases in insulin-induced Thr69 and Thr71-phosphorylation of transcription factor ATF2

Bart Baan, Hans van Dam, Gerard C.M. van der Zon, J. Antonie Maassen and D. Margriet Ouwens

From the Department of Molecular Cell Biology, Section Signal Transduction and Ageing, Leiden University Medical Centre, Leiden, The Netherlands

The stimulation of cells with physiological concentrations of insulin induces a variety of responses, like an increase in glucose uptake, induction of glycogen and protein synthesis, and gene expression. One of the determinants regulating insulin-mediated gene expression may be activating transcription factor 2 (ATF2). Insulin activates ATF2 by phosphorylation of Thr69 and Thr71 via a two-step mechanism, in which ATF2-Thr71-phosphorylation precedes the induction of ATF2-Thr69+71-phosphorylation by several minutes. We previously found that in JNK-/- fibroblasts cooperation of the ERK1/2 and p38-pathways is required for two-step ATF2-Thr69+71-phosphorylation in response to growth factors. As JNK is also capable of phosphorylating ATF2, we assessed the involvement of JNK, next to ERK1/2 and p38 in the insulin-induced two-step ATF2-phosphorylation in JNK-expressing A14 fibroblasts and 3T3L1-adipocytes. The induction of ATF2-Thr71-phosphorylation was sensitive to MEK1/2-inhibition with U0126 and this phosphorylation coincided with nuclear translocation of phosphorylated ERK1/2. Use of the JNK-inhibitor SP600125 or expression of dominant negative JNK-activator SEK1 prevented the induction of ATF2-Thr69+71-, but not ATF2-Thr71-phosphorylation by insulin. ATF2-dependent transcription was also sensitive to SP-treatment. Abrogation of p38-activation with SB203580 or expression of dominant negative MKK6 had no inhibitory effect on these events. In agreement with this, the onset of ATF2-Thr69+71-phosphorylation coincided with the nuclear translocation of phosphorylated JNK. Finally, *in vitro* kinase assays using nuclear extracts indicated that ERK1/2-preceded JNK-translocation. We conclude that sequential activation and nuclear appearance of ERK1/2 and JNK rather than p38 underlies the two-step insulin-induced ATF2-phosphorylation in JNK-expressing cells.

Insulin elicits complex responses in the body in order to maintain glucose and lipid homeostasis. Dependent on the target tissue, insulin regulates a variety of responses, including glucose uptake, glycogen, protein and lipid synthesis and gene expression. Next to the widely studied effects of insulin on the Forkhead/FOXO-transcription factors, also phosphorylation of activating transcription factor 2 (ATF2), may contribute to the effects of insulin on gene expression (1;2).

ATF2 is a ubiquitously expressed member of the cAMP-responsive element (CRE)-binding protein family of basic region-leucine zipper (bZIP) transcription factors also including CREB (3) and ATF3, ATF4, ATF6 and B-ATF (4;5). ATF2 can form homo- and heterodimers with other ATF-family members (5), but also with the activating protein-1 (AP-1) family member cJun (6). The various dimer compositions confer a large repertoire

of target genes on ATF2. Described ATF2 target-genes include cJun, cyclins A and D1, ATF3, Tumor Necrosis Factor α (TNFα) and peroxisome proliferator-activated receptor γ co-activator 1α (PGC1α) (7-13).

In the absence of stimuli, ATF2 is pre-bound to DNA (13;14) and held in an inactive conformation (15). Phosphorylation of residues within the activation domain leads to ATF2 transcriptional activation (16-18). In particular, phosphorylation of two threonine (Thr) residues, Thr69 and Thr71, seems to be required and sufficient for transcriptional activation of ATF2 (7;19).

We previously reported for mouse fibroblasts expressing the human insulin receptor that insulin induces ATF2-activation via phosphorylation of Thr69 and Thr71 via a two-step mechanism (2). Notably, this mechanism involves cooperation of two different pathways. Studies in JNK1,2 -/- embryonic fibroblasts indicated that the ERK1/2-pathway mediates the induction of ATF2-Thr71-phosphorylation, whereas induction of ATF2-Thr69-phosphorylation involves the activity of the p38-pathway (2).

However, JNK is expressed in most cell types and is known to be capable of phosphorylating ATF2 (7;19;20). In addition, purification of endogenous insulin-activated ATF2-kinases identified JNK, next to ERK and p38 as putative candidates (2). These observations prompted us to further determine the contribution of JNK, next to ERK1/2 and p38 in insulin-induced ATF2-phosphorylation in JNK-expressing A14 fibroblasts and 3T3L1 adipocytes. These cell-types were used as representatives of the two major types of insulin-responses: A14 cells respond primarily mitogenic, whereas 3T3L1 adipocytes respond more metabolically to insulin.

We studied *in vivo* and *in vitro* induction of ATF2-Thr71 and ATF2-Th69+71-phosphorylation at various time-points after insulin stimulation using pharmacological inhibitors of the JNK, ERK1/2 and p38-pathways as well as overexpression of dominant negative upstream kinases regulating the activity of JNK and p38. In addition, we examined the insulin-induced nuclear translocation of these kinases by immunofluorescence and assessed nuclear fractions for the presence of *in vitro* nuclear ATF2-kinase activity that could be ascribed to JNK, ERK1/2 or p38.

Results

Differential onset of insulin-induced ATF2-Thr71 and ATF2-Thr69+71-phosphorylation.

Insulin-treatment of A14 fibroblasts induced the phosphorylation of ATF2 on Thr71 within 2-4 minutes, while phosphorylation of ATF2-Thr69+71 was only achieved at 7-10 minutes after addition of insulin (Figure 1A). A comparable situation was found in 3T3L1 adipocytes, in which insulin-induced ATF2-Thr71–phosphorylation was found after 4 minutes and preceded the induction of ATF2-Thr69+71-phosphorylation (Figure 1B). In contrast, the induction of ATF2-Thr69+71-phosphorylation in response to osmotic shock (O.S.) was not preceded by ATF2-Thr71-phosphorylation (Figure 1C). The induction of ATF2-Thr69+71-phosphorylation was accompanied by a retarded mobility of the protein on ATF2-immunoblot, which was preceded by the induction of an intermediate form after 4 minutes of insulin-treatment (Figure 1D). The induction of this intermediate form coincided with the onset of ATF2-Thr71-phosphorylation and underscores the concept that in response to insulin-treatment the ATF2 protein undergoes a transition from the non-phosphorylated form to the ATF2-Thr69+71-phosphorylated form via an intermediate ATF2-Thr71-phosphorylated form.

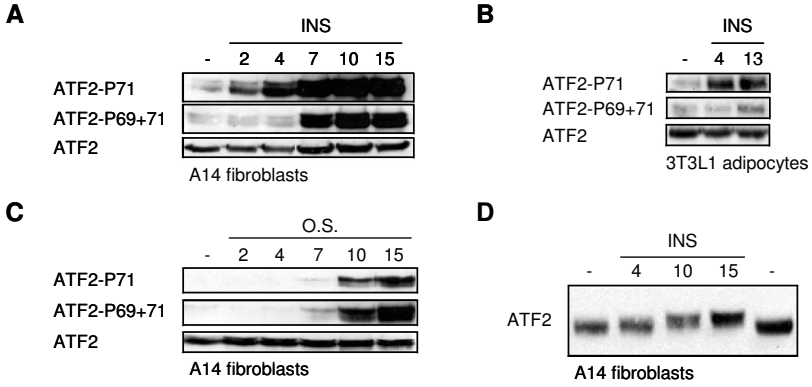

Figure 1. Differential onset of insulin-induced ATF2-Thr71 and ATF2-Thr69+71 phosphorylation. Serum-starved A14 cells (A) or 3T3L1 adipocytes (B) were treated with 10 nM insulin (INS). Total cell lysates were prepared at indicated time-points and analyzed by Western blotting using phospho-specific ATF2-Thr71, ATF2-Thr69+71 antibodies. The faster migrating bands recognized by the phospho-specific ATF2-antibodies seem to represent shorter, alternatively spliced, ATF2 products (2). (C) Cell lysates were prepared from A14 cells treated with 0.5 M NaCl (osmotic shock; O.S.) and immunoblotted as described for A and B. (D) Cell lysates prepared from insulin-treated A14 cells as described above were used for extended electrophoresis and subsequently blotted using ATF2-specific antibody.

Differential onset of insulin-induced MAPK-phosphorylation.

Upon examining the time-course of ERK1/2, p38 and JNK-activation in A14 fibroblasts, we found that ERK1/2 was phosphorylated within 2 minutes of insulin-treatment (Figure 2A). This phosphorylation was accompanied by *in vitro* ATF2-directed kinase activity in ERK-immunoprecipitates (Figure 2B). Also some phosphorylation of p38 and ATF2-directed kinase activity in p38-immunoprecipitates was observed within 2-4 minutes of insulin-treatment of A14 fibroblasts (Figures 2A and B).

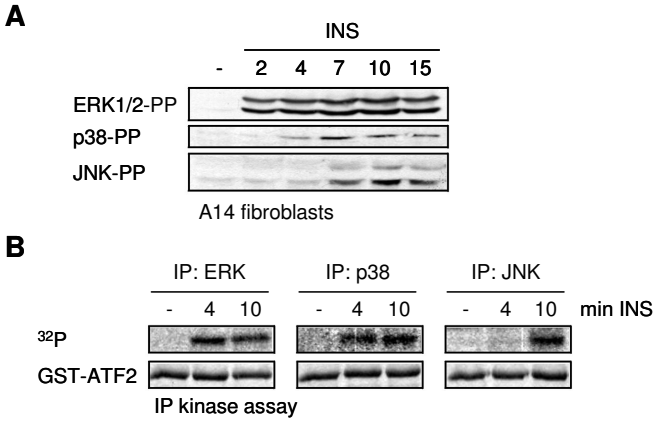

Figure 2. Time course of insulin-induced MAPK-phosphorylation. (A) Lysates from serum-starved A14 cells were prepared at the indicated time points after 10 nM insulin-treatment (INS) and were examined for phosphorylation of ERK1/2, p38 and JNK by immunoblotting with phospho-specific antibodies. (B) ERK1/2-, p38- and JNK-immunoprecipitates were analyzed for ATF2-directed kinase activity in an *in vitro* kinase using GST-ATF2 as substrate for 1hr. The Coomassie-stained gel confirmed equal loading of GST-ATF2.

The onset of JNK-phosphorylation was delayed compared to ERK- and p38-phosphorylation and was observed after 7 minutes of insulin-treatment. The phosphorylation associated with stimulation of ATF2-kinase activity in JNK-immunoprecipitates (Figure 2A and B).

Early insulin-induced ATF2-Thr71 phosphorylation is sensitive to inhibition of the MEK-ERK pathway. As both ERK1/2- and p38-activation coincided with the onset of ATF2-Thr71-phosphorylation, we analyzed the involvement of these MAPKs using pharmacological inhibitors in A14 fibroblasts. Inhibition of p38 using SB203580 (21) had no effect on the induction of ATF2-Thr71 phosphorylation by insulin (Figure 3A). However, prevention of ERK1/2-phosphorylation by the MEK1/2-inhibitor U0126 (22) completely abrogated the induction of ATF2-Thr71 phosphorylation (Figure 3A) and the appearance of the retarded (intermediate) form of ATF2 in response to 4 minutes insulin-treatment (data not shown). Comparable results were obtained in 3T3L1 adipocytes: U0126 prevented insulin-induced increase in ATF2-Thr71-phosphorylation, and pre-treatment with SB203580 had no inhibitory effect on insulin-induced ATF2-Thr71 phosphorylation (Figure 3B).

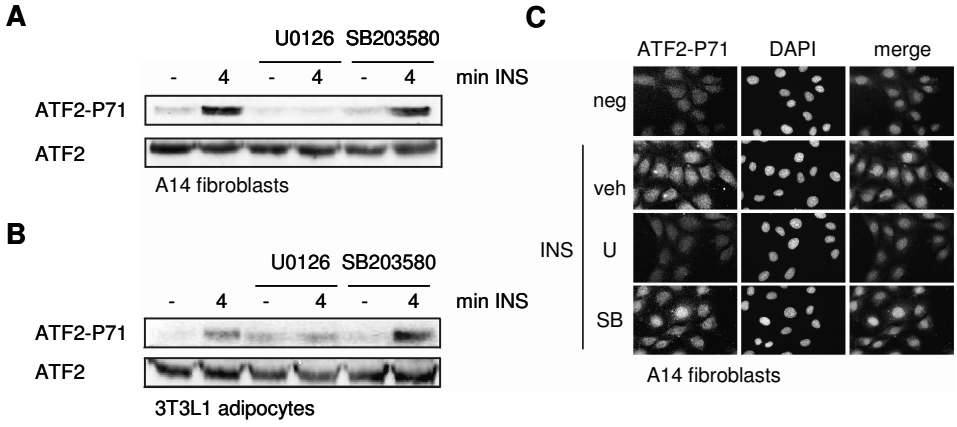

Figure 3. Early insulin-induced ATF2-Thr71 phosphorylation is sensitive to inhibition of the MEK1/2-ERK1/2 pathway. Serum-starved A14 cells (A) or 3T3L1 adipocytes (B) were incubated with 10 μM U0126 (U; 15 minutes) or 2.5 μM SB203580 (SB; 30 minutes) before insulin-stimulation (INS; 10 nM) for 4 minutes. Total ATF2 and ATF2-Thr71-phosphorylation levels were determined by immunoblotting with specific antibodies. (C) A14 cells were treated with inhibitors as described above, prior to stimulation with 10 nM of insulin for 4 minutes. Subsequently, cells were fixed and stained with phospho-specific ATF2-Thr71 antibodies followed by FITC-conjugated secondary antibodies (green). DNA was stained with DAPI (blue). Full-colour illustration can be found at page 124.

In line with these data, immunofluorescence experiments on A14 cells demonstrated nuclear phospho-ATF2-Thr71 immunoreactivity detected after 4 minutes of insulin-treatment, which was abolished upon pre-treatment with U0126, but not with SB203580 (Figure 3C). The nuclear localization of ATF2 did not change during the insulin-stimulation (data not shown). Collectively, these results suggest that ERK1/2, rather than p38 is responsible for the insulin-induced phosphorylation of nuclear ATF2 on Thr71 after 4 minutes of stimulation.

Cooperation of ERK1/2 with p38 or JNK is required for ATF2-Thr69+71-phosphorylation in vitro. When we analyzed lysates prepared from A14 cells treated for 4 minutes with insulin, predominantly ATF2-Thr71 directed kinase activity was found (Figure 4A). This is in line with the observation that ERK1/2 can only phosphorylate ATF2 on Thr71 and not on Thr69 (2;23). In lysates prepared after 15 minutes of insulin-stimulation, ATF2-Thr71 directed kinase activity was similar to that found in 4 min lysates, but the level of ATF2-Thr69+71 directed kinase activity was markedly increased (Figure 4A). To purify the kinase(s) responsible for the induction of ATF2-Thr69+71 phosphorylation, MonoQ fractionation was performed on lysates prepared after 15 min of insulin stimulation, and the obtained fractions were analyzed for the presence of ATF2-Thr71 directed versus ATF2-Thr69+71 directed kinase activity (2). Approximately 90% of the input ATF2-Thr71 directed kinase activity was recovered after anion-exchange chromatography, and the majority of this fraction (80%) co-purified with fractions, containing ERK1/2 (2). The remaining ATF2-Thr71 directed kinase activity was recovered in fractions co-purifying with JNK and p38 respectively (2). These fractions also contained ATF2-Thr69+71 directed kinase activity. However, in contrast to the almost complete recovery of ATF2-Thr71 directed kinase activity, only 5% of the input ATF2-Thr69+71 directed kinase activity was recovered in the fractions containing JNK and p38 (2). Comparable results were obtained for fractionation of lysates from 3T3L1 adipocytes (data not shown). Collectively, these findings raised the possibility that maximal induction of ATF2-Thr69+71-phosphorylation by insulin requires cooperation of ERK1/2 with p38 and/or JNK. To test this possibility, we added partially purified ERK1/2 to the kinase assays on fractions co-purifying with JNK and p38. Indeed, the weak insulin-induced ATF2-Thr71-directed and Thr69+71-directed kinase-activities co-purifying with p38 and JNK were greatly enhanced by addition of ERK1/2-fraction to the assay (Figure 4B). Similar results were obtained upon addition of recombinant ERK1/2 to the kinase assay (data not shown). Together, these findings suggest that phosphorylation of ATF2 on Thr69 by p38 and/or JNK is more efficient when ATF2 is already phosphorylated on Thr71, at least *in vitro*.

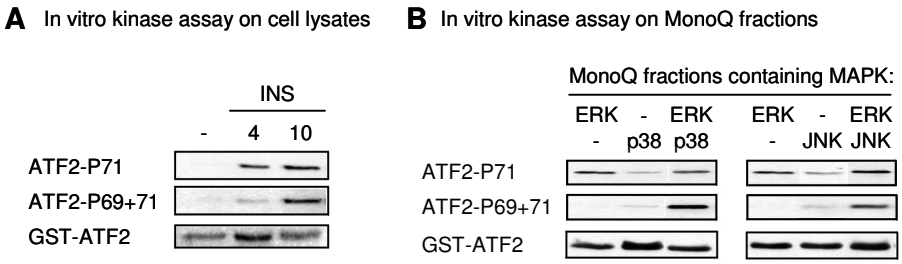

Figure 4. Cooperation of ERK1/2 with p38 or JNK is required for efficient insulin-induced ATF2-Thr69+71-phosphorylation. (A) Lysates from serum-starved A14 fibroblasts treated with 10 nM insulin (INS) for the indicated times were used in ATF2-directed *in vitro* kinase assays. Site-specific phosphorylation of GST-ATF2 was determined by Western blotting using ATF2-Thr71 and ATF2-Thr69+71 phospho-specific antibodies, respectively. (B) MAPK-containing MonoQ fractions of lysates of 15-minute insulin-treated serum-starved A14 cells were used in *in vitro* ATF2-directed kinase assays for 1hr. Site-specific phosphorylation of GST-ATF2 was determined as described above. Ponceau-staining of the same blot is shown to verify equal loading of GST-ATF2.

Inhibition of JNK, but not p38, abrogates insulin-induced ATF2-Thr69+71 phosphorylation and activation. To determine the involvement of p38 and JNK in insulin-induced phosphorylation of ATF2 in intact cells, we used SB203580 and SP600125 (24) to inhibit p38 and JNK, respectively. As shown in Figure 5A and 5B, insulin-induced ATF2-Thr69+71-phosphorylation was abrogated by SP600125, but not SB203580, in both A14 fibroblasts and 3T3L1 adipocytes. Notably, we observed some inhibition of ATF2-Thr71-phosphorylation by SP600125 even under conditions when JNK is not activated, i.e. under basal conditions and at 4 minutes after insulin addition, indicating non-specific side-effects of this inhibitor (Figure 5A). ATF2 band-shift analysis corroborated these results: the slowest migrating (Thr69+71 phosphorylated) form of ATF2 found after 10 minutes was not affected by SB203580, but shifted back to the intermediate form in the presence of SP600125 (Figure 5A).

Similar results were found with the use of dominant negative upstream kinases of p38 and JNK: MKK6-KM and SEK1-KR, respectively (see Figure 5C): Overexpression of SEK1-KR abrogated only the insulin-induced ATF2-Thr69+71 phosphorylation but not the Thr71-phosphorylation found after 15 minutes of insulin-stimulation. Overexpression of MKK6-KM had no effect on insulin-induced ATF2-phosphorylation (Figure 5C).

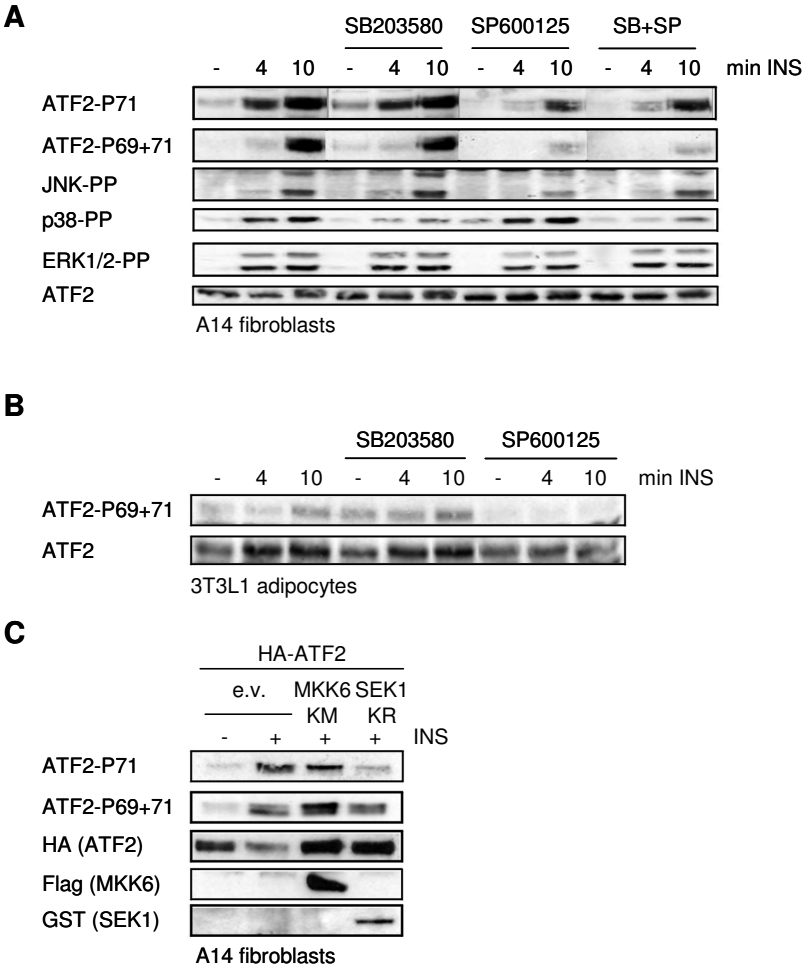

Figure 5. Inhibition of JNK, but not p38, abrogates insulin-induced ATF2-Thr69+71 phosphorylation. Serum-starved A14 fibroblasts (A) or 3T3L1 adipocytes (B) were incubated for 30 minutes with DMSO, 2.5 μM SB203580 (SB), 10 μM SP600125 (SP) or SB+SP prior to stimulation with 10 nM insulin (INS) for the indicated times. Phosphorylation of ATF2-Thr71, ATF2-Thr69+71, JNK, p38 and ERK1/2 was determined with phospho-specific antibodies. (C) A14 fibroblasts were transfected with either an empty vector (e.v.) or expression vectors for epitope-tagged dominant negative MKK6-KM or SEK1-KR together with pBabe-puro and pMT2-HA-ATF2. Puromycin-resistant cells were selected, serum-starved overnight and subsequently stimulated with 10 nM insulin for 15 minutes. Phosphorylation of ATF2-Thr71, ATF2-Thr69+71 was determined with phospho-specific antibodies.

Immunofluorescence experiments showed that 10 minutes of insulin-treatment increased nuclear ATF2-Thr69+71 immunoreactivity compared to 4 minutes and untreated A14 cells, and that this immunoreactivity was sensitive to SP600125 (Figure 6A).

To determine whether modulation of insulin-induced ATF2-Thr69+71-phosphorylation affected ATF2-mediated transcription accordingly, we examined the insulin-induced activation of a GAL4-ATF2-dependent luciferase reporter. Insulin-induced activation was significantly inhibited by SP600125 (P=0.0097), but not by SB203580 (Figure 6B).

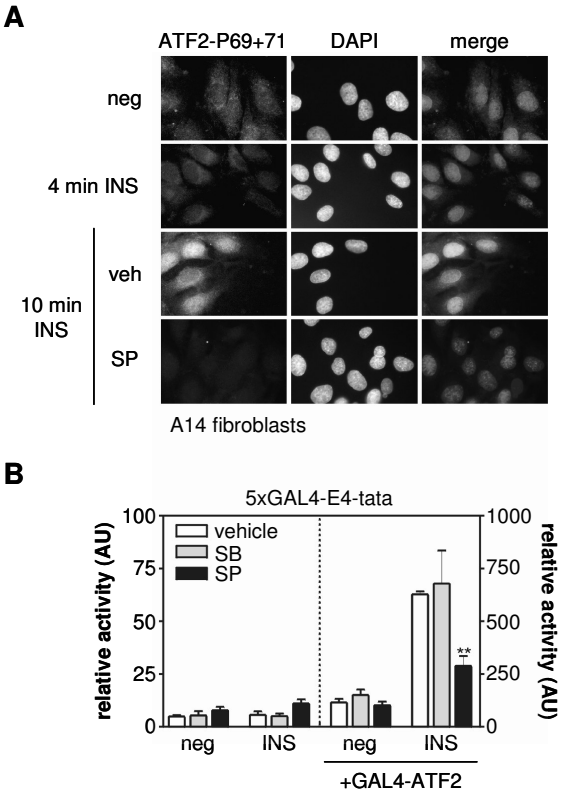

Figure 6. Inhibition of JNK, but not p38, abrogates the insulin-induced ATF2-phosphorylation and activation. (A) Serum-starved A14 cells were treated with inhibitors as described above prior to stimulation with 10 nM insulin (INS) for the indicated times. Cells were fixed and stained with antibodies for Thr69+71-phosphorylated ATF2 followed by FITC-conjugated secondary antibodies (green). DNA was stained with DAPI (blue). (B) Insulin-induced ATF2 transcriptional activity was examined in a GAL4-dependent luciferase reporter assay using the activation domain of ATF2 fused to the GAL4 DNA binding domain (19). Cells were transiently transfected and grown for 8 hours, subsequently serum-starved in DMEM containing 0.5% FBS O/N and treated for 30 minutes with vehicle or inhibitors SB203580 or SP600125 before adding insulin (INS; 10 nM). Cells were lysed 16 hrs later and luciferase activity was determined. The relative firefly luciferase activity is depicted as the mean enhancement of promoter activity in the absence or presence of insulin and/or inhibitors +/- the SD of three independent experiments performed in triplicates. Note the different scaling of the left and right *y*-axis. ** P = 0.0097 in a Student t-test. Full-colour illustration can be found at page 125.

The onset of ATF2-Thr71 and ATF2-Thr69+71-phosphorylation associates with nuclear translocation of ERK1/2 and JNK. The experiments described above suggest that cooperation of ERK1/2 with JNK, rather than with p38, is required for insulin-induced two-step ATF2-Thr69+71-phosphorylation. To corroborate these findings we examined whether ERK1/2 and JNK translocate to the nucleus in response to insulin. We found that within 4 minutes, insulin induced the phosphorylation and nuclear translocation of ERK1/2 (ERK1/2-PP; See Figure 7A). U0126 pre-treatment strongly inhibited the ERK1/2-PP signal and reduced nuclear staining found with a pan-ERK1/2 antibody (Figure 7A and data not shown).

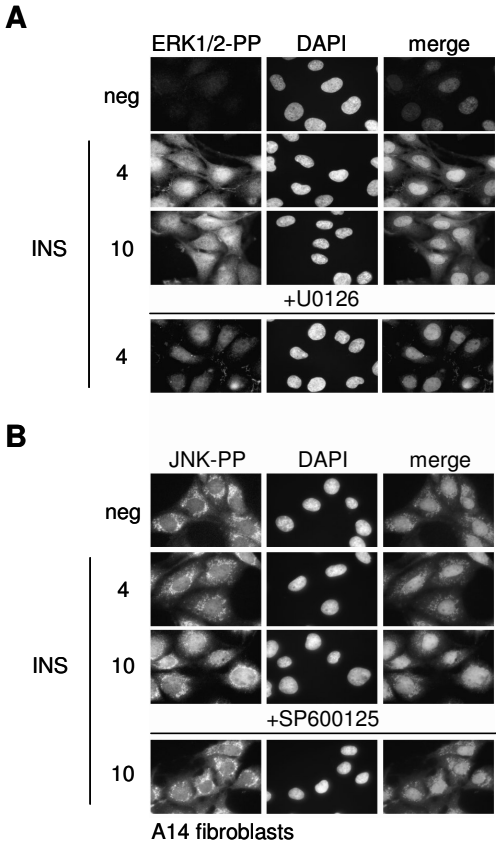

Figure 7. Time course of nuclear translocation of ERK1/2 and JNK. Serum-starved A14 cells were incubated with DMSO, 10 μM U0126 (U) for 15 minutes or 10 μM SP600125 (SP) for 30 minutes prior to stimulation with 10 nM insulin (INS) for the indicated times. Cells were fixed and stained with antibodies for (A) phosphorylated ERK (ERK-PP) or (B) phosphorylated JNK (JNK-PP) and FITC-conjugated secondary antibodies (green). DNA was stained with DAPI (blue). Full-colour illustration can be found at page 126.

Despite the high a-specific background-level of (non-nuclear) phosphorylated JNK (JNK-PP)-signal in the absence of insulin, no increase in JNK-PP staining could be detected after 4 minutes of insulin-treatment (Figure 7B). The amount of JNK-PP in the nucleus was substantially increased after 10 minutes of insulin-stimulation and this response was inhibited by SP600125 (Figure 7B).

In line with the immunofluorescence data, we found that nuclear extracts prepared from cells after 4 minutes of insulin stimulation contained predominantly ATF2-Thr71-directed kinase activity (Figure 8A). This ATF2-Thr71-directed activity could be abrogated by addition of ERK-inhibitor 5-iodotubercidin (Itu (25)) and was absent in nuclear extracts from U0126-treated cells (data not shown). The ATF2-Thr71-directed kinase activity in these nuclear extracts was not affected by SP600125 or SB203580 (Figure 8A).

Nuclear extracts obtained after 10 minutes of insulin-stimulation contained both ATF2-Thr71- and ATF2-Thr69+71-directed kinase activity (Figure 8B). Addition of the JNK-inhibitor SP600125 only abrogated the ATF2-Thr69+71-phosphorylation, but not the ATF2-Thr71-directed activity (Figure 8B). SB203580 did not affect the ATF2-Thr69+71 and ATF2-Thr71 activities, whereas Itu reduced both ATF2-Thr71- and ATF2-Thr69+71 kinase activities.

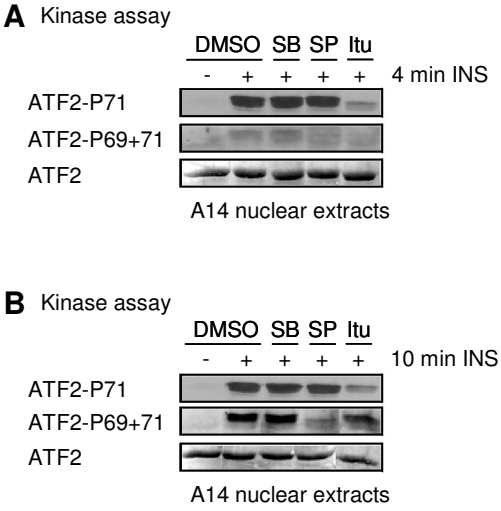

Figure 8. Sequential appearance of ERK1/2- and JNK-dependent ATF2-directed nuclear kinase activities. Serum-starved A14 cells stimulated with 10 nM insulin for 4 minutes (A) or 10 minutes (B). Nuclear proteins were extracted and used in *in vitro* ATF2-directed kinase assays for 2 hrs in the presence of DMSO or inhibitors 2.5 μM SB203580 (SB), 5 μM SP600125 (SP) or 5 μM 5-iodotubercidin (Itu). Site-specific phosphorylation of GST-ATF2 was determined by Western blotting using ATF2-Thr71 and ATF2-Thr69+71 phospho-specific antibodies. Ponceau-staining of the same blot is shown to verify of equal loading of GST-ATF2.

Discussion

The present study addresses the activation of the transcription factor ATF2 by insulin. It extends our previous findings (2) by addressing the mechanism via which insulin accomplishes this activation in A14 cells and 3T3L1 adipocytes. The results of this study suggest the following model for the induction of ATF2-Thr69+71 phosphorylation in response to insulin (summarized in Figure 9): within 2-4 minutes, insulin induces activation of ERK1/2, which translocates to the nucleus and mediates ATF2-Thr71-phosphorylation. Between 5-10 minutes after the addition of insulin, JNK is activated, translocates to the nucleus and mediates Thr69-phosphorylation of phospho-Thr71-ATF2, thereby activating the transcription factor. We propose that the sequential activation and subsequent nuclear appearance of ERK1/2 and JNK are rate limiting for the two-step phosphorylation of ATF2-Thr69+71 in response to insulin.

Previously, we reported that in JNK-/- cells, the ERK1/2- and the p38-pathways cooperate in the growth factor-induced phosphorylation of ATF2-Thr69+71 (2). Although this study indicates that JNK may be dispensable for insulin-mediated ATF2-phosphorylation, pharmacological inhibition of p38 in JNK-expressing cells had no inhibitory effect on the induction ATF2-phosphorylation, suggesting that JNK rather than p38 regulates this response.

Accordingly, various studies have identified JNK as a bona fide ATF2-kinase (2;7;19;20;23). An important finding of the present study, however, is that JNK predominantly functions as ATF2-Thr69-kinase for ATF2 already phosphorylated on Thr71, in the proposed two-step ATF2-Thr69+71 phosphorylation-mechanism induced by insulin. In contrast, in response to inducers of cellular stress like UV, methyl methane sulphonate (MMS), osmotic shock and TNFα, the onset of ATF2-Thr69+71 coincides with the onset of ATF2-Thr71-phosphorylation, and this process seems completely JNK-dependent in JNK-expressing cells (2;7;23 and data not shown).

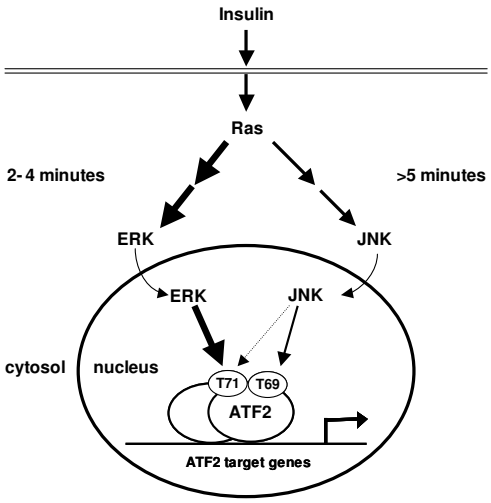

Figure 9. Proposed model for insulin-induced ATF2-activation in A14 cells and 3T3L1 adipocytes. Insulin induces activation of ERK1/2 within 2-4 minutes. ERK1/2 subsequently translocates to the nucleus, where it mediates ATF2-Thr71-phosphorylation. Subsequently JNK is activated, translocates to the nucleus and efficiently phosphorylates Thr71-phosphorylated ATF2 on Thr69, thus inducing transcriptional activation of ATF2.

This raises the question whether activation of JNK alone may be sufficient for the induction of ATF2-phosphorylation in response to insulin-treatment. However, the data shown here are indicative that also ERK1/2 activation seems to biologically relevant for insulin-mediated two-step ATF2-phosphorylation. Biochemical evidence for its involvement is provided by changes in electrophoretic mobility of the ATF2 protein during the course of insulin-mediated phosphorylation. After insulin stimulation, the ATF2-protein undergoes a transition via an ATF2-Thr71 phosphorylated form to an ATF2-Thr69+71 phosphorylated form. More importantly, pharmacological inhibition of ERK-activation prevented early ATF2-Thr71 phosphorylation and the accompanying retarded mobility of the protein. In addition, ERK1/2- and ATF2-Thr71-phosphorylation are found several minutes before JNK-activation and ATF2-Thr69+71 phosphorylation were detectable. Collectively, these findings highlight the importance of ERK1/2 for insulin-induced ATF2-phosphorylation and provide support for our model.

We and others have demonstrated that ERK preferentially phosphorylates ATF2 on Thr71, whereas the kinase seems incapable to efficiently mediate ATF2-Thr69 phosphorylation (2;23). Therefore, cooperation with another kinase seems required for induction of ATF2-Thr69+71 phosphorylation in response to insulin. Interestingly, while MonoQ fractionation of lysates from osmotic-shock treated cells yielded similar recoveries for ATF2-Thr69+71 and ATF2-Thr71 directed kinase activities, in cell extracts from insulin-treated cells, only ~5% of the ATF2-Thr69+71 directed *in vitro* kinase activity was recovered, in contrast to ~80% recovery of ATF2-Thr71 directed activity (for details see reference (2)) Importantly, the weak insulin-induced ATF2-Thr69+71 kinase activities, which co-purified with JNK and p38 respectively, were greatly enhanced by the addition of ERK1/2 to the kinase reaction. Collectively, these findings strongly suggest that insulin-activated MAP kinases cooperate to induce efficient ATF2-Thr69+71 phosphorylation and provide strong support for our two-step model.

Previously, Waas and coworkers (26) found that recombinant active p38 phosphorylates GST-ATF2 via a two-step (double collision) mechanism, involving the dissociation of mono-phosphorylated Thr71-ATF2 or Thr69-ATF2 from the enzyme after the first phosphorylation step. Importantly, these authors found that mono-phosphorylation of ATF2-Thr69 strongly reduces the phosphorylation rate of Thr71, whereas, mono-phosphorylation of Thr71 does not reduce the rate of Thr69 phosphorylation (26). Thus, efficient phosphorylation of ATF2 by recombinant active p38 only occurs in the order Thr71 → Thr69+71. In our model, phosphorylation of ATF2-Thr71 by ERK1/2 might prime ATF2 for subsequent efficient ATF2-Thr69-phosphorylation. As described above, the kinase assays on MonoQ fractions indicate that both p38 and JNK can indeed enhance the phosphorylation of ATF2-Thr69+71 in the presence of activated ERK1/2 *in vitro*. In cultured cell lines expressing both kinases, however, JNK rather than p38 seems to mediate this second phosphorylation. Several lines of evidence point in this direction: First, chemical inhibition of JNK-activity with SP600125, or prevention of JNK-activation by overexpression of dominant negative SEK1 abrogated only the Thr69+71-phosphorylation in response to insulin. Second, prevention of p38-activation by overexpression of dominant negative MKK6 or inhibition of p38 by SB203580 failed to affect insulin-mediated ATF2-phosphorylation in JNK-expressing cells. In part, the absence of the inhibitory effect of SB could be ascribed to an enhanced activation of JNK which was observed in the presence of this inhibitor ((2) see also Figure 5 and Supplementary Figure S1). However, simultaneous addition of SB203580 and SP600125 had the same effect as SP600125 alone, suggesting

that this is not the case. In addition, we could not obtain evidence for nuclear translocation of activated p38 in insulin-treated cells neither in immunofluorescence assays nor in *in vitro* kinase assays on nuclear extracts.

To exclude the possibility that SB203580 was unable to inhibit p38, we analyzed inhibition of p38-activity by SB203580 *in vitro* and *in vivo*. In *in vitro* kinase assays the SB-compound completely abrogated ATF2-directed kinase activity found in p38-containing MonoQ-fractions of insulin-stimulated A14 fibroblasts (data not shown). Also, we found that phosphorylation of p38's downstream nuclear target MAPKAPK2 (MK2 (27)) in response to insulin in JNK-/- cells was sensitive to SB203580-treatment (data not shown). Interestingly, although in A14 fibroblasts p38-activity was induced by insulin and reduced by SB203580-treatment, no MK2-phosphorylation could be detected in these cells (Figure S1). In contrast, O.S. did induce robust phosphorylation of both p38 and MK2, which were reduced and abrogated, respectively by SB203580-treatment (Figure S1). These observations suggest that the SB203580-compound was functional in *in vitro* and *in vivo* assays. In addition, it seems that in JNK-containing A14 cells, insulin-induced phospho-p38 is confined to the cytosol or does not reach its nuclear target MK2, while it does after O.S.-stimulation.

Collectively, these data support the idea that JNK rather than p38 is responsible for the second phosphorylation event, and that p38 seems only capable of inducing ATF2-phosphorylation under conditions that JNK is genetically absent.

Materials and Methods

Cell culture and cell stimulation. A14 cells (NIH 3T3 fibroblasts overexpressing the human insulin receptor (28)) were cultured in Dulbecco's modified Eagle's medium (DMEM) containing 9% fetal bovine serum (FBS) and antibiotics. 3T3L1 fibroblasts were obtained from ATCC and differentiated to adipocytes as described (29). Briefly, 3T3L1 cells were grown to confluence. Two days post-confluence, differentiation was induced by culturing cells for 2 days on DMEM/FBS supplemented with 10 µg/ml of bovine insulin (Sigma), 0.25 µM dexamethasone (Sigma) and 0.5 mM 3-isobutyl-1-methylxanthine (Sigma), followed by DMEM/FBS containing only insulin (10 µg/ml). Differentiated adipocytes were maintained for another 6 days in DMEM/FBS prior to use. Before cell-stimulations, the cells were serum-starved (DMEM w/ 0.5% FBS) for 16h. When inhibitors were used, cells were pre-treated for 30 minutes with 10 µM SP600125 (Biomol) or 2.5 µM SB203580 (Promega) or for 15 minutes with 10 µM U0126 (Promega), before addition of bovine insulin to 10 nM or NaCl (osmotic stress; O.S.) to 500 mM.

Transient transfection and luciferase assays. For overexpression experiments, A14 cells were co-transfected in 6 well plates with a total of 1.5 µg of DNA per well; 0.875 µg of either a carrier vector or expression vectors encoding epitope-tagged dominant negative MKK6-K82M or SEK1-K129R (kindly provided by Dr J. Kyriakis), 0.5 µg pMT2-HA-ATF2 (2) and 0.125 µg pBabe-puro using FUGENE6 transfection reagent (Roche) according to suppliers protocol. Cells were selected with 3 µg/ml of puromycin (Sigma) for 3-5 days, after which cells were serum-starved overnight, stimulated with 10 nM insulin for 15 minutes and lysed and blotted as described above.

For GAL4-luciferase assays, A14 cells were transfected in 6 well plates using the DEAE–dextran method as described (30). For each well 0.25 µg pGl3-GAL4-E4-luciferase reporter (2) was co-transfected with 1 µg of carrier vector psp64 and 1 µg of either pC2-Gal4-ATF2-TAD (19) or the carrier vector. Briefly, DNA was mixed in 1 mg/ml DEAE-

dextran-supplemented TBS [25 mM Tris; pH 7.4, 150 mM NaCl, 5 mM KCl, 0.7 mM $CaCl_2$ and 0.5 mM $MgCl_2$] and added to cells. After a 30-minute incubation, cells were washed and DMEM/FBS was added. After 8 hours, cells were serum-starved in DMEM containing 0.5% FBS and 24 hours after transfection cells were pre-treated with inhibitors before adding insulin (to 10 nM). 16 hours later, cells were lysed in luciferase lysis buffer [25 mM Tris, pH 7.8, 2 mM dithiotreitol, 2 mM 1,2-diaminocyclohexane-*N,N,N',N'*-tetraacetic acid, 10% glycerol and 1% Triton X-100] and luciferase activity was determined according to the manufacturer's protocol (Promega).

Western blot analysis and antibodies. Whole cell lysates were prepared from 9 cm dishes that were rinsed twice with ice-cold phosphate-buffered saline (PBS) and lysed in 750 µl Laemmli sample buffer. Proteins were separated on polyacrylamide slab gels and transferred to Immobilon (Millipore). Blots were stained with Ponceau S before blocking to verify equal loading and appropriate protein transfer. Filters were incubated with antibodies as described previously (2). The antibodies used were: Lamin A and phospho-specific ATF2-Thr69+71, ATF2-Thr71, p38-Thr180/Tyr182, ERK1/2-Thr202/Tyr204 (all polyclonal) and JNK-Thr183/Tyr185 monoclonal (all from Cell Signaling Technology); p38 (N-20), ATF2 (C-19) and ERK1 (K-23) (Santa Cruz) and secondary antibodies: goat anti-rabbit and goat anti-mouse IgG–HRP conjugate (Promega). The total JNK and EF-1β antibodies were described previously (2;31). For ATF2 band shift analysis, immunoblots were prepared after separation of proteins on large 7% polyacrylamide slab gels, and incubated with ATF2 (C-19) antibody.

MonoQ/anion-exchange chromatography. Anion-exchange chromatography was performed essentially as described previously (2). Briefly, stimulated cells were scraped in MonoQ lysis buffer [20 mM Tris (pH 7.0), 0.27 M sucrose, 1 mM EDTA, 1 mM EGTA, 1% Triton X-100, 10 mM sodium β-glycerolphosphate, 50 mM NaF, 5 mM sodium pyrophosphate, 1 mM sodium orthovanadate, 0.1% (v/v) β-mercaptoethanol and Complete protease inhibitors (Roche Biochemicals)]. Lysates of six 9-cm dishes (~8000 mg protein) were diluted twofold with MonoQ buffer [50 mM Tris.Cl (pH 7.5), 1 mM EDTA, 1 mM EGTA, 5% (v/v) glycerol, 0.03% (w/v) Brij-35, 1 mM benzamidine, 0.3 mM sodium orthovanadate, and 0.1% (v/v) β-mercaptoethanol] and applied to a MonoQ HR 5/5 column (Amersham Pharmacia Biotech) equilibrated in MonoQ buffer. After washing, the column was developed with a linear salt gradient to 700 mM NaCl in MonoQ buffer and fractions of 1 ml were collected. Aliquots of 10 µl from each fraction were used in *in vitro* ATF2 kinase assays.

Preparation of nuclear extracts. For extraction of nuclear proteins, cell lysates were prepared from 9 cm dishes that were rinsed twice with ice-cold phosphate buffered saline (PBS) and scraped in 1 ml of cold RIPA buffer [30 mM Tris–HCl pH 7.5, 1mM EDTA, 150 mM NaCl, 0.5% Triton X-100, 0.5% Na-DOC, 1 mM sodium orthovanadate, 10 mM sodium fluoride and Complete protease inhibitors (Roche)]. Nuclei were pelleted by centrifugation (10 min, 14000 rpm, 4°C). Supernatants were collected and stored as cytosolic fractions. Nuclear pellets were washed twice with RIPA and were then incubated on ice for 1hr with 75 µl of extraction buffer [30 mM Tris-HCl pH 7.5, 300 mM NaCl, 1 mM EDTA with Complete protease inhibitors (Roche)] and vortexed every 5 min. After centrifugation, supernatants were collected and used as nuclear protein extracts. Protein content was determined using the BCA-kit (Pierce). Purity of the cell fractions was checked by Western Blotting, using EF-1β and Lamin A antibodies as cytosolic and nuclear markers, respectively (see supplementary Figure S2).

ATF2 kinase assays. For *in vitro* ATF2 kinase assays, equal volumes of MonoQ-fractions and equal amounts of protein from cytosolic or nuclear extracts were incubated at 30°C with 2 μg of purified GST-ATF2-N substrate (7) and 50 μM ATP in a total volume of 60 μl of kinase buffer [25 mM HEPES, pH 7.4, 25 mM MgCl2, 25 mM β-glycerolphosphate, 5 mM β-mercaptoethanol and 100 μM sodium orthovanadate]. When indicated, kinase assays were performed in the presence of vehicle (DMSO) or inhibitors SB203580 (2.5 μM), SP600125 (5 μM) or iodotubercidin (Itu;5 μM (25)). Reactions were terminated by the addition of 20 μl of 4x Laemmli buffer and subsequently analyzed by SDS–PAGE/immunoblotting with phospho-specific ATF2-Thr69+71 and ATF2-Thr71 antibodies. The specificity of these antibodies has been verified previously (2;23).

For immunoprecipitation kinase assays, RIPA cell lysates were prepared as described above and equal aliquots (750 μg) were nutated overnight with 10 μl of p38, JNK, or ERK antibodies coupled to protein A-sepharose beads (Pharmacia) at 4°C. The antibodies used for immunoprecipitation were: ERK 2199 (32), p38 N20 (Santa Cruz) and JNK1 FL (Santa Cruz). Beads were collected by centrifugation and were washed four times with RIPA buffer, and two times with kinase buffer. Subsequently, the beads were incubated with 2 μg of purified GST-ATF2-N substrate (7) and 50 μM ATP, containing 2 μCi [γ-^{32}P]ATP, in a total volume of 60 μl of kinase buffer for 1 at 30°C.

Immunofluorescence. Cells were grown on coverslips. After stimulation, cells were washed twice with ice-cold PBS and subsequently fixed in 3.7% formaldehyde in PBS for 15 minutes at room temperature. Coverslips were washed with Tris buffered saline [TBS; 25 mM Tris, 100 mM NaCl, 5 mM KCl, 0.7 mM $CaCl_2.2H_2O$, 0.5 $MgCl_2.6H2O$] and permeabilised for 5 minutes with 0.1% Triton X-100 in TBS, subsequently washed with 0.2% BSA/TBS, blocked for 30 minutes in 2% BSA/TBS at room temperature and then incubated overnight at 4°C with primary antibodies diluted 1:250 in 0.2% BSA/TBS. After 0.2% BSA/TBS washes, coverslips were incubated with appropriate secondary antibodies diluted 1:100 in 0.2% BSA/TBS for 2 hrs at room temperature. Thereafter coverslips were washed sequentially with 0.2% BSA/TBS and TBS, mounted in DAPI-containing Vectashield solution (Vector Laboratories) and fixed with nail polish. Fluorescence was detected using a Leica DM-RXA microscope. Pictures were acquired as color images (MERGE) and prepared using Photopaint and Coreldraw software.

References

1. Accili D, Arden KC 2004 FoxOs at the crossroads of cellular metabolism, differentiation, and transformation. Cell 117:421-426
2. Ouwens DM, De Ruiter ND, Van Der Zon GC, Carter AP, Schouten J, Van Der Burgt C, Kooistra K, Bos JL, Maassen JA, van Dam H 2002 Growth factors can activate ATF2 via a two-step mechanism: phosphorylation of Thr71 through the Ras-MEK-ERK pathway and of Thr69 through RalGDS-Src-p38. EMBO J 21:3782-3793
3. Mayr B, Montminy M 2001 Transcriptional regulation by the phosphorylation-dependent factor CREB. Nat Rev Mol Cell Biol 2:599-609
4. Hai T, Hartman MG 2001 The molecular biology and nomenclature of the activating transcription factor/cAMP responsive element binding family of transcription factors: activating transcription factor proteins and homeostasis. Gene 273:1-11
5. Hai TW, Liu F, Coukos WJ, Green MR 1989 Transcription factor ATF cDNA clones: an extensive family of leucine zipper proteins able to selectively form DNA-binding heterodimers. Genes Dev 3:2083-2090

6. Hai T, Curran T 1991 Cross-family dimerization of transcription factors Fos/Jun and ATF/CREB alters DNA binding specificity. Proc Natl Acad Sci USA 88:3720-3724
7. van Dam H, Wilhelm D, Herr I, Steffen A, Herrlich P, Angel P 1995 ATF-2 is preferentially activated by stress-activated protein kinases to mediate c-jun induction in response to genotoxic agents. EMBO J 14:1798-1811
8. Shimizu M, Nomura Y, Suzuki H, Ichikawa E, Takeuchi A, Suzuki M, Nakamura T, Nakajima T, Oda K 1998 Activation of the rat cyclin A promoter by ATF2 and Jun family members and its suppression by ATF4. Exp Cell Res 239:93-103
9. Beier F, Lee RJ, Taylor AC, Pestell RG, LuValle P 1999 Identification of the cyclin D1 gene as a target of activating transcription factor 2 in chondrocytes. Proc Natl Acad Sci U S A 96:1433-1438
10. Kool J, Hamdi M, Cornelissen-Steijger P, van der Eb AJ, Terleth C, van Dam H 2003 Induction of ATF3 by ionizing radiation is mediated via a signaling pathway that includes ATM, Nibrin1, stress-induced MAPkinases and ATF-2. Oncogene 22:4235-4242
11. Tsai EY, Jain J, Pesavento PA, Rao A, Goldfeld AE 1996 Tumor necrosis factor alpha gene regulation in activated T cells involves ATF-2/Jun and NFATp. Mol Cell Biol 16:459-467
12. Cao W, Daniel KW, Robidoux J, Puigserver P, Medvedev AV, Bai X, Floering LM, Spiegelman BM, Collins S 2004 p38 Mitogen-Activated Protein Kinase Is the Central Regulator of Cyclic AMP-Dependent Transcription of the Brown Fat Uncoupling Protein 1 Gene. Mol Cell Biol 24:3057-3067
13. Hayakawa J, Mittal S, Wang Y, Korkmaz KS, Adamson E, English C, Omichi M, McClelland M, Mercola D 2004 Identification of Promoters Bound by c-Jun/ATF2 during Rapid Large-Scale Gene Activation following Genotoxic Stress. Mol Cell 16:521-535
14. Herr I, van Dam H, Angel P 1994 Binding of promoter-associated AP-1 is not altered during induction and subsequent repression of the c-jun promoter by TPA and UV irradiation. Carcinogenesis 15:1105-1113
15. Li XY, Green MR 1996 Intramolecular inhibition of activating transcription factor-2 function by its DNA-binding domain. Genes Dev 10:517-527
16. Sakurai A, Maekawa T, Sudo T, Ishii S, Kishimoto A 1991 Phosphorylation of cAMP response element-binding protein, CRE-BP1, by cAMP-dependent protein kinase and protein kinase C. Biochem Biophys Res Commun 181:629-635
17. Sevilla A, Santos CR, Vega FM, Lazo PA 2004 Human vaccinia-related kinase 1 (VRK1) activates the ATF2 transcriptional activity by novel phosphorylation on Thr-73 and Ser-62 and cooperates with JNK. J Biol Chem 279:27458-27465
18. Ban N, Yamada Y, Someya Y, Ihara Y, Adachi T, Kubota A, Watanabe R, Kuroe A, Inada A, Miyawaki K, Sunaga Y, Shen ZP, Iwakura T, Tsukiyama K, Toyokuni S, Tsuda K, Seino Y 2000 Activating transcription factor-2 is a positive regulator in CaM kinase IV-induced human insulin gene expression. Diabetes 49:1142-1148
19. Livingstone C, Patel G, Jones N 1995 ATF-2 contains a phosphorylation-dependent transcriptional activation domain. EMBO J 14:1785-1797
20. Gupta S, Campbell D, Derijard B, Davis RJ 1995 Transcription factor ATF2 regulation by the JNK signal transduction pathway. Science 267:389-393

21. Cuenda A, Rouse J, Doza YN, Meier R, Cohen P, Gallagher TF, Young PR, Lee JC 1995 SB 203580 is a specific inhibitor of a MAP kinase homologue which is stimulated by cellular stresses and interleukin-1. FEBS Lett 364:229-233
22. Favata MF, Horiuchi KY, Manos EJ, Daulerio AJ, Stradley DA, Feeser WS, Van Dyk DE, Pitts WJ, Earl RA, Hobbs F, Copeland RA, Magolda RL, Scherle PA, Trzaskos JM 1998 Identification of a novel inhibitor of mitogen-activated protein kinase kinase. J Biol Chem 273:18623-18632
23. Morton S, Davis RJ, Cohen P 2004 Signalling pathways involved in multisite phosphorylation of the transcription factor ATF-2. FEBS Lett 572:177-183
24. Bennett BL, Sasaki DT, Murray BW, O'Leary EC, Sakata ST, Xu W, Leisten JC, Motiwala A, Pierce S, Satoh Y, Bhagwat SS, Manning AM, Anderson DW 2001 SP600125, an anthrapyrazolone inhibitor of Jun N-terminal kinase. Proc Natl Acad Sci U S A 98:13681-13686
25. Fox T, Coll JT, Xie X, Ford PJ, Germann UA, Porter MD, Pazhanisamy S, Fleming MA, Galullo V, Su MS, Wilson KP 1998 A single amino acid substitution makes ERK2 susceptible to pyridinyl imidazole inhibitors of p38 MAP kinase. Protein Sci 7:2249-2255
26. Waas WF, Lo HH, Dalby KN 2001 The kinetic mechanism of the dual phosphorylation of the ATF2 transcription factor by p38 mitogen-activated protein (MAP) kinase alpha. Implications for signal/response profiles of MAP kinase pathways. J Biol Chem 276:5676-5684
27. Ben Levy R, Hooper S, Wilson R, Paterson HF, Marshall CJ 1998 Nuclear export of the stress-activated protein kinase p38 mediated by its substrate MAPKAP kinase-2. Curr Biol 8:1049-1057
28. Burgering BM, Medema RH, Maassen JA, van de Wetering ML, van der Eb AJ, McCormick F, Bos JL 1991 Insulin stimulation of gene expression mediated by p21ras activation. EMBO J 10:1103-1109
29. van den Berghe N, Ouwens DM, Maassen JA, van Mackelenbergh MG, Sips HC, Krans HM 1994 Activation of the Ras/mitogen-activated protein kinase signaling pathway alone is not sufficient to induce glucose uptake in 3T3-L1 adipocytes. Mol Cell Biol 14:2372-2377
30. Angel P, Hattori K, Smeal T, Karin M 1988 The jun proto-oncogene is positively autoregulated by its product, Jun/AP-1. Cell 55:875-885
31. Sanders J, Brandsma M, Janssen GM, Dijk J, Moller W 1996 Immunofluorescence studies of human fibroblasts demonstrate the presence of the complex of elongation factor-1 beta gamma delta in the endoplasmic reticulum. J Cell Sci 109:1113-1117
32. Pronk GJ, Vries-Smits AM, Ellis C, Bos JL 1993 Complex formation between the p21ras GTPase-activating protein and phosphoproteins p62 and p190 is independent of p21ras signalling. Oncogene 8:2773-2780

Supplemental figures to Chapter 4

S1

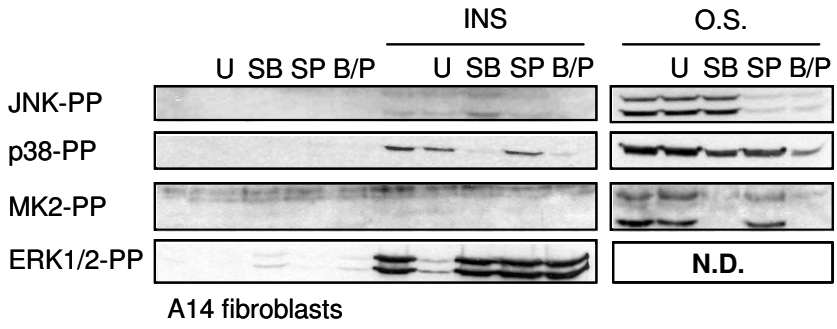

SUPPL. FIG S1. Serum-starved A14 cells were treated with DMSO or 10 µM U0126 (U; 15 minutes), 2.5 µM SB203580 (SB; 30 minutes), 10 µM SP600125 (SP; 30 minutes) or SB and SP (B/P; 30 minutes) prior to 15 minute-treatments with 10 nM insulin (INS) or osmotic shock (O.S.; 0.5M NaCl). Cell lysates were prepared and analyzed with antibodies specific for phosphorylated JNK, p38, MAPKAPK2 (MK2) and ERK. N.D. is not determined.

S2

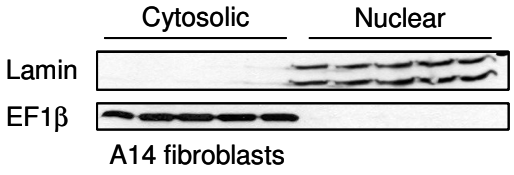

SUPPL. FIG. S2. Crude cell fractions were prepared from serum-starved, insulin-stimulated A14 fibroblasts as described in Materials and Methods. Cytosolic and nuclear fractions were immunoblotted using EF-1β and Lamin A antibodies as cytosolic and nuclear markers, respectively. No cytosolic leak could be detected in the nuclear pellets used for protein extraction.

5

Identification of insulin-regulated ATF2-target genes in 3T3L1 adipocytes and A14 fibroblasts

Manuscript in preparation

Chapter 5

Chapter 5

Identification of insulin-regulated ATF2-target genes in 3T3L1 adipocytes and A14 fibroblasts

Bart Baan[1], Terrence A.T. Wanga[1], Gerard C.M. van der Zon[1], J. Antonie Maassen[2] and D. Margriet Ouwens[1]

From the [1]Department of Molecular Cell Biology, Leiden University Medical Centre, Leiden, [2]Department of Endocrinology/Diabetes Centre, VU University Medical Centre, Amsterdam, the Netherlands

Activating transcription factor 2 (ATF2) is strongly associated with the response to inducers of cellular stress, like viral infection and DNA damage. However, ATF2 has also been identified as a component of insulin signalling, both *in vitro and in vivo*. Studies in mouse and Drosophila have linked ATF2 to the regulation of glucose and lipid metabolism via induction of PPARγ coactivator 1α (PGC1α) and phosphoenolpyruvatecarboxykinase (PEPCK) expression. This study aimed at detailing the role of ATF2 in insulin action and metabolic control through the characterization of ATF2 target genes in insulin-sensitive cell lines. Therefore, we analyzed the expression of 16 putative ATF2-target genes by real-time PCR in 3T3L1 adipocytes and A14 cells. Using the JNK-inhibitor SP600125, which abrogates the induction of ATF2 phosphorylation by insulin, and shRNA-mediated silencing of the ATF2 gene, we identified ATF3, *c-jun*, Egr1, MKP1, and SREBP1c as insulin-induced ATF2-dependent genes. Furthermore, we found that the induction of adiponectin by insulin is JNK-dependent.

Activating transcription factor 2 (ATF2), a ubiquitously expressed member of the cAMP-responsive element binding protein family of basic region leucine-zipper transcription factors, has been implicated in multiple responses in mammalian cells by regulating the expression of a broad spectrum of target genes (1-3). Among the ATF2 target genes are cell cycle regulators (cyclin A, cyclin D1), proteins related with invasion (MMP2, UPA), cell adhesion molecules (E-selectin, P-selectin, and VCAM), anti-apoptotic factors (Bcl-2), transcription factors (*c-jun*, ATF3, CHOP, *c-fos*, junB), growth factor receptors and cytokines (PDGFRα, IL8, Fas ligand, TNFα, IL1β, and IL6), and proteins engaged in the response to endoplasmic reticulum (ER) stress and DNA damage (Grp78,ATM, XPA) (1-4). The nature of these target genes indicates a key role for ATF2 in oncogenesis and protection against cellular stress and DNA damage.

Activation of ATF2, however, is not confined to inducers of cellular stress. Also insulin has been shown to activate ATF2 *in vitro* and *in vivo* (5-8). Moreover, ATF2 has been implicated in the regulation of proteins involved in metabolic control, including expression of PPARγ coactivator 1α (PGC1α) in brown adipose tissue (9) and phosphoenolpyruvate carboxykinase (PEPCK) in the liver and white adipose tissue (10-12). Finally, selective ablation of ATF2 in the Drosophila fat body, the fly equivalent of mammalian liver and adipose tissue, not only confirms ATF2 regulation of PEPCK expression, but also identifies ATF2 as critical regulator of lipid metabolism (13).

Collectively, these findings strongly suggest that ATF2 also has an important function in the regulation of metabolic control by insulin.

To detail the role of ATF2 in insulin action, the present study aimed to characterize insulin-regulated ATF2 target genes in 3T3L1 adipocytes and A14 fibroblasts. We used real-time PCR to examine the effects of insulin on the expression of 16 putative ATF2 targets identified in previous studies (1;3;4). To validate these genes as bona fide ATF2 targets, the expression of the insulin-regulated genes was subsequently studied following treatment with the JNK-inhibitor SP600125, which abrogates insulin-mediated ATF2 phosphorylation (5), and after shRNA-mediated silencing of the ATF2 gene.

Results

Regulation of gene expression by insulin. Using real-time PCR, we examined the effect of insulin on the expression 16 putative ATF2-target genes in 3T3L1 adipocytes. The candidate genes, which are listed in Table 1, were selected on the basis of previous studies and have regulatory functions in insulin action and lipid metabolism. Adiponectin was included as potential ATF2 target gene based on a promoter analysis, which identified two potential cyclic AMP response elements (CRE), the binding site for ATF2, at position -3177 (TGACGTAA) and -335 (TGACGTCC), respectively.

Table 1. Potential ATF2 target genes

Target	References	Role in insulin action & metabolism
Transcriptional regulators		
ATF3	(1;3;20)	apoptosis
FOXO3a	(4)	metabolic gene expression
c-jun	(1;3;4)	proliferation
CREB1	(1;3)	metabolic gene expression
Egr1	(4)	proliferation
HIF1α	(4)	Angiogenesis
PGC1α	(9)	metabolic gene expression
PPARα	(4)	metabolic gene expression
SREBP1c	(4)	lipid metabolism
Hormones		
adiponectin		positive regulation insulin action
IGF2	(4)	adipocyte function
IGFBP6	(4)	
IL1β	(1;21)	β-cell destruction, inflammation
TNFα	(21)	inhibition of insulin signalling
Metabolic enzymes		
MKP1	(4;49)	inhibition of insulin signalling
PEPCK	(10;11;13)	gluconeogenesis, glyceroneogenesis

Figure 1 shows that a 30 min incubation with insulin increased the expression of 7 genes (adiponectin, ATF3, *c-jun*, Egr1, IGFBP6, MKP1, and PEPCK), lowered the levels of 3 genes (FOXO3a, IGF2, PPARα), and did not affect the abundance of 4 genes (CREB1, HIF1α, PGC1α, and SREBP1c) in 3T3L1 adipocytes. No reproducible data were obtained for IL1β and TNFα. Except for ATF3, all insulin-mediated alterations in gene expression,

both positive and negative, were transient. Compared to 30 min of insulin incubation, the levels of *c-jun* and Egr1 were lower after 60 min exposure to insulin, or had returned to basal level in the case of adiponectin, IGFBP6, MKP1, and PEPCK (Figure 1).

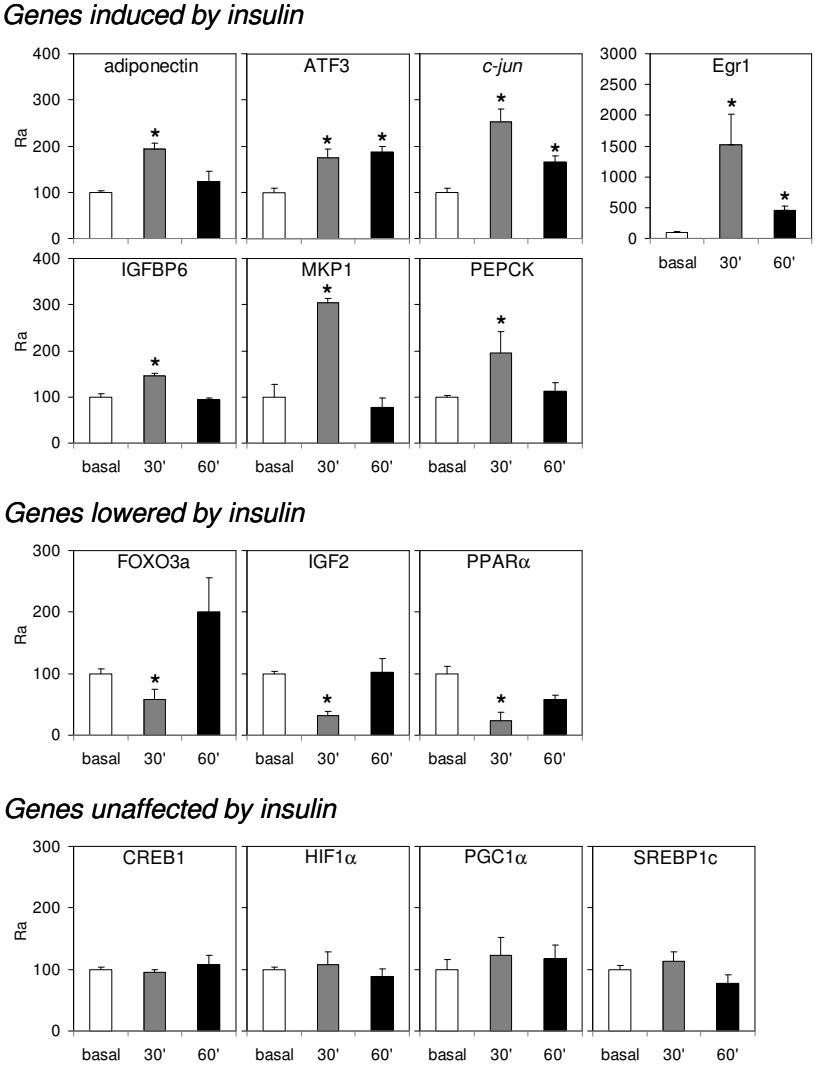

Figure 1. Regulation of gene expression by insulin in 3T3L1 adipocytes. Serum-starved 3T3L1 adipocytes were kept untreated (basal; open bars), or stimulated for 30 min (30'; grey bars) or 60 min (60'; black bars) with 10 nM insulin. Gene expression levels were determined by real-time PCR. The relative mRNA abundance (Ra) in untreated cells was set at 100. Data are mean ± SEM of 3 independent experiments performed in duplicate. *, $P<0.05$ versus basal.

We used A14 cells to substantiate the insulin-mediated induction of putative ATF2-target genes. Compared to 3T3L1 adipocytes, insulin increased the mRNA levels of ATF3, *c-jun*, Egr1 and MKP1 in A14 cells (Figure 2). Only in A14 cells, insulin also induced HIF1α and SREBP1c mRNA (Figure 2). The levels of CREB1, IGFBP6, and PGC1α were either lowered or unaffected by insulin (Figure 2). We did not determine the abundance of adiponectin and PPARα, as these metabolic genes are not expressed in A14 cells, and failed to obtain reproducible results for IGF2, IL1β, TNFα, and FOXO3a. Finally, whereas the insulin effects in 3T3L1 adipocytes were transient, the increases in gene expression in A14 fibroblasts were more linear in time (Figure 2).

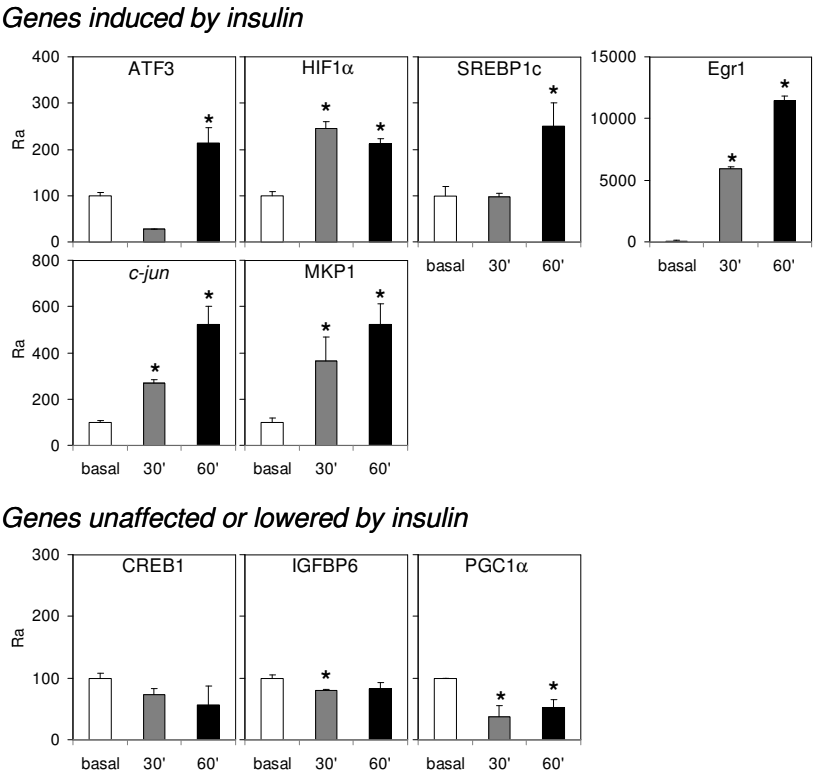

Figure 2. Regulation of gene expression by insulin in A14 fibroblasts. Serum-starved A14 cells were kept untreated (basal; open bars), or stimulated for 30 min (30'; grey bars) or 60 min (60'; black bars) with 10 nM insulin. Gene expression levels were determined by real-time PCR. The relative mRNA abundance (Ra) in untreated cells was set at 100. Data are mean ± SEM of 3 independent experiments performed in duplicate. *, $P<0.05$ versus basal.

Inhibition of JNK abrogates insulin-mediated gene induction in 3T3L1 adipocytes and A14 cells. We have previously shown that the JNK inhibitor SP600125 blocks insulin-mediated ATF2 activation (5). Therefore, we used SP600125 to ascribe the induction of the insulin-regulated genes to activation of the JNK/ATF2-pathway. As shown in Figure 3, SP600125 completely abrogated insulin-induced ATF2-Thr69 phosphorylation both in 3T3L1 adipocytes and A14 fibroblasts (Figure 3) without significantly affecting other components of insulin action, like PKB-S473 phosphorylation and the ERK1/2-dependent ATF2-Thr71 phosphorylation (Figure 3).

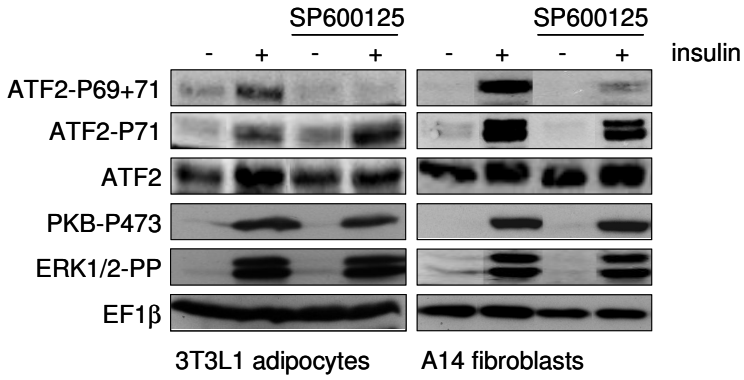

Figure 3. Effect of SP600125 on ATF2-phosphorylation and insulin signalling. Serum-starved 3T3L1 adipocytes and A14 fibroblasts were treated with DMSO or SP600125 (10 μM) for 30 min prior to stimulation with 10 nM insulin. Total cell lysates were prepared after 15 minutes and analyzed by Western blotting using phospho-specific ATF2-Thr71, ATF2-Thr69+71 and total ATF2 antibodies or phospho-specific antibodies directed against PKB-P473 and ERK1/2- P202/204. Equal loading was confirmed using an EF1β antibody.

In 3T3L1 adipocytes, SP600125 blocked the induction of adiponectin, ATF3, c-jun, Egr1, and MKP1, but not of IGFBP6 and PEPCK, mRNA by 30 min insulin treatment (Figure 4A). Similarly, in A14 cells, SP600125 significantly blunted the increase in c-jun, Egr1, MKP1, HIF1α and SREBP1c mRNA by 60 min of insulin exposure (Figure 4B). Thus, the insulin-mediated induction of ATF3, c-jun, Egr1, HIF1α, MKP1, and SREBP1c, but not PEPCK and IGFBP6, requires activation of the JNK/ATF2-pathway.

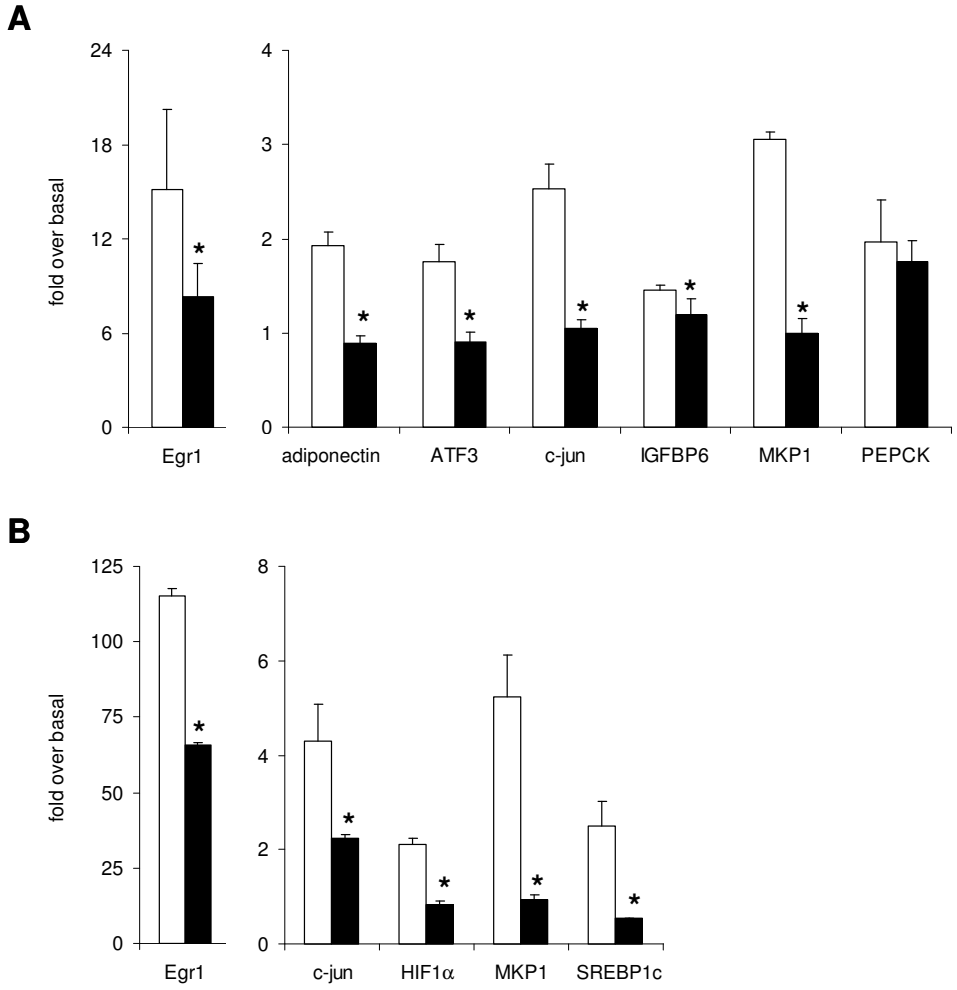

Figure 4. Inhibition of insulin-mediated gene expression by SP600125. Serum-starved 3T3L1 adipocytes (A) and A14 fibroblasts (B) were treated with DMSO (open bars) or with 10 μM SP600125 (black bars) for 30 min prior to stimulation with 10 nM insulin for 30 min (3T3L1 adipocytes) or 60 min (A14 cells). Gene expression levels were determined by real-time PCR. The effect of insulin is expressed as fold over basal. Data are mean ± SEM of 3 independent experiments performed in duplicate. *, $P<0.05$ versus DMSO.

ATF2 silencing and insulin-mediated gene induction in A14 fibroblasts. Next, we examined the effect of silencing of the ATF2 gene on insulin-mediated gene induction in A14 fibroblasts. Expression of mATF2#1 or mATF2#2 downregulated ATF2 mRNA levels by 70 and 82 %, respectively when compared to cells transfected with pSuper (Figure 5A). ATF2 silencing also resulted in an almost complete knock-down of ATF2 protein expression, but did not significantly interfere with the phosphorylation of PKB-S473 and ERK1/2 in response to insulin (Figure 5B).

Figure 5C shows that silencing of the ATF2 gene blunted the insulin-mediated induction of ATF3, Egr1, MKP1, and SREBP1c mRNA, and to a lesser extent *c-jun* mRNA. We did not observe induction of HIF1α by insulin in A14 cells transfected with pSuper (Figure 5C).

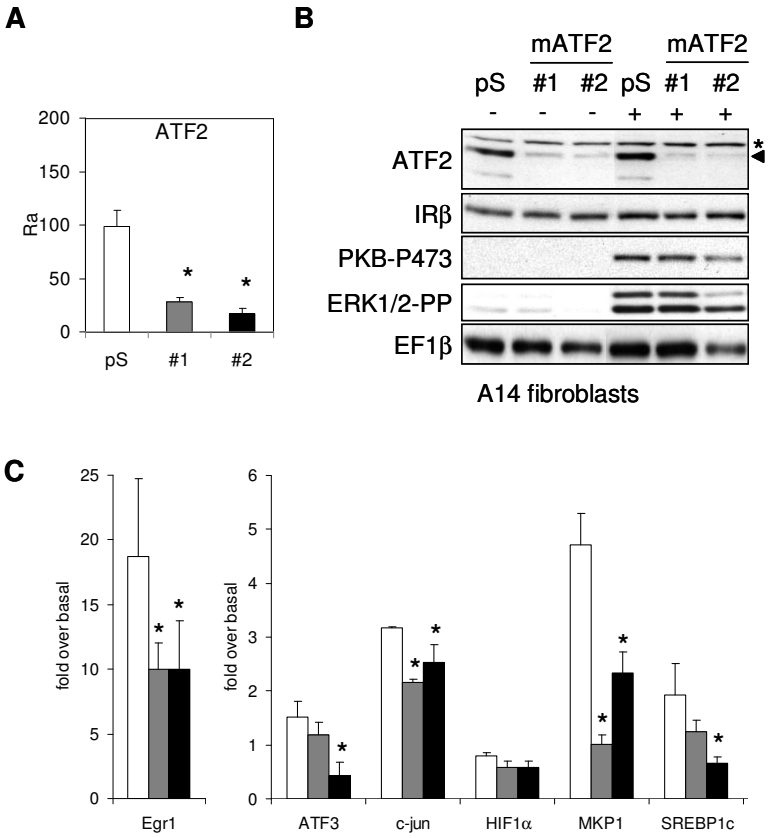

Figure 5. Effect of ATF2 silencing on insulin signalling and insulin-mediated gene expression. A14 cells were transfected with pSuper (pS) or ATF2-specific shRNA (#1 and #2). A. Effect of ATF2 silencing on relative ATF2 mRNA abundance (Ra). Data are mean± SEM of 2 independent experiments performed in duplicate. *, $P<0.05$ versus pSuper. B. Western blot analysis of cells kept untreated (-) or stimulated for 15 min with 10 nM insulin (+) using antibodies for ATF2, phospho-specific antibodies directed against PKB-P473 and ERK1/2- P202/204. Equal loading was confirmed using insulin receptor β-subunit and EF1β antibodies. * marks a background band C. Relative mRNA abundance (Ra) of ATF2 target genes in A14 cells transfected with pSuper (open bars), mATF2#1 (grey bars) or mATF2#2 (black bars). The effect of 60 min incubation with 10 nM insulin is expressed as fold over basal. Data are mean ± SEM of 2 independent experiments performed in duplicate. *, $P<0.05$ versus pSuper.

Thus, in A14 cells, ATF2 contributes to the induction of ATF3, *c-jun*, Egr1, MKP1, and SREBP1c mRNA by insulin.

Discussion

To detail the role of ATF2 activation in insulin action and metabolic control, insulin-regulated ATF2-dependent genes were characterized in both 3T3L1 adipocytes and A14 fibroblasts. The terminally differentiated 3T3L1 adipocytes display metabolic responses, like insulin-mediated glucose uptake, triglyceride synthesis, and inhibition of lipolysis (14-16), as well as secretion of adipokines (17). A limitation of 3T3L1 adipocytes is that both conventional gene transfer methods, like transient transfections, and lentivirus-mediated delivery of shRNA-constructs are inefficient in this cell type. To circumvent this problem, we also included A14 fibroblasts in this study. These cells respond to insulin in a more 'mitogenic' manner, such as induction of the immediate early genes *c-jun* and *c-fos*, and DNA synthesis (18;19). Both cell types were exposed to insulin for 30-60 min, not only to reduce secondary responses, but also because ATF2 activation and *c-jun* induction occur within 4-10 min and 30-60 min after the addition of insulin, respectively (5;8;19).

Potential ATF2 target genes were selected on the basis of a promoter analysis for CRE-binding sites, or previous studies (1;3;4;10;11;13;20;21). For a number of selected genes ATF3, *c-jun*, Egr1, MKP1, and SREBP1c, the mRNA levels were increased by insulin, and this induction was blunted both by the JNK-inhibitor SP600125 and by silencing of the ATF2 gene. In 3T3L1 adipocytes, we also found that the insulin-mediated induction of adiponectin was inhibited by SP600125. As this gene is not expressed in A14 fibroblasts, we could not validate this finding using shRNAs. Activation of luciferase reporter constructs fused to the adiponectin promoter by ATF2-VP16, a hybrid protein in which the potent transactivation domain of the viral transactivator VP16 is fused to the carboxyl terminus of ATF2 (22), or chromatin immunoprecipitation assays, could further detail a role for ATF2 in the regulation of adiponectin.

Although previous studies have identified PEPCK, PGC1α, IL1β, and TNFα (1;9-11;13;21) as ATF2-target genes, we could not confirm a role for ATF2 in the regulation of these genes by insulin in A14 cells and/or 3T3L1 adipocytes. In the case of IL1β and TNFα, we did not obtain reproducible amplification of these genes. It seems plausible that these genes are not expressed in these cell types under the experimental conditions used. Studies in murine tissues, including the liver, have demonstrated that the primer sets used to amplify these genes are functional (6).

Various possibilities may underlie the absence of regulation PEPCK and PGC1α expression by the insulin-ATF2 pathway. ATF2 binds to DNA either as homodimer, or as heterodimer with other ATF family members, like ATF3, ATF4, ATF6, and B-ATF, or *c-jun* family members(1-3). In addition, at least 21 distinct isoforms of mouse ATF2 have been identified so far. These various isoforms combined in different (hetero)dimer compositions confer a large repertoire of target genes on ATF2, depending on tissue-specific expression levels and the activating stimulus. In case of PEPCK, which was identified as an ATF2 target gene in rat hepatoma cells, but also in the fat-body, the fly equivalent of the mammalian liver and fat tissue (10;11;13), differences in the activating stimulus, rather than tissue-specific factors seem to underlie the absence of gene-regulation by the insulin-ATF2 pathway in the cell-types examined.

Both tissue- and stimulus-specific differences may contribute to the lack of PGC1α-induction by insulin in 3T3L1 adipocytes, and its downregulation in A14 fibroblasts, as PGC1α was characterized as target of the p38-ATF2 pathway in response to

β-adrenergic stimulation of brown adipose tissue (9). Other insulin-activated signaling pathways may be dominant over the ATF2-pathway in 3T3L1 and A14 cells. For example, the PKB/FOXO pathway, which is strongly activated by insulin, has been shown to lower the expression of PGC1α (23).

An important question arising from this study is how the identified target genes impact on insulin action and metabolic control. The gene most strongly induced by insulin in both 3T3L1 adipocytes and A14 fibroblasts, is the zinc-finger transcription factor Egr1. In β-cells, insulin-regulated induction of Egr1, like *c-jun*, regulates proliferation and differentiation (24-27), amongst others by Egr1-dependent induction of the homeodomain transcription factor pancreas duodenum homeobox-1 (PDX1), a key regulator of insulin expression and pancreatic β-cell development, function, and survival (25). In adipocytes, insulin-mediated regulation of Egr1 contributes to the induction of tissue factor and macrophage colony-stimulating factor, two cardiovascular risk factors (28;29). Furthermore, in endothelial cells, the insulin-induced Egr1-target genes, like platelet-derived growth factor, TNFα, intracellular adhesion molecule-1, monocyte chemotactic protein-1, plasminogen activator inhibitor-1, and vascular adhesion molecule-1, are strongly linked to the development of atherosclerosis (30;31) and also expressed in adipocytes. Intriguingly, both in adipocytes and endothelial cells, the induction of Egr1 by insulin was not altered under conditions of insulin resistance (29;31). Thus, whereas the function of Egr1 induction in adipocytes is unclear under normal conditions, deregulation of this response in type 2 diabetes may contribute to the development of vascular complications.

Also the role of ATF3, a transcription factor belonging to the same family as ATF2, in normal insulin action requires further studies. Although ATF3 has been implicated in the downregulation of PEPCK in the liver (32), other studies strongly link ATF3 to cellular damage and apoptosis. For example, the induction of ATF3 in response to pro-inflammatory cytokines, nitric oxide, hyperglycemia, high levels of palmitate, or endoplasmic reticulum stress precedes apoptosis in β-cells (11;33;34).

cJun is another member of the bZip-containing family of transcription factors and has been implicated in the regulation of cell growth and differentiation (2). cJun is an important dimer-partner of ATF2 (35). In addition, one of the major kinases phosphorylating both cJun and ATF2: JNK, is activated by insulin (5;36). Insulin-induced JNK-dependent cJun-phosphorylation has been reported in A14 cells ((7), BB and DMO, unpublished results). Thus, cJun could cooperate with ATF2 in regulating insulin-induced ATF2-dependent gene expression. However, it should be noted that, increasing evidence also supports a role for JNK in the development of insulin resistance in a number of tissues (reviewed in (37-39)) suggesting that cJun, perhaps in combination with ATF2, could also be involved in the development of insulin resistance.

MKP1 belongs to the MAP kinase phosphatase family of dual specificity phosphatases, which negatively regulate the activity of MAP kinases, like JNK, p38 and ERK1/2 (40). Interestingly, levels of phosphorylated ATF2 in insulin-treated cells remain elevated when the induction of MKP1 is abolished (DMO, unpublished data). This observation raises the possibility that MKP1 induction may serve to prevent sustained ATF2 activation by insulin and dampen a prolonged expression of detrimental ATF2-target genes. Accordingly, MKP1 has an inhibitory effect on the production of monocyte chemoattractant protein 1 (MCP-1), a chemokine highly associated with the development of adipocyte dysfunction in insulin resistance (41).

The transcription factor SREBP1c is a pivotal regulator of glucose and lipid metabolism, amongst others by inducing the expression of glucokinase and genes involved in lipogenesis (42). Insulin is a known inducer of SREBP1c in various tissues (43). Although SREBP1c was identified as ATF2-regulated gene before (4), analysis of the insulin-regulated part of the SREBP1c promoter did not (yet) identify putative ATF2-binding sites (43). It is therefore plausible that ATF2 regulates the SREBP1c promoter through the transcriptional co-activator p300/CBP (43;44). Like Egr1 and ATF3, however, deregulation of SREBP1c activity by high fat feeding, endoplasmic reticulum stress and hyperinsulinemia, contributes to the development of hepatic steatosis, which aggravates of insulin resistance (42;45).

Collectively, this study identifies ATF3, *c-jun*, Egr1, MKP1 and SREBP1c as insulin-regulated ATF2 target genes. Intriguingly, deregulation of (downstream targets of) these genes is highly linked to the pathogenesis of insulin resistance, β-cell dysfunction and vascular complications found in type 2 diabetes. Therefore, this study not only substantiates a role for ATF2 in insulin action, but also suggests that aberrant ATF2 activation under conditions of insulin resistance may contribute to the development of type 2 diabetes.

Materials and methods

Materials. Tissue culture media were obtained from Invitrogen (Carlsbad, Ca, USA), and SP600125 was from Biomol (Plymouth meeting, PA, USA). Antibodies recognizing phospho-T71-ATF2 (#9221), phospho-T69/T71-ATF2 (#9225), phospho-T202/Y204-ERK1/2 (#9101), and phospho-S473-PKB (#9271) were from Cell Signaling Technology (Beverly, MA, USA), anti-ATF2 (C19) and anti-insulin receptor β-subunit (C19) were from SantaCruz Biotechnology (Santa Cruz, CA, USA). Anti-elongation factor 1β (EF1β) has been described (46).

Generation of shRNA ATF2 constructs. To produce mouse-specific ATF2 shRNA constructs, we used the siRNA target finder to select oligonucleotides that were subsequently verified for specificity for mouse ATF2 (mATF2) by BLAST analysis of the mouse genome database. Sense and antisense versions of two silencing oligonucleotides, i.e. 5'-TGAGGAGCCTTCTGTTGTA-3' (mATF2#1), and 5'-GTGCCAAGCAGTCCACATA-3' (mATF2#2), corresponding to nucleotides 727-745 and 1685-1703, respectively, of the predicted mRNA ATF2 sequence in the mouse genome database were inserted into forward (5'-gatccccSENSEttcaagagaANTISENSEtttttggaaa-3') and reverse oligonucleotides (5'-agcttttccaaaaaSENSEtctcttgaaANTISENSEggg-3') purchased from Eurogentec (Liege, Belgium). Oligonucleotide pairs were annealed and phosphorylated and ligated into *Bgl*II- and *Hind*III-digested pSuperH1 (47). The pSuper-shATF2 constructs were verified by restriction and sequence analysis.

Cell culture and transient transfections. 3T3L1 adipocytes were purchased from the American Type Culture Collection (Manassas, VA, USA), and cultured and differentiated in adipocytes as described previously (48). A14 cells are NIH3T3 fibroblasts overexpressing the human insulin receptor, and grown in DMEM supplemented with 10% fetal bovine serum and antibiotics (19). For silencing experiments, A14 cells were transfected in 6-well plates with 500 ng of the pSuper ShRNA construct and 125 ng of pBabe-puro using Fugene 6 reagent (Roche Biochemicals, Indianapolis, IN). The next day, the cells were split into 2 6-well dishes, and selected with 3 μg/ml of puromycin (Sigma Aldrich, St. Louis, MO, USA) for 2 days, after which cells were serum-starved overnight and stimulated with insulin where indicated.

RNA extraction and real-time PCR analysis. Cells were homogenized in RLT-buffer (Qiagen, Venlo, The Netherlands), whereafter total RNA was extracted using RNeasy mini columns (Qiagen, Venlo, The Netherlands). DNase I digestion was performed to ensure complete removal of DNA. Purity and quantity of nucleic acids was determined by spectrophotometric analysis at 260 and 280 nm. Integrity of the RNA was verified by agarose gel electrophoresis. A total of 1.0 µg RNA was transcribed into complementary DNA using a Superscript™ first strand synthesis kit (Invitrogen, Breda, The Netherlands) using oligo-dT priming. mRNA abundance was measured using real-time PCR. Primers are listed in Table 2, and were designed using Primer Express version 3.0 software (Applied Biosystems, Foster City, CA, USA).

Table 2. Sequences of primers used for real-time PCR

Gene name	Accession number	Forward primer (5'->3')	Reverse primer (5'->3')
18S rRNA	NR_003278	gactcaacacgggaaacctc	agacaaatcgctccaccaac
adiponectin	NM_009605	ggaatgacaggagctgaagg	cgaatgggtacattgggaac
ATF2	NM_001025093	gactccaacgccaacaagat	aggtaaagggctgtcctggt
ATF3	NM_007498	aacacctctgccatc	ttatttctttctcgccgcctc
β-actin	NM_007393	agagggaaatcgtgctgac	caatagtgatgacctggccgt
c-jun	NM_010591	caacatgctcagggaacaggt	tgcgttagcatgagttggca
CREB1	NM_133828	ggagcttgtaccaccggtaa	gggctaatgtggcaatctgt
EF1α	NM_010106	aattggaggcattggcac	aaaggtaaccaccatgccagg
Egr1	NM_007913	aacactttgtggcctgaacc	aggcagaggaagacgatgaa
FABP4	NM_024406	aagaagtgggagtgggcttt	ctgtcgtctgcggtgattt
FOXO3a	NM_019740	ttcccatataccgccaagag	tgacgcaaggagttcagaga
HIF1α	NM_010431	cctggaaacgagtgaaagga	ctgccttgtatgggagcatt
IGF2	NM_010514	gagttcagagaggccaaacg	tagtgtgggacgtgatggaa
IGFBP6	NM_008344	cagagaccggcagaagaatc	ctcggaagacctcagtctgg
IL1β	NM_008361	caggcaggcagtatcactca	aggtgctcatgtcctcatcc
MKP1	NM_013642	ctcatgggagctggtcctta	gcgaagaaactgcctcaaac
PEPCK	NM_011044	tctgaggccacagctgctg	gggtcgcatggcaaagg
PGC1α	NM_008904	tttttggtgaaattgaggaatgc	cggtaggtgatgaaaccatagct
PPARα	NM_011144	caacccgccttttgtcatac	cctctgcctctttgtcttcg
SREBP1c	NM_011480	ggagccatggattgcacatt	cctgtctcacccccagcata
TNFα	NM_013693	gtccccaaagggatgagaag	cacttggtggtttgctacga

Reactions were carried out in the presence of 1x SYBR® Green PCR Master Mix (Applied Biosystems), 0.5µM of each forward and reverse primer on a StepOne Plus Real-time PCR system (Applied Biosystems) with the following cycle conditions: 95°C for 10 min followed by 40 cycles of 95°C for 15", 60°C for 30", and 72°C for 30". The threshold cycle number (C_t) was calculated using StepOne Plus software version 2.0 (Applied Biosystems) and an automated setting of the baseline. Data were analyzed using a comparative critical threshold (C_t) method in which the amount of target is normalized to the amount of endogenous control using the equation $R_a=2^{-\Delta Ct}$ in which R_a = the relative mRNA abundance, and $\Delta C_t=C_t$(gene of interest)-C_t(endogenous control), and C_t(endogenous control) is calculated as the geomean(C_t) of FABP4, ATF2, EF1α, and β-actin in 3T3L1 adipocytes, and geomean(C_t) of 18S rRNA, EF1α, β-actin in A14 fibroblasts, respectively.

The expression of the genes used as endogenous control was not affected by the experimental conditions used in this study.

Analysis of insulin signaling. Cells were washed twice with ice-cold PBS and lysed in 30 mM Tris.Cl, pH 7.5, 150 mM NaCl, 0.5% Triton X-100, 0.5% sodium deoxycholate, 1% SDS, 1 mM Na_3VO_4, 10 mM NaF and protease inhibitors (Complete, Roche). Cell lysates were cleared by centrifugation (13.200 rpm; 15 min, 4°C), and protein content was determined using a bicinchoninic acid protein assay kit (Pierce, Rockford, IL, USA). Expression and phosphorylation of proteins was studied by SDS-PAGE and Western blotting as described (5).

Statistical analysis. Data are expressed as means ± SE. Differences between groups were determined by unpaired students two-tailed *t*-test using SPSS version 16.0. $P<0.05$ was considered statistically significant.

References

1. Bhoumik, A., Lopez-Bergami, P., and Ronai, Z. (2007) *Pigment Cell Res.* **20,** 498-506
2. van Dam, H. and Castellazzi, M. (2001) *Oncogene.* **20,** 2453-2464
3. Vlahopoulos, S. A., Logotheti, S., Mikas, D., Giarika, A., Gorgoulis, V., and Zoumpourlis, V. (2008) *Bioessays* **30,** 314-327
4. Hayakawa, J., Mittal, S., Wang, Y., Korkmaz, K. S., Adamson, E., English, C., Ohmichi, M., McClelland, M., and Mercola, D. (2004) *Mol. Cell.* **16,** 521-535
5. Baan, B., van Dam H., van der Zon, G. C., Maassen, J. A., and Ouwens, D. M. (2006) *Mol. Endocrinol.* **20,** 1786-1795
6. Baan et al., *Manuscript in preparation* (Chapter 6)
7. de Ruiter, N. D., Wolthuis, R. M., van Dam, H., Burgering, B. M., and Bos, J. L. (2000) *Mol. Cell Biol.* **20,** 8480-8488
8. Ouwens, D. M., de Ruiter, N. D., van der Zon, G. C., Carter, A. P., Schouten, J., van der Burgt, C., Kooistra, K., Bos, J. L., Maassen, J. A., and van Dam H. (2002) *EMBO J.* **21,** 3782-3793
9. Cao, W., Daniel, K. W., Robidoux, J., Puigserver, P., Medvedev, A. V., Bai, X., Floering, L. M., Spiegelman, B. M., and Collins, S. (2004) *Mol. Cell Biol.* **24,** 3057-3067
10. Cheong, J., Coligan, J. E., and Shuman, J. D. (1998) *J. Biol. Chem.* **273,** 22714-22718
11. Lee, M. Y., Jung, C. H., Lee, K., Choi, Y. H., Hong, S., and Cheong, J. (2002) *Diabetes* **51,** 3400-3407
12. Reshef, L., Olswang, Y., Cassuto, H., Blum, B., Croniger, C. M., Kalhan, S. C., Tilghman, S. M., and Hanson, R. W. (2003) *J. Biol. Chem.* **278,** 30413-30416
13. Okamura, T., Shimizu, H., Nagao, T., Ueda, R., and Ishii, S. (2007) *Mol. Biol. Cell.* **18,** 1519-1529
14. Green, H. and Kehinde, O. (1975) *Cell* **5,** 19-27
15. Green, H. and Meuth, M. (1974) *Cell* **3,** 127-133
16. Rosen, E. D. and Spiegelman, B. M. (2000) *Annu. Rev. Cell Dev. Biol.* **16,** 145-171
17. Scherer, L. J. and Rossi, J. J. (2003) *Nat. Biotechnol.* **21,** 1457-1465
18. Osterop, A. P., Medema, R. H., Ouwens, D. M., van der Zon, G. C., Moller, W., and Maassen, J. A. (1994) *Biochemistry* **33,** 7453-7459
19. Burgering, B. M., Medema, R. H., Maassen, J. A., van de Wetering, M. L., van der Eb, A. J., McCormick, F., and Bos, J. L. (1991) *EMBO J.* **10,** 1103-1109
20. Kool, J., Hamdi, M., Cornelissen-Steijger, P., van der Eb, A. J., Terleth, C., and van Dam H. (2003) *Oncogene.* **22,** 4235-4242

21. Reimold, A. M., Kim, J., Finberg, R., and Glimcher, L. H. (2001) *Int. Immunol.* **13,** 241-248
22. Liu, F. and Green, M. R. (1990) *Cell* **61,** 1217-1224
23. Daitoku, H., Yamagata, K., Matsuzaki, H., Hatta, M., and Fukamizu, A. (2003) *Diabetes* **52,** 642-649
24. Breant, B., Lavergne, C., and Rosselin, G. (1990) *Diabetologia* **33,** 586-592
25. Eto, K., Kaur, V., and Thomas, M. K. (2007) *J. Biol. Chem.* **282,** 5973-5983
26. Garnett, K. E., Chapman, P., Chambers, J. A., Waddell, I. D., and Boam, D. S. (2005) *J. Mol. Endocrinol.* **35,** 13-25
27. Leibiger, I. B. and Berggren, P. O. (2008) *Annu. Rev. Nutr.* **28,** 233-251
28. Alexander-Bridges, M., Buggs, C., Giere, L., Denaro, M., Kahn, B., White, M., Sukhatme, V., and Nasrin, N. (1992) *Mol. Cell Biochem.* **109,** 99-105
29. Sartipy, P. and Loskutoff, D. J. (2003) *J. Biol. Chem.* **278,** 52298-52306
30. Hasan, R. N., Phukan, S., and Harada, S. (2003) *Arterioscler. Thromb. Vasc. Biol.* **23,** 988-993
31. Wang, C. C., Sharma, G., and Draznin, B. (2006) *Am. J. Hypertens.* **19,** 366-372
32. Allen-Jennings, A. E., Hartman, M. G., Kociba, G. J., and Hai, T. (2002) *J. Biol. Chem.* **277,** 20020-20025
33. Eizirik, D. L., Cardozo, A. K., and Cnop, M. (2008) *Endocr. Rev.* **29,** 42-61
34. Hartman, M. G., Lu, D., Kim, M. L., Kociba, G. J., Shukri, T., Buteau, J., Wang, X., Frankel, W. L., Guttridge, D., Prentki, M., Grey, S. T., Ron, D., and Hai, T. (2004) *Mol. Cell Biol.* **24,** 5721-5732
35. Benbrook, D. M. and Jones, N. C. (1990) *Oncogene* **5,** 295-302
36. Miller, B. S., Shankavaram, U. T., Horney, M. J., Gore, A. C., Kurtz, D. T., and Rosenzweig, S. A. (1996) *Biochemistry* **35,** 8769-8775
37. Yang, R. and Trevillyan, J. M. (2008) *Int. J. Biochem. Cell Biol.* **40,** 2702-2706
38. Wellen, K. E. and Hotamisligil, G. S. (2005) *J. Clin. Invest* **115,** 1111-1119
39. Tilg, H. and Moschen, A. R. (2008) *Mol. Med.* **14,** 222-231
40. Owens, D. M. and Keyse, S. M. (2007) *Oncogene* **26,** 3203-3213
41. Ito, A., Suganami, T., Miyamoto, Y., Yoshimasa, Y., Takeya, M., Kamei, Y., and Ogawa, Y. (2007) *J. Biol. Chem.* **282,** 25445-25452
42. Ferre, P. and Foufelle, F. (2007) *Horm. Res.* **68,** 72-82
43. Raghow, R., Yellaturu, C., Deng, X., Park, E. A., and Elam, M. B. (2008) *Trends Endocrinol. Metab* **19,** 65-73
44. Karanam, B., Wang, L., Wang, D., Liu, X., Marmorstein, R., Cotter, R., and Cole, P. A. (2007) *Biochemistry* **46,** 8207-8216
45. Shimomura, I., Matsuda, M., Hammer, R. E., Bashmakov, Y., Brown, M. S., and Goldstein, J. L. (2000) *Mol. Cell* **6,** 77-86
46. Sanders, J., Brandsma, M., Janssen, G. M., Dijk, J., and Moller, W. (1996) *J. Cell Sci.* **109 (Pt 5),** 1113-1117
47. Brummelkamp, T. R., Bernards, R., and Agami, R. (2002) *Science.* **296,** 550-553
48. van den Berghe N, Ouwens, D. M., Maassen, J. A., van Mackelenbergh, M. G., Sips, H. C., and Krans, H. M. (1994) *Mol. Cell Biol.* **14,** 2372-2377
49. Breitwieser, W., Lyons, S., Flenniken, A. M., Ashton, G., Bruder, G., Willington, M., Lacaud, G., Kouskoff, V., and Jones, N. (2007) *Genes Dev.* **21,** 2069-2082

Chapter 5

6

Increased *in vivo* phosphorylation of ATF2 by insulin and high fat diet-induced insulin resistance in mice

Manuscript in preparation

Chapter 6

Chapter 6

Increased *in vivo* phosphorylation of ATF2 by insulin and high fat diet-induced insulin resistance in mice

Bart Baan[1], Peter J. Voshol[2], Gerard C.M. van der Zon[1], Jan Kriek[1], Elena Korsheninnikova[1], Johannes A. Romijn[2], J. Antonie Maassen[1,3] and D. Margriet Ouwens[1]

[1]Departments of Molecular Cell Biology, and [2]Endocrinology, Leiden University Medical Centre, Leiden, The Netherlands, and [3]Department of Endocrinology/Diabetes Centre, VU University Medical Centre, Amsterdam, the Netherlands

Activating transcription factor 2 (ATF2) has been identified as a component of insulin signalling in cultured cells. ATF2-activation has been linked to the regulation of metabolic enzymes, but also to β-cell apoptosis, inflammation and diabetic neuropathy. To detail the function of ATF2 in insulin action, we studied the induction of ATF2-phosphorylation and potential ATF2 target genes by insulin *in vivo* and examined the effects of high-fat diet (HFD) induced insulin resistance on these parameters in mice. Insulin infusion induced a transient increase in ATF2-phosphorylation in the liver, white adipose tissue (WAT) and pancreas. In the liver, insulin infusion increased the expression of the potential ATF2-target genes ATF3, *c-jun*, Egr1, and SREBP1c. In the absence of insulin, basal ATF2 phosphorylation was increased in the liver and WAT of HFD-fed mice. This was accompanied by increased hepatic mRNA levels of the pro-inflammatory cytokines IL1β and TNFα, in addition to ATF3, *c-jun*, Egr1, and SREBP1c. Furthermore, the livers from HFD-fed mice were resistant for the induction of ATF2-target genes by insulin. We conclude that ATF2 has a dual role in insulin action as it is activated both by insulin infusion and under conditions of HFD-induced insulin resistance. The induction of pro-inflammatory cytokines in the liver of HFD-fed mice only suggests a state of chronic inflammation, which may contribute to the development of type 2 diabetes.

Activating transcription factor 2 (ATF2) is a component of the insulin signaling system. In A14 fibroblasts and 3T3L1 adipocytes, insulin rapidly phosphorylates ATF2 on its transactivation sites, Thr69 and Thr71 (1;2). This phosphorylation results in activation of the protein and induction of ATF2-target genes, including ATF3, *c-jun*, Egr1, MKP1 and SREBP1c (3). Also other studies indicate a role for ATF2 in metabolic control. In skeletal muscle and brown adipose tissue, the p38/ATF2 pathway regulates the expression of PPARγ coactivator 1α (PGC1α) (4;5), and of phosphoenolpyruvate carboxykinase (PEPCK) in the hepatoma cells (6;7). Finally, studies on the Drosophila fat body, the equivalent of the mammalian liver and adipose tissue, identify the p38/ATF2/PEPCK pathway as critical regulator of lipid metabolism (8).

It should be noted, however, that several ATF2-target genes are also highly linked to the pathogenesis of insulin resistance, β-cell dysfunction and complications found in type 2 diabetes. In β-cells, the ATF2-mediated induction of both the pro-inflammatory cytokine interleukin 1β (IL1β) and ATF3, in response to nitric oxide, hyperglycemia, high levels of palmitate, pro-inflammatory cytokines or endoplasmic reticulum stress, precedes apoptosis

(9-11). In endothelial cells, Egr1-regulated genes, like platelet-derived growth factor, TNFα, intracellular adhesion molecule-1, monocyte chemotactic protein-1, plasminogen activator inhibitor-1, and vascular adhesion molecule-1, have been implicated in the development of atherosclerosis (12;13). Finally, uncontrolled activation of SREBP1c has been implicated in the development of hepatic steatosis, which aggravates insulin resistance (14;15). Interestingly, also the upstream regulator of ATF2, JNK, has been linked to the pathogenesis of insulin resistance. Hirosumi et al. found elevated JNK activity in liver, adipose tissue and skeletal muscle of obese insulin resistant mice, and knockout of *Jnk1* (*Jnk1*$^{-/-}$) or inhibition of JNK-activity restores insulin sensitivity in mouse models of insulin resistance (16;17). It has been proposed that JNK phosphorylates the insulin receptor substrate 1 on Ser307, thereby inhibiting the insulin-mediated activation of protein kinase B, a master regulator of glucose metabolism (18;19).

The elevated basal activity of JNK, and the involvement of, amongst others, ATF3, IL1β, Egr1, and SREBP1c in β-cell apoptosis and insulin resistance, suggests that deregulation of ATF2 activity may contribute to the pathogenesis of type 2 diabetes mellitus. The present study aimed at detailing the role of ATF2 in insulin action and insulin resistance. Therefore, we analyzed the *in vivo* phosphorylation of ATF2 and the expression of ATF2-target in insulin target tissues of mice before and after an insulin infusion. Furthermore, we examined whether these responses were altered under conditions of high-fat diet-induced insulin resistance and obesity.

Results

Insulin induces ATF2 phosphorylation in vivo. We used male C57/Bl6J mice, fasted overnight, to examine ATF2 phosphorylation following an infusion with either PBS or insulin. To ascribe alterations in ATF2 phosphorylation levels to insulin rather than changes in blood glucose levels, glucose was co-infused to maintain euglycemia. Table 1 lists the animal characteristics at sacrifice. Mean body weight was similar among the experimental groups. Plasma insulin levels were 77±10 pmol/L in PBS-infused mice and 435±96 pmol/L and 467±84 pmol/L following 10 and 20 min of insulin infusion (both $P<0.01$ versus PBS). Blood glucose levels were similar in all groups (Table 1).

Table 1. Characteristics of overnight fasted mice following PBS or insulin infusion

	PBS (n=7)	**10 min INS (n=6)**	**20 min INS (n=7)**
Body weight at sacrifice (gram)	24.2±0.6	23.6±0.7	22.9±0.7
Fasting blood glucose (mmol/L)	6.2±0.7	5.6±0.6	6.4±0.7
Glucose at sacrifice (mmol/L)	5.7±0.4	4.7±0.4	4.8±0.4
Insulin at sacrifice (pmol/L)	77±17	435±96*	467±84*

Values are mean±SEM, *, $P<0.05$ versus PBS

Immunohistochemical staining (IHC) with phospho-ATF2-Thr71 antibodies shows a nuclear staining throughout the liver and pancreas of insulin-infused mice only (Figure 1). Notably, in the pancreas, ATF2-Thr71 phosphorylation tended to be enriched in the insulin-secreting β-cells (Figure 1). Application of the phospho-ATF2-Thr69+71 antibody failed to produce a detectable signal in IHC (data not shown).

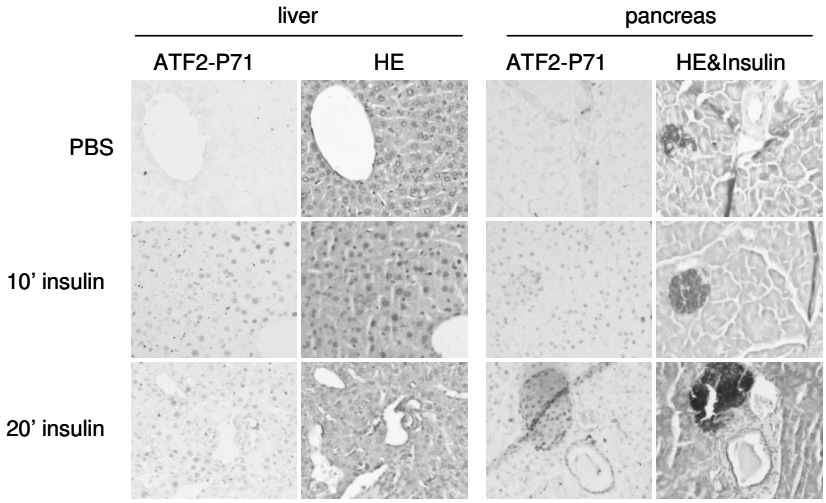

Figure 1. Immunohistochemical staining of mouse liver and pancreas tissue sections with phospho-ATF2-Thr71 antibodies (ATF2-P71), or hematoxylin (HE; blue) in combination with insulin (brown). Mice were infused with either PBS or insulin for the indicated times. Photographs are representative of 2-3 independent animals. Full-colour illustration can be found at page 127.

Instead, we examined the insulin-mediated induction of ATF2-Thr71 and ATF2-Thr69+71 phosphorylation in homogenates of insulin target tissues. Ten minutes after initiation of the insulin infusion, ATF2-Thr71 phosphorylation levels were increased 2.9-fold in liver (P<0.05 versus PBS-infusion, Figure 2). At this time point, phosphorylation levels of ATF2-Thr69+71 were increased 2.6-fold (P<0.05 versus PBS infusion, Figure 2). Hepatic ATF2 was still phosphorylated after 20 min insulin infusion (Figure 2), but had returned to basal levels 2 hrs after insulin infusion (data not shown).

In epididymal adipose tissue, all phospho-ATF2 antibodies detected a band migrating at ~64-kDa rather than the 70-kDa band observed in the liver. This protein was also detected by an antibody recognizing the aminoterminal part of ATF2 and was downregulated upon silencing the ATF2 gene in murine fibroblasts (data not shown). Therefore, it is likely that the observed immunoreactivity in adipose tissue results from an alternative splice variant of ATF2 (Chapter 2). The immunoreactivity of phospho-ATF2-Thr71 was increased by 2.3- and 2.5-fold after 10 and 20 min of insulin infusion, respectively (P<0.05; Figure 2). In contrast to the liver, ATF2-Thr69+71 phosphorylation was not significantly affected by insulin in adipose tissue (Figure 2).

Because of the multiple cell types present in the pancreas, we used cultured rat INS-1E insulinoma cells to confirm insulin-mediated ATF2 phosphorylation in insulin-secreting β-cells. Insulin rapidly increased both ATF2-Thr71- and ATF2-Thr69+71-phosphorylation, with peak levels occurring at 5 min after insulin addition, followed by a gradual decrease after 15 and 30 min (Figure 2). The increases in ATF2 phosphorylation by western blot could not be ascribed to major changes in ATF2 protein levels (Figure 2).

In heart and skeletal muscle, we could not detect the induction of ATF2 phosphorylation following insulin infusion, despite the presence of ATF2 protein in these tissues (data not shown). Activation of insulin signalling in all tissues was confirmed by increased phosphorylation of the PKB/Akt substrate PRAS40 (20) in insulin-infused animals (Figure 2, data not shown).

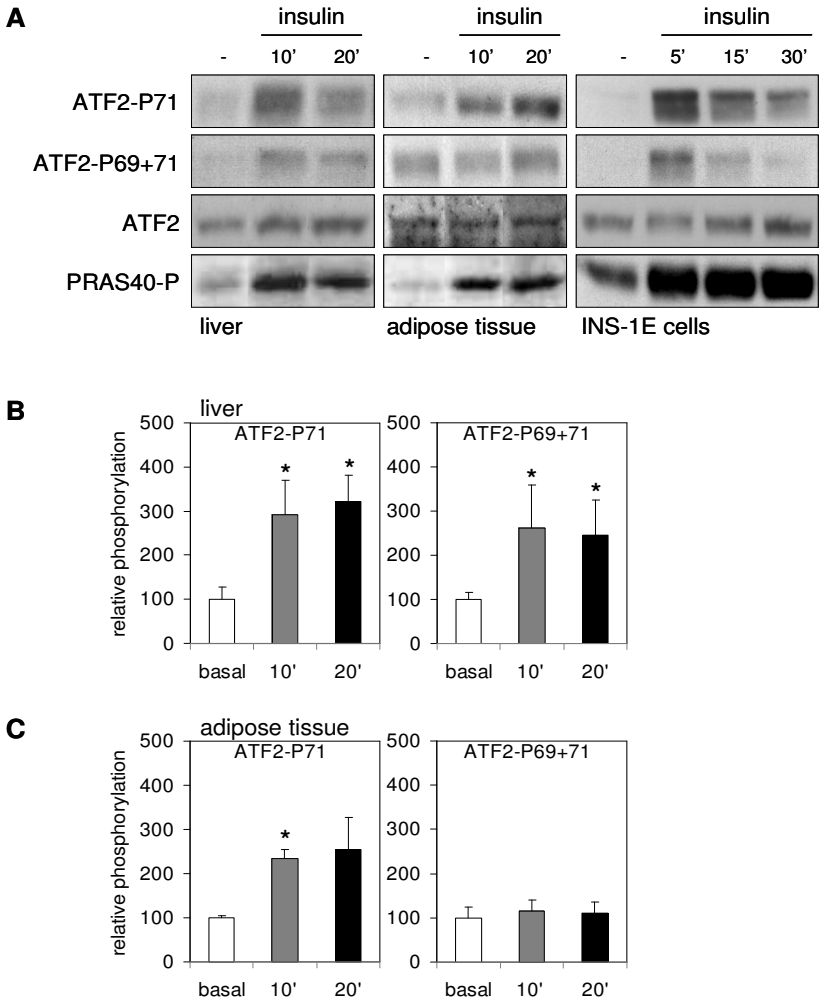

Figure 2. A. Phosphorylation of ATF2 and PRAS40, and expression of ATF2 in mouse liver and adipose tissue homogenates following infusion with PBS or insulin, and INS-1E cells, following incubation with 1 μM insulin for the indicated amounts of time. Western blots are representative of 7 independent mice per group or 2 independent experiments and verified for equal loading by PonceauS staining (not shown). B/C. Quantification of ATF2 phosphorylation in the liver (B) and adipose tissue (C). The relative ATF2 phosphorylation after PBS infusion (basal) was set at 100. Data are expressed as mean ± SEM of 7 independent mice per group. *, $P<0.05$ versus basal.

Induction of ATF2-target genes by insulin. Using real-time PCR, we examined the expression of 10 potential ATF2-target genes, i.e. ATF3, *c-jun*, Egr1, HIF1α, IL1β, MKP1, PEPCK, PGC1α, SREBP1c, TNFα in mouse livers. Livers were isolated from chow-fed mice, after an overnight fast or 2 h after initiation of a hyperinsulinemic euglycemic clamp. Table 2 shows that the mean body weight was similar between the experimental groups. Plasma insulin levels were 136±18 pmol/L in PBS-infused mice and 454±108 pmol/L following 2 h hyperinsulinemia. Blood glucose levels were similar between the groups (Table 2).

As shown in Figure 3, hyperinsulinemia increased the expression of ATF3, c-jun, Egr1 and SREBP1c by 1.4-, 1.4-, 2.7- and 3.0 fold (all $P<0.05$ vs basal), respectively. Furthermore, insulin lowered the levels of 4 genes (HIF1α, PEPCK, PGC1α and TNFα) and did not affect the abundance of IL1β and MKP1 (Figure 3).

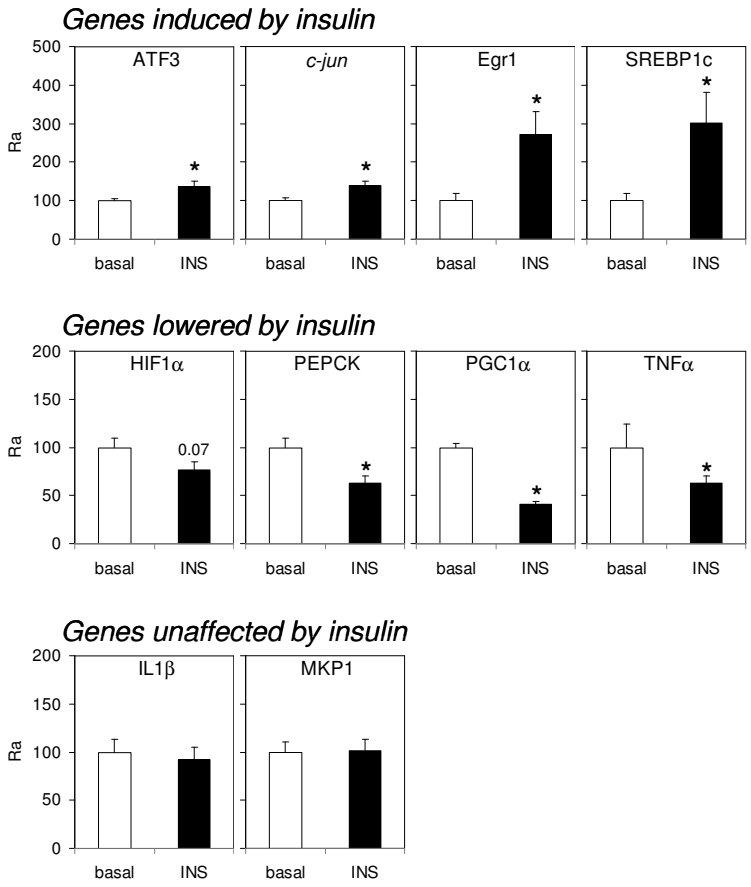

Figure 3. Effect of hyperinsulinemia on the expression of ATF2-target genes. Mice, fasted overnight, were sacrificed before (basal; open bars) or 2 h after initiation of a hyperinsulinemic euglycemic clamp (INS; black bars). Gene expression levels in the liver were determined by real-time PCR. The relative mRNA abundance (Ra) in the liver from fasted mice was set at 100. Data are expressed as mean ± SEM. *, $P<0.05$ versus basal (n=6-8 mice/group).

Table 2. Body and plasma characteristics before and after initiation of a hyperinsulinemic euglycemic clamp in mice fed a chow or HFD for 6 weeks.

	basal		hyperinsulinemia	
	chow (n=7)	HFD (n=7)	Chow (n=5)	HFD (n=6)
Body weight at sacrifice (gram)	24.3±0.6	28.1±1.0*	26.1±1.1	30.6±1.3*
Fasting blood glucose (mmol/L)	4.2±0.4	4.2±0.2	4.6±0.5	4.4±0.2
Fasting plasma insulin (pmol/L)	136±18	190±42*	139±25	185±31*
Glucose at sacrifice (mmol/L)	4.2±0.4	4.2±0.2	4.4±0.2	4.2±0.2
Insulin at sacrifice (pmol/L)	136±18	190±42*	454±108	592±188

Values are mean±SEM, *, $P<0.05$ versus chow

Insulin resistance increases basal ATF2 phosphorylation in mice. The effects of insulin resistance on ATF2-phosphorylation were determined in tissues from high-fat diet (HFD) fed mice (21). Table 2 shows that compared to chow fed mice, a 6-wk exposure to a HFD induced obesity. Whereas fasting blood glucose levels were not affected by high-fat feeding, fasting plasma insulin levels were elevated in HFD-fed mice. We previously reported that HFD-feeding blunted the suppression of hepatic glucose production by insulin (21), indicating insulin resistance.

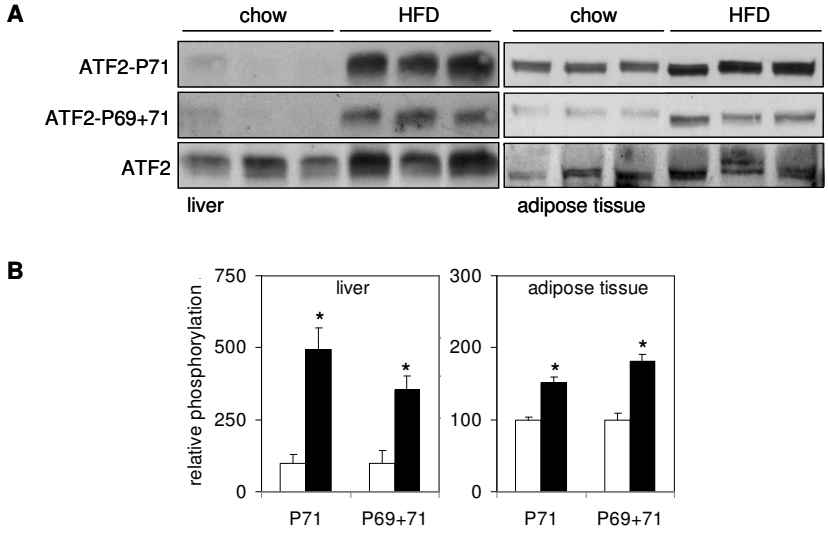

Figure 4. Western blot (A) and quantification (B) ATF2 phosphorylation in the liver and adipose tissue of chow (open bars) or high-fat diet fed mice (black bars). Tissue homogenates of were analyzed by immunoblotting with antibodies recognizing total ATF2, phospho-ATF2-Thr71 (ATF2-P71) or phospho-ATF2-Thr69+71 (ATF2-P69+71) antibodies. PonceauS staining confirmed equal loading of the Western blots (not shown). The relative ATF2 phosphorylation in chow fed mice was set at 100. Data are expressed as mean±SEM of 4 independent mice per group. *, $P<0.05$ versus chow.

In the liver, HFD-feeding induced a 4.9- and 3.6-fold increase in ATF2-Thr71 and ATF2-Thr69+71 phosphorylation, respectively (Figure 4; P<0.005 and P<0.01 respectively). Also in epididymal adipose tissue, phosphorylation levels of ATF2-Thr71 and ATF2-Thr69+71 were increased in HFD-fed mice by 1.5- (P<0.001) and 1.8-fold (P<0.005), respectively (Figure 4). This increase in basal levels of phosphorylated ATF2 could not be ascribed to alterations in ATF2 protein expression (Figure 4).

Increased mRNA levels of ATF2-target genes in the liver of HFD-fed mice. We also determined whether the elevated levels of phosphorylated ATF2 in livers from HFD-fed mice were accompanied by alterations in the expression of potential ATF2-target genes. Figure 5A shows that the abundance of ATF3, *c-jun*, Egr1, IL1β, SREBP1c and TNFα was 1.7-, 1.8-, 4.0-, 1.7-, 12.8- and 2.1-fold higher, respectively, in livers from HFD- versus CH-fed mice (all *P*<0.05).

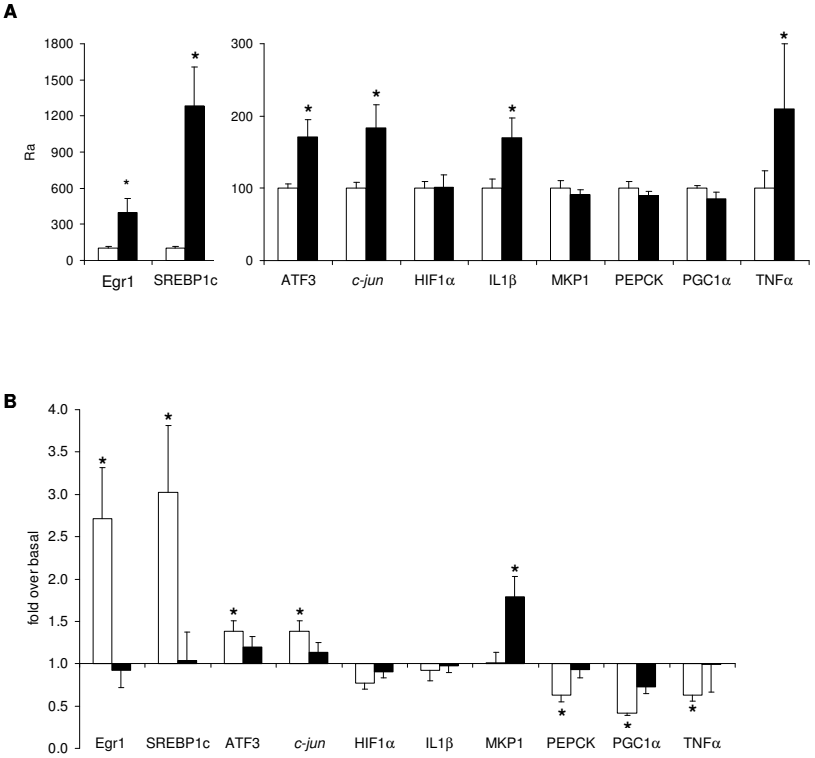

Figure 5. Effect of high-fat feeding on the expression of ATF2-target genes. A. Gene expression levels determined by real-time PCR in livers, isolated after an overnight fast, from mice fed a chow (open bars) or a high-fat diet (black bars). The relative mRNA abundance (Ra) in the liver from chow-fed mice was set at 100. Data are expressed as mean ± SEM. *, *P*<0.05 versus basal (*n*=6-8 mice/group). B. Effect of 2h hyperinsulinemia on the expression of ATF2 target genes in chow (open bars) and high-fat diet (black bars) fed mice. The effect of insulin is expressed as fold over basal. Data are mean ± SEM. *, *P*<0.05 versus basal (*n*=6-8 mice/group).

HFD-feeding had no effect on the expression of HIF1α, MKP1, PEPCK and PGC1α mRNA (Figure 5A). Except for MKP1, hyperinsulinemia did not significantly alter the expression of the examined genes, indicating that HFD-induced insulin resistance also affects insulin regulation of the ATF2 signaling pathway (Figure 5B).

Discussion

In this study, we examined the effects of insulin and HFD-feeding on the phosphorylation of the transcription factor ATF2. We show that insulin infusion induced phosphorylation of ATF2 on Thr69 and Thr71 in the liver, epididymal adipose tissue and the pancreas, but not in cardiac and skeletal muscle. In the liver, insulin increased the expression of the ATF2-regulated genes ATF3, *c-jun*, Egr1 and SREBP1c. Compared to chow-fed mice, HFD-feeding increased ATF2 phosphorylation in liver and adipose tissue. Elevated mRNA-levels of the (putative) ATF2-target genes ATF3, *c-jun*, Egr-1, SREBP1c, but also of the pro-inflammatory cytokines IL1β and TNFα accompanied these HFD-induced changes in the liver. Finally, livers from HFD-fed mice were resistant for the induction of ATF2-target genes in response to insulin.

The present study extends our previous findings (1;2) and identifies ATF2 as a component of physiological insulin action *in vivo*. The study described here was performed with insulin concentrations normally achieved following food intake and under euglycemic conditions, thereby excluding the possibility that the observed phosphorylation of ATF2 results from alterations in plasma glucose levels.

Strikingly, in the fasted state with low plasma concentrations of insulin, the levels of phosphorylated ATF2 were markedly increased in both the liver and epididymal adipose tissue from insulin resistant HFD-fed mice. This indicates a role for ATF2 both in insulin action and insulin resistance. The predominant kinases regulating ATF2 phosphorylation are ERK1/2, p38 and JNK (1;2;22-25). Numerous studies have demonstrated elevated activity of predominantly JNK under conditions of insulin resistance (16;17;19;26;27). Therefore, the sustained ATF2 phosphorylation in tissues from HFD-fed animals is likely to result from elevated JNK-activity.

To detail the dual function of ATF2 in insulin action and insulin resistance, the expression levels of potential downstream targets of ATF2 were determined in the livers from CH- and HFD-fed mice. Four genes that have been linked with ATF2-activation in previous reports, i.e. HIF1α (28), PEPCK (6-8), PGC1α (4;5) and MKP1 (28;29), were neither induced by hyperinsulinemia in CH-fed mice nor by HFD-feeding. Tissue-specific differences in the expression of ATF2 isoforms which affect the composition of ATF2-containing heterodimers may contribute to the absence of ATF2-regulation of these genes. Furthermore, also other insulin- or HFD-induced signaling pathways may be dominant over the ATF2-pathway. For example, the PKB/FOXO pathway, which is strongly activated by insulin, has been shown to lower the expression of PEPCK (30) and PGC1α (31).

Intriguingly, both HFD-feeding and hyperinsulinemia in CH-fed mice increased the abundance of 4 potential ATF2-regulated transcription factors, i.e. ATF3, *c-jun*, Egr1 and SREBP1c mRNA (3;22;28;32). It should be noted, however, that the magnitude of the induction caused by HFD-feeding, in particular of Egr1 and SREBP1c and to a lesser extent ATF3 and *c-jun*, is much higher than that caused by hyperinsulinemia in CH-fed mice. Furthermore, IL1β and TNFα mRNA levels were increased in the livers of HFD-fed mice only.

It is unknown whether these changes can be ascribed to the duration of ATF2 phosphorylation, which is transient in response to insulin and continuous after HFD-feeding, or to changes in the composition of ATF2-containing dimers. In this respect, it should be noted that cJun is not only an important dimer partner of ATF2 (33), but that it is also phosphorylated by JNK (22;23). Thus, increases in both the phosphorylation and expression of c-jun may affect the activity and formation of cJun/ATF2 heterodimers in HFD-fed mice.

The identification of ATF3, like ATF2, a member of the ATF/CREB family of transcription factors (34), as insulin-regulated gene is surprising. Although ATF3 has been implicated in the downregulation of PEPCK (35), induction of ATF3 is strongly linked to inducers of (endoplasmic reticulum) stress and apoptosis. Elevated levels of ATF3 in β-cells, caused by exposure to hyperglycemia, IL1β or nitric oxide (36), induce apoptosis via repression of the IRS2 gene (37). Furthermore, ATF3 is linked to mitochondrial dysfunction in C2C12 cells and negatively regulates the expression of adiponectin in 3T3L1 adipocytes (38;39).

Egr1 is linked to the regulation of cell proliferation and differentiation, amongst others by the induction of the homeodomain transcription factor pancreas duodenum homeobox-1 (PDX1), a key regulator of insulin expression and pancreatic β-cell development, function and survival (40). Also insulin signalling itself is critical for β-cell proliferation (41). Thus, an impaired induction of Egr1 by insulin may result in a decreased ability of the pancreas to compensate for the increased demand for insulin secretion under conditions of insulin resistance. Deregulation of Egr1 activity has further been linked to the development of atherosclerosis through enhanced expression of Egr1-target genes in endothelial cells (12;13) and adipocytes (42;43).

SREBP1c is a pivotal regulator of glucose and lipid metabolism, amongst others by inducing the expression of glucokinase and genes involved in lipogenesis (14;44). Both insulin and HFD-feeding are known inducers of SREBP1c in various tissues (45;46). However, unregulated activation of SREBP1c in the liver leads to hepatic steatosis, which aggravates insulin resistance (16).

The pathogenesis of type 2 diabetes is closely associated with chronic inflammation as illustrated by abnormal pro-inflammatory cytokine production by various tissues (47). The selective increases in IL1β and TNFα in the livers of HFD-fed mice only support these findings. These pro-inflammatory cytokines are not only target of ATF2, but also potent inducers of ATF2 activation. A limitation of this study is that we could not determine the plasma levels of IL1β and TNFα. However, it seems plausible that increases in circulating levels of pro-inflammatory cytokines may underlie the increased phosphorylation of ATF2 in the liver and WAT of HFD-fed mice, as has been observed by others (27;47).

Although the use of animal models can provide valuable information on deregulation of ATF2 under conditions of insulin resistance when compared to cultured cell lines, a major limitation is that we cannot formally ascribe the observed changes in gene expression to increases in ATF2 phosphorylation. Furthermore, we cannot exclude that the increased expression of IL1β and TNFα in HFD-fed mice results from Kupffer cells or infiltrated macrophages (27;47). To resolve these issues, studies on mice with tissue-specific ablation of the ATF2 gene are required.

We conclude that we have identified ATF2 as a component of the insulin signalling system in the liver, pancreas and WAT. However, we also show that ATF2-

activity is elevated in the liver and WAT of HFD-fed mice, which may contribute to the development of type 2 diabetes. This dual role of ATF2 suggests that regulation of ATF2 activity plays a critical role in insulin action and insulin resistance.

Materials and methods

Animals. The investigation conformed to the Guide for the Care and Use of Laboratory Animals as published by the NIH (NIH Publication No. 85-23, revised 1996) and the regulations of the Institutional Animal Care and Use Committee.

The effects of insulin infusion on ATF2-phosphorylation were studied in adult male C57Bl6J mice. Overnight fasted mice were anaesthetized by intraperitoneal injection with a combination of 6.25 mg/kg body weight (BW) acetylpromazine (Sanofi Santé Nutrition Animale, Libourne Cedex, France), 6.25 mg/kg BW midazolam (Roche, Mijdrecht, Netherlands) and 0.3125 mg/kg BW fentanyl (Janssen-Cilag, Tilburg, Netherlands). Insulin was infused through the tail-vein at 24.5 pmol/kg BW/min as described (48). Glucose was co-infused with insulin at 105 µmol/min to maintain euglycemia. At 10 and 20 min following initiation of the insulin infusion, mice were sacrificed by cervical dislocation. Control animals were sacrificed following infusion with PBS. After sacrifice, organs were removed and either immersion-fixed in 4% buffered formaldehyde solution, or snap-frozen in liquid nitrogen and stored at –80^{o}C until further use. The effects of insulin resistance were examined in high-fat diet fat mice. Male C57Bl6/J mice were randomly divided in two groups and fed either standard lab chow or a high-fat diet (HFD). After 6 weeks on the diet, mice were sacrificed following infusion with PBS or 2-hrs after initiation of a hyperinsulinemic euglycemic clamp (insulin infusion rate: 24.5 pmol/kg BW/min) as described (21). Then, tissues were removed, snap-frozen in liquid nitrogen and stored at -80^{o}C until further use.

Diets. High-fat diet was obtained from Arie Blok Diervoeding (Woerden, The Netherlands, cat#4031.05) and consisted (in % of total energy) of 44% bovine fat, 19% protein and 37% carbohydrate. Chow diet consisted of 32% proteins, 54% carbohydrates and 14% crude fat. Both diets were supplemented with vitamins and microelements.

Plasma determinations. Blood glucose was measured using a FreeStyle hand glucometer (Therasense, Disetronic Medical Systems, Vianen, Netherlands). Plasma insulin levels were determined using ELISA (Ultrasensitive mouse insulin kit, Mercodia AB, Uppsala, Sweden).

Cell culture. Ins-1E insulinoma cells (49) were kindly provided by Dr. C. Wollheim (University Medical Center, Geneva, Switzerland) and cultured in RPMI 1640 supplemented with 9% fetal bovine serum (FBS), 25 mM HEPES, glutamax, 1 mM sodium pyruvate and antibiotics.

Immunohistochemistry. Fixed tissues were prepared by routine paraffin embedding, sections were cut and mounted on slides. Sections were deparaffinized and washed with water for 5 min. Antigen retrieval was performed for ATF2 by boiling in 10 mM citrate buffer at pH 6 for 10 min followed by cooling for 20 min. Sections were washed three times for 5 minutes with water and endogenous peroxidase activity was blocked in 1% H_2O_2 for 20 min. After washing in water and PBS, sections were preincubated with 5% normal goat serum in PBS for 1 h. Incubation with ATF2-phospho-Thr71 antibodies (#9221; Cell Signaling Technology, Beverly, MA, USA) (1:50) was overnight at 4°C (50). Sections were then washed with PBS, incubated with rabbit Envision-HRP for 30 min, washed again and developed using DAB with 0.7% $NiCl_2$ for 10 min (black/blue precipitate). Separate sections were counterstained with hematoxylin (blue) or in case of the

pancreas with insulin (brown) and hematoxylin (blue) (51). Therefore, sections were incubated with 1% H_2O_2, washed and incubated overnight with the insulin-antibody (Dako, Glostrup, Denmark) (1:200) at room temperature, followed by washing with PBS, incubation with rabbit Envision-HRP for 30 min, washing and developing using DAB for 10 min. Sections were inspected using a Leica DM-LB light microscope (Leica, Rijswijk, The Netherlands) and digital images were captured using a Leica DC500 digital camera and software.

Western blotting. Cell- and tissue homogenates were prepared in 30 mM Tris.Cl, pH 7.5, 150 mM NaCl, 0.5% Triton X-100, 0.5% sodium deoxycholate, 1% SDS, 1 mM Na_3VO_4, 10 mM NaF and protease inhibitors (Complete, Roche) and cleared by centrifugation (13.200 rpm; 15 min, 4°C). Protein content was determined using a BCA protein assay kit (Pierce, Rockford, IL, USA). Expression and phosphorylation of proteins was determined by SDS-PAGE and immunoblotting (2). The antibodies used were: anti-phospho-Thr71-ATF2 (#9221), anti-phospho-Thr69+71-ATF2 (#9225) (both from Cell Signaling Technology, Beverly, MA, USA), anti-ATF2 (C19) (Santa Cruz Biotechnology, Inc., Santa Cruz, CA, USA) and anti-phospho-PRAS40-Thr246 (#44-100G) (Biosource International, Camarillo, CA, USA). PonceauS staining of the membranes confirmed correct protein transfer and equal loading. Bound antibodies were visualized by enhanced chemiluminescence. Immunoblots were quantified by densitometric analysis of the films (52).

RNA extraction and real-time PCR analysis. Frozen tissue biopsies (~30 mg) were homogenized in RLT-buffer (Qiagen, Venlo, The Netherlands), whereafter total RNA was extracted using RNeasy mini columns (Qiagen, Venlo, The Netherlands). DNase I digestion was performed to ensure complete removal of DNA. Purity and quantity of nucleic acids was determined by spectrophotometric analysis at 260 and 280 nm. Integrity of the RNA was verified by agarose gel electrophoresis. A total of 1.0 µg RNA was transcribed into complementary DNA using a Superscript™ first strand synthesis kit (Invitrogen, Breda, The Netherlands) using oligo-dT priming. mRNA abundance was measured using real-time PCR. Primers are listed in Table 3 and were designed using Primer Express version 3.0 software (Applied Biosystems, Foster City, CA, USA). Reactions were carried out in the presence of 1x SYBR® Green PCR Master Mix (Applied Biosystems), 0.5µM of each forward and reverse primer on a ABI PRISM® 7900HT Sequence Detection System (Applied Biosystems) with the following cycle conditions: 95°C for 10 min followed by 40 cycles of 95°C for 15", 60°C for 30" and 72°C for 30". The threshold cycle number (C_t) was calculated using SDS software version 2.2 (Applied Biosystems) and an automated setting of the baseline. Data were analyzed using a comparative critical threshold (C_t) method in which the amount of target is normalized to the amount of endogenous control using the equation $R_a=2^{-\Delta Ct}$ in which R_a = the relative mRNA abundance and $\Delta C_t=C_t$(gene of interest)-C_t(endogenous control) and C_t(endogenous control) is calculated as the geomean(C_t) of β-actin and EF1α. The expression of these genes was not affected by the experimental conditions used in this study.

Statistical analysis. Data are expressed as means ± SE. Differences between groups were determined by unpaired students two-tailed *t*-test using SPSS version 16.0. $P<0.05$ was considered statistically significant.

Table 3. Sequences of primers used for real-time PCR

Gene name	Accession number	Forward primer (5'->3')	Reverse primer (5'->3')
ATF2	NM_001025093	gactccaacgccaacaagat	aggtaaagggctgtcctggt
ATF3	NM_007498	aacacctctgccatc	ttatttctttctcgccgcctc
β-actin	NM_007393	agagggaaatcgtgctgac	caatagtgatgacctggccgt
c-jun	NM_010591	caacatgctcagggaacaggt	tgcgttagcatgagttggca
EF1α	NM_010106	aattggaggcattggcac	aaaggtaaccaccatgccagg
Egr1	NM_007913	aacactttgtggcctgaacc	aggcagaggaagacgatgaa
IL1β	NM_008361	caggcaggcagtatcactca	aggtgctcatgtcctcatcc
MKP1	NM_013642	ctcatgggagctggtcctta	gcgaagaaactgcctcaaac
PEPCK	NM_011044	tctgaggccacagctgctg	gggtcgcatggcaaagg
PGC1α	NM_008904	tttttggtgaaattgaggaatgc	cggtaggtgatgaaaccatagct
SREBP1c	NM_011480	ggagccatggattgcacatt	cctgtctcacccccagcata
TNFα	NM_013693	gtccccaaagggatgagaag	cacttggtggtttgctacga

Acknowledgements

The authors acknowledge Dr. Claes Wollheim (University Medical Center, Geneva, Switzerland) for the kind gift of INS-1E cells and the contribution of Annemieke van der Wal (Leiden University Medical Center, Dept. of Pathology) and Dr. Ng Hang Le (Leiden University Medical Center, Dept. of Human Genetics) to the immunohistochemistry experiments. The support of the Dutch Diabetes Research Foundation (grants 2001.00.046, 2002.00.032 and 2005.01.003) and the European Science Foundation (COST-Action BM0602) is greatly acknowledged. P.J.V. is the recipient of a VIDI-Innovational Research Grant from the Netherlands Organization for Health Research and Development.

References

1. Ouwens, D. M., de Ruiter, N. D., van der Zon, G. C., Carter, A. P., Schouten, J., van der Burgt, C., Kooistra, K., Bos, J. L., Maassen, J. A., and van Dam H. (2002) *EMBO J.* **21,** 3782-3793
2. Baan, B., van Dam H., van der Zon, G. C., Maassen, J. A., and Ouwens, D. M. (2006) *Mol. Endocrinol.* **20,** 1786-1795
3. Baan et al., *Manuscript in preparation* (Chapter 5)
4. Yan, Z., Li, P., and Akimoto, T. (2007) *Exerc. Sport Sci. Rev.* **35,** 97-101
5. Cao, W., Daniel, K. W., Robidoux, J., Puigserver, P., Medvedev, A. V., Bai, X., Floering, L. M., Spiegelman, B. M., and Collins, S. (2004) *Mol. Cell Biol.* **24,** 3057-3067
6. Cheong, J., Coligan, J. E., and Shuman, J. D. (1998) *J. Biol. Chem.* **273,** 22714-22718
7. Lee, M. Y., Jung, C. H., Lee, K., Choi, Y. H., Hong, S., and Cheong, J. (2002) *Diabetes* **51,** 3400-3407
8. Okamura, T., Shimizu, H., Nagao, T., Ueda, R., and Ishii, S. (2007) *Mol. Biol. Cell.* **18,** 1519-1529
9. Ammendrup, A., Maillard, A., Nielsen, K., Aabenhus, A. N., Serup, P., Dragsbaek, M. O., Mandrup-Poulsen, T., and Bonny, C. (2000) *Diabetes.* **49,** 1468-1476

10. Zhang, S., Liu, H., Liu, J., Tse, C. A., Dragunow, M., and Cooper, G. J. (2006) *FEBS J.* **273,** 3779-3791
11. Reimold, A. M., Kim, J., Finberg, R., and Glimcher, L. H. (2001) *Int. Immunol.* **13,** 241-248
12. Wang, C. C., Sharma, G., and Draznin, B. (2006) *Am. J. Hypertens.* **19,** 366-372
13. Hasan, R. N., Phukan, S., and Harada, S. (2003) *Arterioscler. Thromb. Vasc. Biol.* **23,** 988-993
14. Ferre, P. and Foufelle, F. (2007) *Horm. Res.* **68,** 72-82
15. Shimomura, I., Matsuda, M., Hammer, R. E., Bashmakov, Y., Brown, M. S., and Goldstein, J. L. (2000) *Mol. Cell* **6,** 77-86
16. Hirosumi, J., Tuncman, G., Chang, L., Gorgun, C. Z., Uysal, K. T., Maeda, K., Karin, M., and Hotamisligil, G. S. (2002) *Nature* **420,** 333-336
17. Stebbins, J. L., De, S. K., Machleidt, T., Becattini, B., Vazquez, J., Kuntzen, C., Chen, L. H., Cellitti, J. F., Riel-Mehan, M., Emdadi, A., Solinas, G., Karin, M., and Pellecchia, M. (2008) *Proc. Natl. Acad. Sci. U. S. A* **105,** 16809-16813
18. de Luca C. and Olefsky, J. M. (2008) *FEBS Lett.* **582,** 97-105
19. Hotamisligil, G. S. (2005) *Diabetes.* **54 Suppl 2:S73-8.,** S73-S78
20. Nascimento, E. B., Fodor, M., van der Zon, G. C., Jazet, I. M., Meinders, A. E., Voshol, P. J., Vlasblom, R., Baan, B., Eckel, J., Maassen, J. A., Diamant, M., and Ouwens, D. M. (2006) *Diabetes.* **55,** 3221-3228
21. Korsheninnikova, E., van der Zon, G. C., Voshol, P. J., Janssen, G. M., Havekes, L. M., Grefhorst, A., Kuipers, F., Reijngoud, D. J., Romijn, J. A., Ouwens, D. M., and Maassen, J. A. (2006) *Diabetologia.* **49,** 3049-3057
22. van Dam, H., Wilhelm, D., Herr, I., Steffen, A., Herrlich, P., and Angel, P. (1995) *EMBO J.* **14,** 1798-1811
23. Gupta, S., Campbell, D., Derijard, B., and Davis, R. J. (1995) *Science.* **267,** 389-393
24. Raingeaud, J., Gupta, S., Rogers, J. S., Dickens, M., Han, J., Ulevitch, R. J., and Davis, R. J. (1995) *J. Biol. Chem.* **270,** 7420-7426
25. Kyriakis, J. M. and Avruch, J. (2001) *Physiol Rev.* **81,** 807-869
26. Solinas, G., Naugler, W., Galimi, F., Lee, M. S., and Karin, M. (2006) *Proc. Natl. Acad. Sci. U. S. A.* **103,** 16454-16459
27. Wellen, K. E. and Hotamisligil, G. S. (2005) *J. Clin. Invest* **115,** 1111-1119
28. Hayakawa, J., Mittal, S., Wang, Y., Korkmaz, K. S., Adamson, E., English, C., Ohmichi, M., McClelland, M., and Mercola, D. (2004) *Mol. Cell.* **16,** 521-535
29. Breitwieser, W., Lyons, S., Flenniken, A. M., Ashton, G., Bruder, G., Willington, M., Lacaud, G., Kouskoff, V., and Jones, N. (2007) *Genes Dev.* **21,** 2069-2082
30. Barthel, A. and Schmoll, D. (2003) *Am. J. Physiol Endocrinol. Metab* **285,** E685-E692
31. Daitoku, H., Yamagata, K., Matsuzaki, H., Hatta, M., and Fukamizu, A. (2003) *Diabetes* **52,** 642-649
32. Liang, G., Wolfgang, C. D., Chen, B. P., Chen, T. H., and Hai, T. (1996) *J. Biol. Chem.* **271,** 1695-1701
33. Benbrook, D. M. and Jones, N. C. (1990) *Oncogene* **5,** 295-302
34. Hai, T. W., Liu, F., Coukos, W. J., and Green, M. R. (1989) *Genes Dev.* **3,** 2083-2090
35. Allen-Jennings, A. E., Hartman, M. G., Kociba, G. J., and Hai, T. (2002) *J. Biol. Chem.* **277,** 20020-20025
36. Hartman, M. G., Lu, D., Kim, M. L., Kociba, G. J., Shukri, T., Buteau, J., Wang, X., Frankel, W. L., Guttridge, D., Prentki, M., Grey, S. T., Ron, D., and Hai, T. (2004) *Mol. Cell Biol.* **24,** 5721-5732

Chapter 6

37. Li, D., Yin, X., Zmuda, E. J., Wolford, C. C., Dong, X., White, M. F., and Hai, T. (2008) *Diabetes* **57,** 635-644
38. Kim, H. B., Kong, M., Kim, T. M., Suh, Y. H., Kim, W. H., Lim, J. H., Song, J. H., and Jung, M. H. (2006) *Diabetes.* **55,** 1342-1352
39. Lim, J. H., Lee, J. I., Suh, Y. H., Kim, W., Song, J. H., and Jung, M. H. (2006) *Diabetologia.* **49,** 1924-1936
40. Eto, K., Kaur, V., and Thomas, M. K. (2007) *J. Biol. Chem.* **282,** 5973-5983
41. Leibiger, I. B. and Berggren, P. O. (2008) *Annu. Rev. Nutr.* **28,** 233-251
42. Alexander-Bridges, M., Buggs, C., Giere, L., Denaro, M., Kahn, B., White, M., Sukhatme, V., and Nasrin, N. (1992) *Mol. Cell Biochem.* **109,** 99-105
43. Sartipy, P. and Loskutoff, D. J. (2003) *J. Biol. Chem.* **278,** 52298-52306
44. Eberle, D., Hegarty, B., Bossard, P., Ferre, P., and Foufelle, F. (2004) *Biochimie* **86,** 839-848
45. Raghow, R., Yellaturu, C., Deng, X., Park, E. A., and Elam, M. B. (2008) *Trends Endocrinol. Metab* **19,** 65-73
46. Lin, J., Yang, R., Tarr, P. T., Wu, P. H., Handschin, C., Li, S., Yang, W., Pei, L., Uldry, M., Tontonoz, P., Newgard, C. B., and Spiegelman, B. M. (2005) *Cell* **120,** 261-273
47. Hotamisligil, G. S. (2006) *Nature* **444,** 860-867
48. Voshol, P. J., Haemmerle, G., Ouwens, D. M., Zimmermann, R., Zechner, R., Teusink, B., Maassen, J. A., Havekes, L. M., and Romijn, J. A. (2003) *Endocrinology.* **144,** 3456-3462
49. Merglen, A., Theander, S., Rubi, B., Chaffard, G., Wollheim, C. B., and Maechler, P. (2004) *Endocrinology.* **145,** 667-678
50. Le, N. H., van der Wal A, van der Bent P, Lantinga-van Leeuwen, I., Breuning, M. H., van Dam H, de Heer E, and Peters, D. J. (2005) *J. Am. Soc. Nephrol.* **16,** 2724-2731
51. Pinkse, G. G., Steenvoorde, E., Hogendoorn, S., Noteborn, M., Terpstra, O. T., Bruijn, J. A., and de Heer E. (2004) *Diabetologia.* **47,** 55-61
52. Ouwens, D. M., Boer, C., Fodor, M., de, G. P., Heine, R. J., Maassen, J. A., and Diamant, M. (2005) *Diabetologia* **48,** 1229-1237

7

Summary and Discussion

Chapter 7

Chapter 7

Summary and Discussion

Insulin elicits complex responses in peripheral tissues like skeletal muscle, adipose tissue, the heart, the liver and brain to maintain glucose and lipid homeostasis. Insulin resistance and type 2 diabetes are associated with impaired insulin action in these target tissues. In order to understand the molecular mechanisms underlying insulin resistance and to develop novel (therapeutic) strategies to improve peripheral insulin sensitivity, it is crucial to understand the complex responses that are induced by insulin in its target tissues. Insulin action is initiated by binding of insulin to its receptor and eventually leads to activation of two major effector pathways: the PI-3K-dependent PKB/Akt-pathway and the Ras-dependent MAPK-pathway. Activation of the PKB/Akt pathway has been linked to the regulation of lipid and glucose metabolism, gene expression and cell survival. The MAPK-pathway contributes to activation of gene expression and cell proliferation. In contrast to the PKB/Akt-pathway, the role of the Ras/MAPK in physiological insulin action is less well defined.

We have identified the transcription factor activating transcription factor 2 (ATF2) as a downstream target of the Ras/MAPK signaling pathway and novel component of insulin signaling (1). In the research described in this thesis we have further characterized the role of ATF2 in insulin action by (i) detailing the mechanism of insulin-induced ATF2 phosphorylation, (ii) identifying genes whose expression depends on ATF2 and (iii) investigating whether the induction of ATF2-phosphorylation and ATF2-regulated genes is altered under conditions of insulin resistance.

Chapters 3 and 4 address the mechanism of ATF2-activation in response to insulin. The data reported in these chapters extend the previous findings by further detailing the mechanism with which insulin induces ATF2-phosphorylation in the genetic absence and presence of JNK. Where stresses seem to induce activation of ATF2 via simultaneous phosphorylation of the transactivating residues Thr69+71 dependent on one kinase, insulin (and mitogens in general) utilizes a Ras-dependent two-step mechanism employing two kinases to achieve this. The data presented in chapters 3 and 4 suggest the following model for the induction of ATF2-Thr69+71 phosphorylation in response to insulin in cultured cells (summarized in Figure 1): in both JNK-deficient and JNK-containing cells, insulin induces early activation of the ERK1/2 via the Ras-Raf-pathway. Active ERK1/2 then translocates to the nucleus and mediates ATF2-Thr71-phosphorylation. Minutes later, after Ras-RalGDS-Ral dependent activation of p38/JNK, nuclear translocation of active p38 (in JNK-deficient cells) or active JNK (in JNK-expressing cells) is responsible for the activation of ATF2 by phosphorylation of Thr71-phosphorylated ATF2 on Thr69. We propose that, in both JNK-/- and JNK-expressing cells, the difference between the nuclear appearance of ERK1/2 and the ATF2-Thr69-phosphorylating SAPK (p38 or JNK) is rate limiting for the two-step phosphorylation of ATF2-Thr69+71 in response to insulin.

Importantly, the data described in chapter 6 confirmed insulin-induced ATF2-phosphorylation in several mouse tissues *in vivo*. However, the question whether *in vivo* ATF2-phosphorylation is also regulated via a two-step mechanism dependent on two cooperating kinases remains unanswered. No evidence was found to support a two-step process, but as hepatic ATF2 was already found to be phosphorylated on both Thr69+71 at the earliest time-point examined (10 minutes after start of insulin infusion), analysis of earlier time-points may potentially reveal differential kinetics in phosphorylation of the

different ATF2 sites and/or correlating differences in MAPK-activation in response to insulin. Experimental procedures to measure in vivo ATF2 phosphorylation at these early time points are however difficult to perform. In adipose tissue and liver, we observed a weak and transient induction of p38 and ERK1/2 phosphorylation at the time-points examined. Although phosphorylation of JNK could not be detected on western blots, due to the presence of interfering background bands and a poor signal-to-noise-ratio, pharmacological inhibition of JNK (using SP600125), and not of p38 (with SB203580) severely reduced only the ATF2-Thr69 *in vitro* kinase activity, and not the ATF2-Thr71 directed activity present in lysates from insulin-treated mouse livers (BB/DMO, unpublished results). These preliminary data suggest a potential role for JNK in the *in vivo* Thr69-phosphorylation of ATF2 induced by insulin. Further experimentation, using cell-permeable inhibitors of JNK that have been described to be functional in whole animals (2;3) or JNK-knockout mice (4) can potentially be used to substantiate the involvement of JNK in the insulin-induced *in vivo* ATF2-phosphorylation. Alternatively, the *in vivo* regulation of ATF2-phosphorylation may differ from the mechanism found in cells, and other kinases can be involved in this process *in vivo*. For a more general identification of ATF2-kinases activated by insulin *in vivo*, anion-exchange chromatography of insulin-treated tissue lysates in combination with ATF2-directed kinase assays can be employed (1;5).

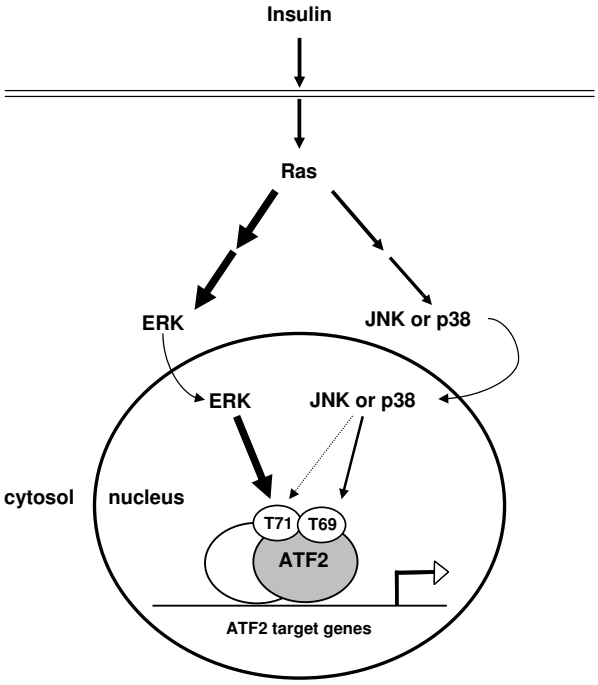

Figure 1. Proposed model for insulin-induced ATF2 activation in cultured cells. First, insulin induces Ras-dependent activation of ERK1/2. ERK1/2 subsequently translocates to the nucleus, where it mediates ATF2-Thr71 phosphorylation. Subsequently, JNK or (in JNK-deficient cells) p38 is activated. JNK (or p38) then translocates to the nucleus, and efficiently phosphorylates Thr71-phosphorylated ATF2 on Thr69, thus inducing transcriptional activation of ATF2.

To begin to detail the role of ATF2 in insulin action, we identified ATF2 target genes in insulin-sensitive cell lines and determined their hepatic expression levels in response to insulin-stimulation *in vivo*. In chapter 2, an overview is given on the potential role of ATF2 and ATF2-regulated genes in metabolic control and/or insulin action. Chapter 5 describes the identification of ATF3, *c-jun*, Egr1, MKP1 and SREBP1c as insulin-induced genes, whose expression is ATF2-dependent in both A14 fibroblasts and 3T3L1-adipocytes. Although *in vivo* insulin-inducibility could also be established for most of the identified ATF2-dependent genes in mouse liver (ATF3, *c-jun,* Egr1, and SREBP1c), a role for ATF2 therein was not formally proven (chapter 6). To obtain such evidence, adenovirus-mediated knockdown of hepatic ATF2 and/or Chromatin Immuno Precipitation (ChIP) studies for (phosphorylated) ATF2 (which is also possible in other tissues than liver) could be performed. Unfortunately, the ATF2 knockout mice or the phospho-dead $ATF2^{AA}$ expressing knock-in mice can not be used in studies on insulin action in adult animals, as they die shortly after birth (6;7). However, ATF2m/m mice, that express a mutant ATF2-isoform at low levels (7-9), have been employed to identify ATF2-dependent gene transcription and could therefore be suitable in further detailing the function of ATF2 in physiological insulin action. Other mouse-models include tissue-specific ATF2-knockout mice, which are currently being generated (10), or tissue-specific (inducible) expression of dominant negative forms of ATF2. Combination of these experimental setups with large-scale gene expression-profiling methods, such as microarray or solexa sequencing, could produce a higher yield of potential candidates and can provide more insight in the role of ATF2 in insulin-induced gene expression.

For some of the examined genes that were previously described as ATF2 targets, we could not establish ATF2-dependency in either one or both of our cell- or mouse-based studies. For example, we could not find any correlation between *in vivo* ATF2-phosphorylation and MKP1 expression in mouse livers, despite the fact that MKP1 expression was found to be ATF2-dependent in cultured cells stimulated with insulin (chapter 5) and expression of a number of MKPs (including MKP1) was reported to be dependent on intact ATF2-phosphorylation in embryonic livers (6). Apparently, other, potentially ATF2-independent, regulatory mechanisms govern the *in vivo* MKP1 expression in the adult animal.

Some of the other described ATF2-regulated genes (PEPCK, PGC1α, IL1β and TNFα) did not show any ATF2-dependency in response to insulin in cultured cells. In addition, *in vivo* insulin-treatment either lowered or had no effect on the expression of these genes in liver. For the cytokines IL1β and TNFα, it is not unthinkable that they are not expressed in the cell- or tissue-types and/or experimental conditions discussed here (see also below).

Several explanations can be given for the absence of regulation of the described ATF2 targets MKP1, PEPCK and PGC1α expression by insulin, both independent of and dependent on ATF2. Stimulus- and tissue-specific responses can underlie the apparent ATF2-independent regulation of these genes by insulin. The expression of most genes is regulated by a high number of factors and depending on the stimulus and cell- or tissue-type, other signaling pathways may be dominant over the ATF2-pathway. For example, the PKB/FOXO pathway, which is strongly activated by insulin in liver, could be crucial in the regulation of insulin-induced PGC1α expression (11).

Alternatively, expression of different ATF2-isoforms and/or ATF2-binding partners, some of which have been reported to repress transcription (e.g. ATF2d (12) and ATF3 (13)), can have opposing effects on ATF2-dependent gene regulation. Our

unpublished results suggest that several ATF2-isoforms are (co-)expressed in a tissue-specific manner (see figure 2). Differences in promoter-, co-factor- or dimer partner-specific characteristics would then determine which isoform of the ATF2 protein would be dominant in regulating a specific gene.

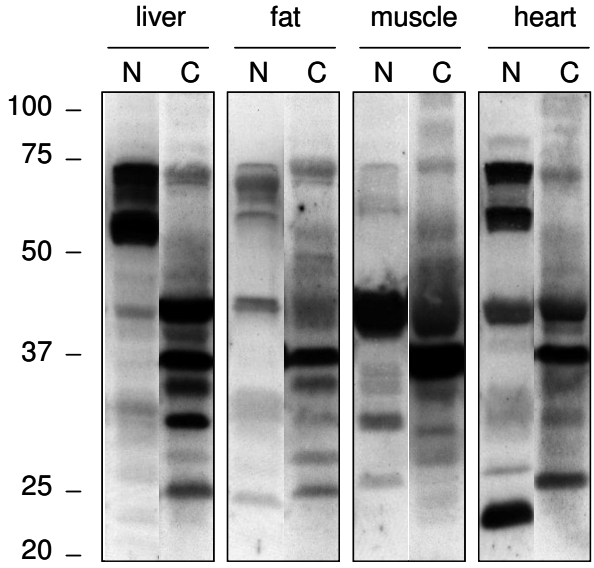

Figure 2. Expression of ATF2 isoforms in target tissues for insulin action. Lysates from mouse liver, adipose tissue, skeletal and cardiac muscle were analyzed by Western blotting using antibodies recognizing the first 96 (N) or last 19 (C) amino acids of ATF2.

A still unanswered question is how the identified ATF2-target genes impact on insulin action and metabolic control. Most of the positively identified insulin-induced ATF2-dependent genes encode transcription factors (e.g. Egr1, ATF3, *c-jun* and SREBP1c), whose targets have been postulated to be involved in several aspects of normal insulin action, like proliferation and differentiation of β-cells (for Egr1 and cJun (14-16)), control of hepatic fat and glucose metabolism (SREBP1, ATF3, cJun and Egr1 (13;17-19)). Further studies in relevant physiological models could be used to address their role in normal insulin action. One can think of ectopic expression of these factors in ATF2-'deficient' models (ATF2m/m mice (9) or (virus-mediated) knockdown of ATF2 in cellular model systems or in mouse liver), but not after a role for ATF2 in the regulation of these genes is established more firmly.

Finally, deregulation of a number of (potential) ATF2-target genes described in chapters 2 and 5 has also been associated with pathogenesis of insulin resistance, e.g. β-cell dysfunction and vascular complications found in type 2 diabetes (see chapter 2 for references). In addition, cytokine- or ER-stress-induced activation of one of the major ATF2 kinases: JNK, has been described to play a role in the development of insulin resistance in a number of tissues (reviewed in (20-22)). This suggests that next to a role in normal insulin action, ATF2 and its target genes could also be involved in the development of an insulin-resistant state and/or T2D(-associated complications).

To assess if insulin-resistance impacted on ATF2-phosphorylation, we examined ATF2-phosphorylation and expression of ATF2-dependent genes in tissues of high fat diet (HFD)-induced insulin-resistant mice. We found that already in the fasting state with low plasma concentrations of insulin, HFD induced increased ATF2-phosphorylation in livers and adipose tissue of insulin-resistant mice (chapter 6). As numerous studies have described elevated JNK-activity in HFD-induced insulin resistant states (4;23), the increased ATF2 phosphorylation found here, is probably (at least partially) mediated by JNK.

Correlating with the increased ATF2-phosphorylation found in these mice, HFD induced basal hepatic expression of the ATF2-dependent genes identified in chapter 5: ATF3, *c-jun*, Egr1 and SREBP1c. The described ATF2 target genes IL1-β and TNFα were also significantly induced by the HFD in liver, presumably produced by hepatic Kupfer cells or infiltrated macrophages activated by the HFD-induced state of chronic inflammation. The insulin-induced enhancement of all of these genes was severely reduced in the HFD-fed animals, correlating with the inability of insulin-administration to further increase ATF2 phosphorylation.

To ascertain the ATF2-involvement in this process, similar experiments as suggested above could be performed, e.g. comparison of (phospho-)ATF2-ChIPs in chow vs HFD-fed mouse tissues and/or analysis of the development of HFD-induced insulin-resistance in ATF2m/m mice or in mice with tissue-specific inactivation of ATF2 (10). Notably, as ATF2 is highly expressed in the brain (24;25) and there is increasing evidence for metabolic control via the brain (25-29), potential regulation of metabolism via central (neuronal) ATF2 should be considered. To further define the potential role of ATF2 in JNK-dependent HFD-induced insulin resistance analysis of the ATF2-phosphorylation status and ATF2-dependent gene expression in JNK-knockout mice (4;23;30;31) and/or combination of ATF2- and JNK-deficient mouse models could also be useful.

As a number of other genes related to metabolic control (such as PEPCK (32;33)) or the development of diabetes and/or its associated complications (for example the pro-inflammatory cytokine TNFα (9)) have been shown to be ATF2-dependent in several different experimental settings (see chapter 2), including these genes as targets in ChIP–on-chip experiments or larger scale expression profiling in several of the models described above could be particularly interesting.

In conclusion, we have identified ATF2 as a component of the cellular and *in vivo* insulin signaling systems. Insulin induced ATF2-phosphorylation in A14 fibroblasts, 3T3L1 adipocytes and several mouse tissues *in vivo*. In cell lines, the insulin-induced ATF2-phosphorylation was dependent on cooperation between two Ras-dependent MAPK-pathways: ERK and p38/JNK. Analysis of several described ATF2-target genes identified insulin-induced expression of Egr1, ATF3, *c-jun* and SREBP1c as being ATF2-dependent in cell lines. Quantitative PCR analysis showed increased mRNA expression of these genes in mouse livers correlating with hepatic ATF2-phosphorylation induced by insulin, but also in response to HFD-induced insulin resistance. Although the elucidation of the exact role of ATF2 activation under these conditions needs further experimentation, the data presented in this thesis suggest a potential dual function for ATF2 as a mediator of insulin action on the one hand and a putative regulator of the development or maintenance of insulin resistance on the other.

Chapter 7

References

1. Ouwens, D. M., de Ruiter, N. D., van der Zon, G. C., Carter, A. P., Schouten, J., van der Burgt, C., Kooistra, K., Bos, J. L., Maassen, J. A., and van Dam, H. (2002) *EMBO J.* **21,** 3782-3793
2. Kaneto, H., Nakatani, Y., Miyatsuka, T., Kawamori, D., Matsuoka, T. A., Matsuhisa, M., Kajimoto, Y., Ichijo, H., Yamasaki, Y., and Hori, M. (2004) *Nat. Med.* **10,** 1128-1132
3. Stebbins, J. L., De, S. K., Machleidt, T., Becattini, B., Vazquez, J., Kuntzen, C., Chen, L. H., Cellitti, J. F., Riel-Mehan, M., Emdadi, A., Solinas, G., Karin, M., and Pellecchia, M. (2008) *Proc. Natl. Acad. Sci. U. S. A* **105,** 16809-16813
4. Hirosumi, J., Tuncman, G., Chang, L., Gorgun, C. Z., Uysal, K. T., Maeda, K., Karin, M., and Hotamisligil, G. S. (2002) *Nature* **420,** 333-336
5. Baan, B., van Dam, H., van der Zon, G. C., Maassen, J. A., and Ouwens, D. M. (2006) *Mol. Endocrinol.* **20,** 1786-1795
6. Breitwieser, W., Lyons, S., Flenniken, A. M., Ashton, G., Bruder, G., Willington, M., Lacaud, G., Kouskoff, V., and Jones, N. (2007) *Genes Dev.* **21,** 2069-2082
7. Maekawa, T., Bernier, F., Sato, M., Nomura, S., Singh, M., Inoue, Y., Tokunaga, T., Imai, H., Yokoyama, M., Reimold, A., Glimcher, L. H., and Ishii, S. (1999) *J. Biol. Chem.* **274,** 17813-17819
8. Reimold, A. M., Grusby, M. J., Kosaras, B., Fries, J. W., Mori, R., Maniwa, S., Clauss, I. M., Collins, T., Sidman, R. L., Glimcher, M. J., and Glimcher, L. H. (1996) *Nature* **379,** 262-265
9. Reimold, A. M., Kim, J., Finberg, R., and Glimcher, L. H. (2001) *Int. Immunol.* **13,** 241-248
10. http://www.paterson.man.ac.uk/cellregulation/atf2.stm.
11. Daitoku, H., Yamagata, K., Matsuzaki, H., Hatta, M., and Fukamizu, A. (2003) *Diabetes* **52,** 642-649
12. Chyan, Y. J., Rawson, T. Y., and Wilson, S. H. (2003) *Gene* **312,** 117-124
13. Allen-Jennings, A. E., Hartman, M. G., Kociba, G. J., and Hai, T. (2002) *J. Biol. Chem.* **277,** 20020-20025
14. Eto, K., Kaur, V., and Thomas, M. K. (2007) *J. Biol. Chem.* **282,** 5973-5983
15. Leibiger, I. B. and Berggren, P. O. (2008) *Annu. Rev. Nutr.* **28,** 233-251
16. Breant, B., Lavergne, C., and Rosselin, G. (1990) *Diabetologia* **33,** 586-592
17. Raghow, R., Yellaturu, C., Deng, X., Park, E. A., and Elam, M. B. (2008) *Trends Endocrinol. Metab* **19,** 65-73
18. Drosatos, K., Sanoudou, D., Kypreos, K. E., Kardassis, D., and Zannis, V. I. (2007) *J. Biol. Chem.* **282,** 19556-19564
19. Wang, C. C., Sharma, G., and Draznin, B. (2006) *Am. J. Hypertens.* **19,** 366-372
20. Hotamisligil, G. S. (2005) *Diabetes* **54 Suppl 2,** S73-S78
21. Tilg, H. and Moschen, A. R. (2008) *Mol. Med.* **14,** 222-231
22. Yang, R. and Trevillyan, J. M. (2008) *Int. J. Biochem. Cell Biol.* **40,** 2702-2706
23. Solinas, G., Naugler, W., Galimi, F., Lee, M. S., and Karin, M. (2006) *Proc. Natl. Acad. Sci. U. S. A.* **103,** 16454-16459
24. Pearson, A. G., Curtis, M. A., Waldvogel, H. J., Faull, R. L., and Dragunow, M. (2005) *Neuroscience* **133,** 437-451
25. Maekawa, T., Sakura, H., Kanei-Ishii, C., Sudo, T., Yoshimura, T., Fujisawa, J., Yoshida, M., and Ishii, S. (1989) *EMBO J.* **8,** 2023-2028
26. Pocai, A., Obici, S., Schwartz, G. J., and Rossetti, L. (2005) *Cell Metab* **1,** 53-61

27. Lam, T. K., Gutierrez-Juarez, R., Pocai, A., Bhanot, S., Tso, P., Schwartz, G. J., and Rossetti, L. (2007) *Nat. Med.* **13,** 171-180
28. Plum, L., Belgardt, B. F., and Bruning, J. C. (2006) *J. Clin. Invest* **116,** 1761-1766
29. Schwartz, M. W., Woods, S. C., Porte, D., Jr., Seeley, R. J., and Baskin, D. G. (2000) *Nature* **404,** 661-671
30. Solinas, G., Vilcu, C., Neels, J. G., Bandyopadhyay, G. K., Luo, J. L., Naugler, W., Grivennikov, S., Wynshaw-Boris, A., Scadeng, M., Olefsky, J. M., and Karin, M. (2007) *Cell Metab* **6,** 386-397
31. Sabio, G., Das, M., Mora, A., Zhang, Z., Jun, J. Y., Ko, H. J., Barrett, T., Kim, J. K., and Davis, R. J. (2008) *Science* **322,** 1539-1543
32. Cheong, J., Coligan, J. E., and Shuman, J. D. (1998) *J. Biol. Chem.* **273,** 22714-22718
33. Okamura, T., Shimizu, H., Nagao, T., Ueda, R., and Ishii, S. (2007) *Mol. Biol. Cell.* **18,** 1519-1529

Chapter 7

8

Nederlandse Samenvatting

Chapter 8

Nederlandse Samenvatting

Insulin induceert complexe responsen in perifere weefsel zoals de skeletspier, vet, hart, lever en het brein om glucose- en vet-homeostase te bewerkstelligen. Een verminderde insulinewerking met betrekking tot de glucose-huishouding in deze organen wordt insuline resistentie genoemd en is een kenmerk van type 2 diabetes. Teneinde op een moleculair niveau de mechanismen te begrijpen welke ten grondslag liggen aan insuline resistentie en nieuwe strategieën te ontwikkelen om de insuline resistentie te verminderen is beter inzicht in het moleculaire mechanisme van de cellulaire insuline-respons vereist. Binding van insuline aan zijn receptor leidt tot activatie van twee intracellulaire signaal-transductie routes: een PI-3K-afhankelijke PKB/Akt route en een Src/Ras-afhankelijke MAPK route. Activatie van de PKB/Akt route is vooral belangrijk voor de acute regulatie van het vet- en glucose-metabolisme. Tevens reguleert deze route tevens gen-expressie en cel-overleving. De MAPK-route lijkt vooral belangrijk voor activatie van gen-expressie en cellulaire proliferatie. In tegenstelling tot de PKB/Akt-route, is er nog weinig bekend over de rol van de Ras/MAPK-route bij de fysiologische insuline werking.

In onze onderzoeksgroep is de transcriptie factor ATF2 geïdentificeerd als een van de componenten van de Ras/MAPK signaalroute en tevens als nieuw onderdeel van de insuline signaal-transductieketen. In dit proefschrift hebben we de rol van ATF2 in de insuline-geïnduceerde respons verder onderzocht. Het onderzoek beschreven in dit proefschrift valt in de volgende drie deelvragen uiteen:

1. Wat is het mechanisme van insuline-geïnduceerde ATF2-fosforylering?
2. Welke insuline-gereguleerde genen zijn ATF2-afhankelijk?
3. Is de regulatie van ATF2-fosforylering en ATF2-afhankelijke genen veranderd in een situatie van insuline resistentie?

In de hoofstukken 3 en 4 wordt het onderzoek naar het mechanisme van de insuline-geïnduceerde fosforylatie van ATF2 beschreven. De hierbij verkregen resultaten sluiten aan bij de eerder gepubliceerde bevindingen (zie Ouwens et al. EMBO J 2002). In tegenstelling tot stress-stimuli, die een min of meer gelijktijdige fosforylering van ATF2 op de Threonine (Thr)69 en Thr71 induceren - een reactie die vermoedelijk uitgevoerd wordt door één kinase - induceren insuline en verwante groeifactoren ATF2-fosforylering op Thr69 en Thr71 via een Ras-afhankelijk twee-staps mechanisme waarin twee MAPK-routes samenwerken. Op basis van de resultaten beschreven in hoofdstuk 3 en 4 lijkt het volgende mechanisme voor insuline-geïnduceerde ATF2-fosforylering waarschijnlijk: Insuline activeert het MAPK ERK1/2, via activatering van de Ras-Raf-route. Actief Erk1/2 beweegt naar de kern waar het ATF2 fosforyleert op aminozuur Thr71. Minuten later, na een Ras-Ral-afhankelijke activatering van de stress-kinases p38 en/of JNK, migreren deze kinases naar de kern waar ze Thr71-gefosforyleerd ATF2 opnieuw fosforyleren, nu op Thr69. Door gebruik te maken van cellen die specifiek JNK missen, hebben we tevens aangetoond dat het kinase p38 op zich al in staat is om deze fosforylering te bewerkstelligen. In JNK-bevattende cellen lijkt echter het grootste deel van de Thr69-fosforylering via JNK te verlopen. De verkregen resultaten suggereren dat samenwerking tussen deze routes noodzakelijk is en dat het verschil in de migratiesnelheid tussen actief ERK1/2 en respectievelijk JNK/p38 verantwoordelijk is voor de twee-staps fosforylering van ATF2 in respons op insuline.

In hoofdstuk 6 beschrijven we dat deze situatie van ATF2 fosforylering zich ook voordoet in levende dieren. In een muizen-model kon worden bevestigd dat infusie van insuline *in vivo* tot ATF2-fosforylering in lever, vet-weefsel en de pancreatische β-cel leidt. Of dit proces in de muis via precies dezelfde stappen verloopt als bij de gekweekte cellen, konden we vanwege technische redenen niet in detail vaststellen.

In hoofdstuk 2 wordt op basis van literatuuronderzoek bediscussieerd welke rol ATF2 en ATF2-gereguleerde genen potentieel zouden kunnen spelen bij metabole regulatie en de insuline respons in het bijzonder. Om een begin te maken de fysiologische rol van ATF2 in insuline actie te begrijpen, is van een aantal van deze insuline-gereguleerde genen de ATF2-afhankelijkheid onderzocht in insuline-gevoelige cellijnen (hoofdstuk 5). Vervolgens hebben we in een *in vivo* situatie onderzocht in hoeverre de expressie van deze genen in de lever, *in vivo*, onder controle van insuline staat (hoofdstuk 6). Met behulp van farmacologische remming van ATF2-activatie en via ATF2-knockdown experimenten werd in A14 fibroblasten en 3T3L1-adipocyten aangetoond dat voor efficiënte insuline-geïnduceerde expressie van een aantal genen (ATF3, *c-jun*, Egr1, MKP1 en SREBP1c) ATF2-activatie, dan wel expressie van ATF2 cruciaal is (hoofdstuk 5). Hoewel de meeste van deze ATF2-afhankelijke genen (ATF3, *c-jun,* Egr1 en SREBP1c) ook *in vivo* door insuline in muizen-levers werden geïnduceerd (hoofdstuk 6), hebben we hierbij de betrokkenheid van ATF2 niet kunnen onderbouwen.

Een aantal van de (potentieel) ATF2-afhankelijke genen beschreven in hoofdstuk 2 en 5 is betrokken bij de pathogenese van insuline resistentie/type 2 diabetes. Bovendien draagt hyperactivatie van de het ATF2-kinase JNK ook sterk bij aan dit proces. Op basis van bovenstaande gegevens lijkt er in de ontwikkeling van insuline resistentie/type 2 diabetes een rol voor ATF2 te zijn weggelegd. Om die reden hebben we in hoofdstuk 6 ook gekeken naar de staat van ATF2-fosforylering en (insuline-geïnduceerde) expressie van ATF2-gereguleerde genen in een *in vivo* insuline resistente situatie. Daarvoor zijn muizen resistent voor insuline gemaakt door ze een aantal weken een 'hoog-vet' dieet (HVD) te voeren. Ten opzichte van de controle dieren werd er in de lever en het vetweefsel van insuline resistente muizen een significante verhoging van ATF2-fosforylering gevonden. In de levers van de HVD-muizen ging de basaal verhoogde ATF2-fosforylering gepaard met een verhoogde expressie van de in hoofdstuk 5 beschreven ATF2-afhankelijke genen. In tegenstelling tot de controle dieren had insuline-infusie geen additioneel inducerend effect meer op de hepatische expressie van deze ATF2-target genen. Bovendien was de expressie van eerder beschreven ATF2-target genen betrokken bij de immuun respons (IL1β en TNFα) ook verhoogd in de HVD-situatie.

Samenvattend kan gesteld worden dat het hier beschreven onderzoek ATF2 heeft geïdentificeerd als component van de insuline signaal-transductie route, zowel *in vitro* als *in vivo*. In cellijnen werd de insuline-geïnduceerde ATF2-fosforylering gemedieerd door samenwerking van twee Ras-afhankelijke MAPK-routes: ERK en p38/JNK. Het lijkt waarschijnlijk dat een soortgelijk mechanisme *in vivo* plaatsvindt.

Door analyse van beschreven ATF2-target genen in cellijnen hebben we laten zien dat de insuline-geïnduceerde expressie van Egr1, ATF3, *c-jun* en SREBP1c afhankelijk is van ATF2. Het bleek dat het *in vivo* expressie niveau van deze genen correleerde met een verhoogde ATF2-fosforylering in respons op insuline enerzijds, maar anderzijds ook in response op HVD-geïnduceerde insuline resistentie. Opmerkelijk is dat een hoog vet dieet insuline resistentie induceert en een verdere fosforylering van ATF2 door insuline verhindert. Ondanks het feit dat het ophelderen van de precieze rol van ATF2 fosforylering

in deze situaties nader onderzoek vereist, suggereren de hier beschreven data dat ATF2 mogelijk een duale rol speelt: enerzijds als een mediator van normale insuline werking, anderzijds als potentiële regulator bij het ontstaan van insuline resistentie.

Chapter 8

Curriculum vitae

The author of this thesis was born on the 10th of June 1977 in Leiden, the Netherlands. After graduating from the Gymnasium Haganum in The Hague in 1995, he started a study Biology at the University of Utrecht. During his master he did a first internship within the faculty of Biology at the EMSA-department (Drs. Esther Hulleman and Dr. Johannes Boonstra). In 1999, he was secretary of the Board of the Dutch National Student Orchestra (NSO) and played the double bass in the orchestra. Returning to his study, he did a second master-internship at the Virology-department of the faculty of Veterinary Science (Drs. Marel de Wit and Prof. Dr. Peter Rottier). After concluding his master studies with a literature review at the Hubrecht-laboratory in 2002 (Dr. Hendrik Korswagen), he started the research described in this thesis at the department of Molecular Cell Biology of the Leiden University Medical Centre, supervised by Dr. Margriet Ouwens and Prof. Dr. Ton Maassen. Since 2006, the author is employed as a postdoctoral researcher in the group of Dr. Hans van Dam at the department of Molecular Cell Biology of the Leiden University Medical Centre.

List of publications

Baan B, Van Dam JAF and Ouwens DM. ATF2, a novel player in insulin action and insulin resistance? *Manuscript in preparation.*

Baan B, Wanga TAT, Van der Zon GCM, Maassen JA and Ouwens DM. Identification of insulin-regulated ATF2-target genes in 3T3L1 adipocytes and A14 fibroblasts. *Manuscript in preparation.*

Baan B, Voshol PJ, Van der Zon GCM, Kriek J, Korsheninnikova E, Romijn JA, Maassen JA and Ouwens DM. Increased *in vivo* phosphorylation of activating transcription factor 2 by insulin and high fat diet-induced insulin resistance in mice. *Manuscript in preparation.*

Baan B, Van der Zon GCM, Maassen JA and Ouwens DM. The nuclear appearance of ERK and p38 determines the sequential induction of ATF2-Thr71 and ATF-Thr69-phosphorylation by serum in JNK deficient cells. *Manuscript conditionally accepted.*

Korsheninnikova E, Voshol PJ, Baan B, Van der Zon GCM, Havekes LM, Romijn JA, Maassen JA and Ouwens DM. Dynamics of insulin signalling in liver during hyperinsulinemic euglycaemic clamp conditions *in vivo* and the effects of high fat feeding in male mice. *Arch Physiol Biochem (2007) 113(4-5):173-185*

Nascimento EBM, Fodor M, van der Zon GCM, Jazet IM, Meinders AE, Vlasblom R, Baan B, Eckel J, Maassen JA, Diamant M and Ouwens DM. Insulin-stimulated phosphorylation of the proline-rich Akt substrate PRAS40 is impaired in insulin target tissues of high fat diet-fed rats. *Diabetes (2006) 55(12): 3221-3228*

Baan B**,** Van Dam JAF, Van der Zon GCM, Maassen JA and Ouwens DM. The role of JNK, p38 and ERK MAP-kinases in insulin-induced Thr69 and Thr71-phosphorylation of transcription factor ATF2. *Mol Endocrinology (2006) 20(8): 1786-1795*

Appendix

Full-colour Illustrations

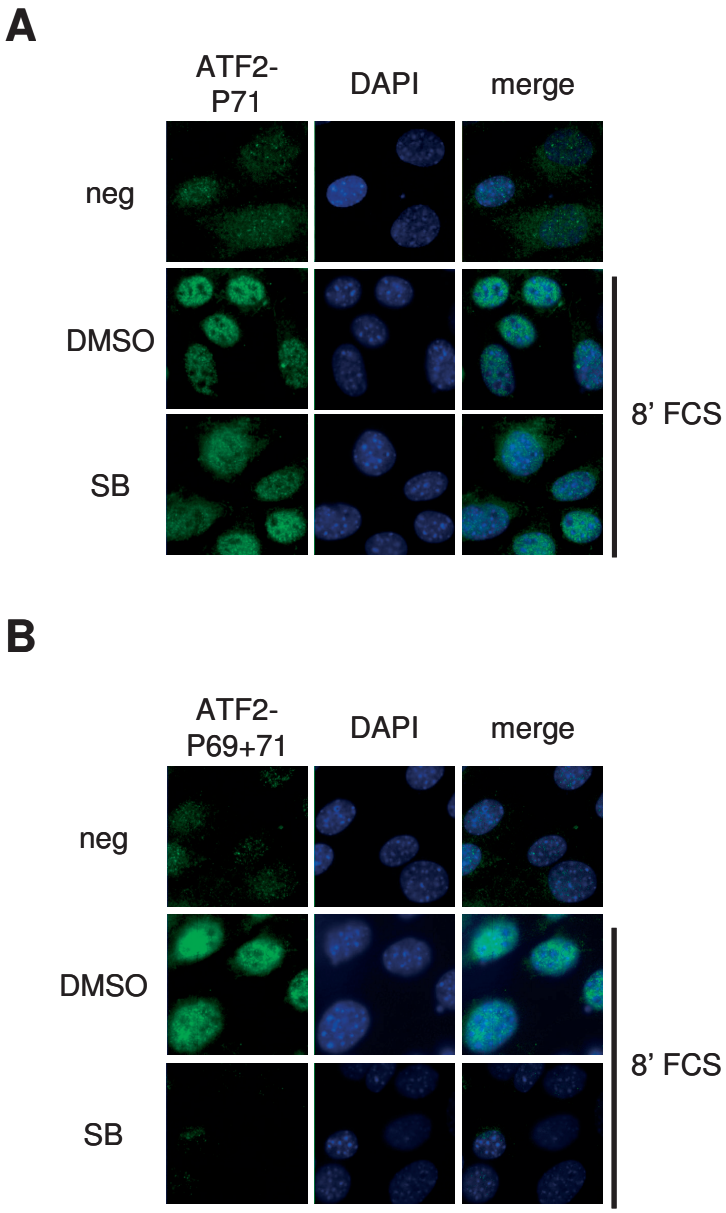

Figure 3. Serum-induced ATF2-Thr69+71, but not Thr71-phosphorylation is SB203580-sensitive in JNK-/- cells. Serum-starved JNK-/- cells were treated with SB203580 (SB) for 30 minutes prior to stimulation with 20% serum (FCS) for 8 minutes. Cells were fixed and stained with antibodies for (A) Thr71- or (B) Thr69+71-phosphorylated ATF2 followed by FITC-conjugated secondary antibodies (green). DNA was stained with DAPI (blue).

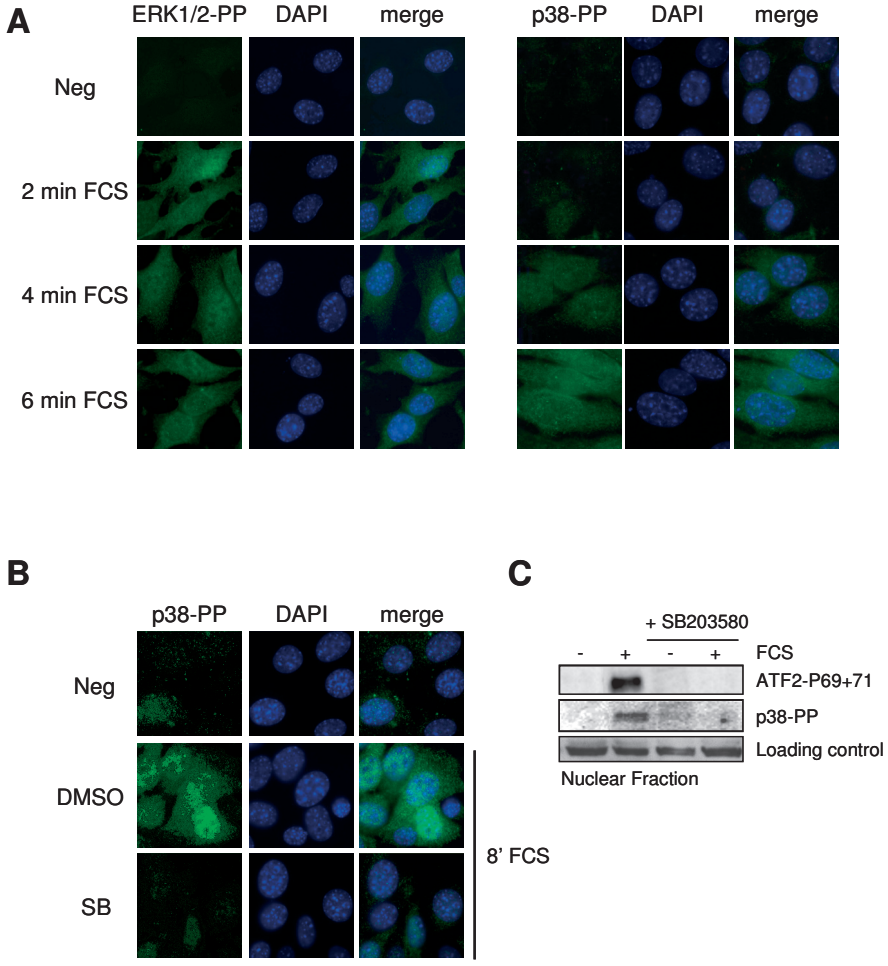

Figure 5. The onset of ATF2-Thr71 and ATF2-Thr69+71-phosphorylation associates with nuclear translocation ERK1/21/2 and p38. (A) Serum-starved JNK-/- cells were stimulated with 20% serum (FCS) and fixed at the times indicated. The fixed cells were stained with antibodies for phospho-ERK1/2 (ERK1/2-PP) or phospho-p38 (p38-PP) followed by FITC-conjugated secondary antibodies (green). DNA was stained with DAPI (blue). (B) Serum-starved JNK-/- cells pre-treated with vehicle or SB203850 for 30 minutes prior to 8 minute FCS-stimulation were fixed and stained for phospho-p38 (p38-PP) as described above. (C) Serum-starved JNK-/- cells, pre-treated with vehicle or SB203850 were serum-stimulated for 8 minutes, after which cellular fractions were prepared and the nuclear fractions examined for p38- and ATF2-Thr69+71 phosphorylation by immunoblotting with phospho-specific antibodies as described.

Chapter 4

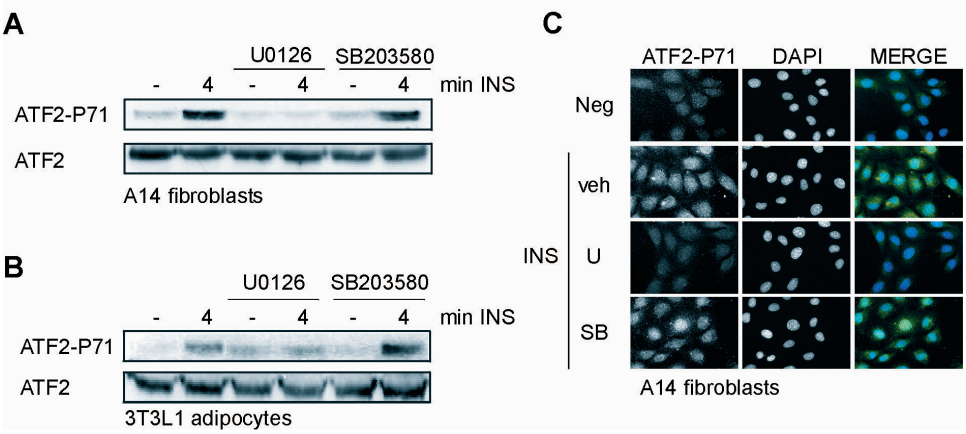

Figure 3. Early insulin-induced ATF2-Thr71 phosphorylation is sensitive to inhibition of the MEK1/2-ERK1/2 pathway. Serum-starved A14 cells (A) or 3T3L1 adipocytes (B) were incubated with 10 μM U0126 (U; 15 minutes) or 2.5 μM SB203580 (SB; 30 minutes) before insulin-stimulation (INS; 10 nM) for 4 minutes. Total ATF2 and ATF2-Thr71-phosphorylation levels were determined by immunoblotting with specific antibodies. (C) A14 cells were treated with inhibitors as described above, prior to stimulation with 10 nM of insulin for 4 minutes. Subsequently, cells were fixed and stained with phospho-specific ATF2-Thr71 antibodies followed by FITC-conjugated secondary antibodies (green). DNA was stained with DAPI (blue).

Chapter 4

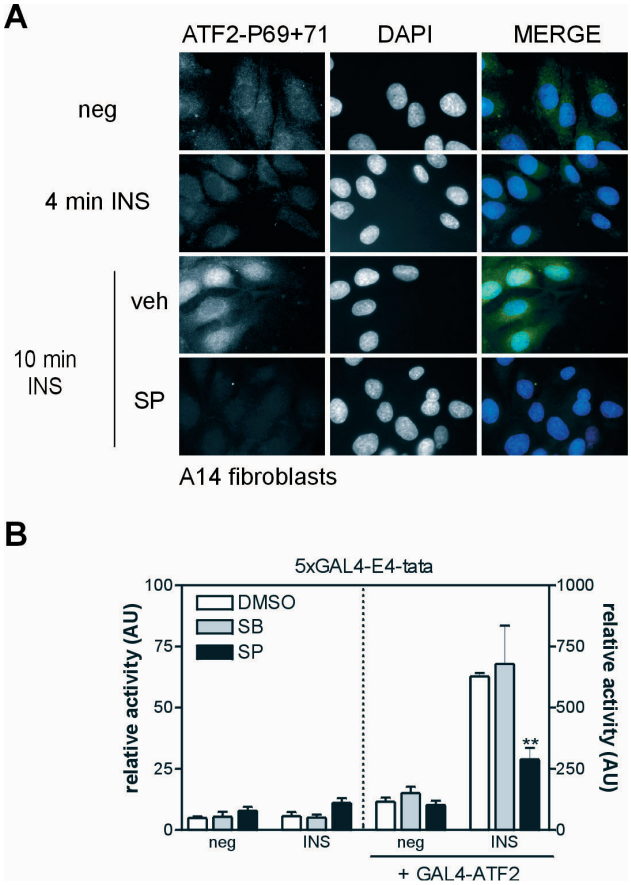

Figure 6. Inhibition of JNK, but not p38, abrogates the insulin-induced ATF2 phosphorylation and activation. (A) Serum-starved A14 cells were treated with inhibitors as described above prior to stimulation with 10 nM insulin (INS) for the indicated times. Cells were fixed and stained with antibodies for Thr69+71-phosphorylated ATF2 followed by FITC-conjugated secondary antibodies (green). DNA was stained with DAPI (blue). (B) Insulin-induced ATF2 transcriptional activity was examined in a GAL4-dependent luciferase reporter assay using the activation domain of ATF2 fused to the GAL4 DNA binding domain (19). Cells were transiently transfected and grown for 8 hours, subsequently serum-starved in DMEM containing 0.5% FBS O/N and treated for 30 minutes with vehicle or inhibitors SB203580 or SP600125 before adding insulin (INS; 10 nM). Cells were lysed 16 hrs later and luciferase activity was determined. The relative firefly luciferase activity is depicted as the mean enhancement of promoter activity in the absence or presence of insulin and/or inhibitors +/- the SD of three independent experiments performed in triplicates. Note the different scaling of the left and right *y*-axis. ** P = 0.0097 in a Student t-test.

Chapter 4

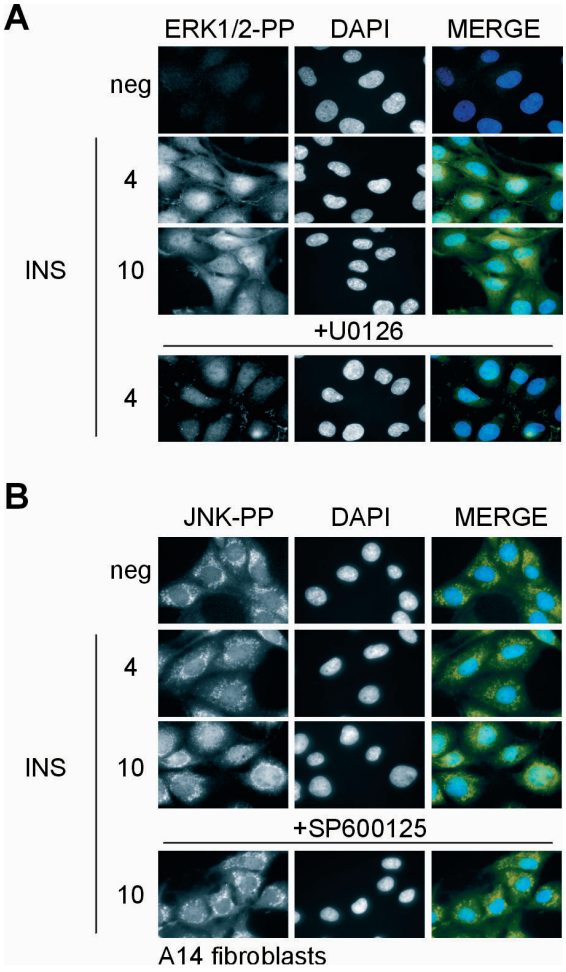

Figure 7. Time course of nuclear translocation of ERK1/2 and JNK. Serum-starved A14 cells were incubated with DMSO, 10 µM U0126 (U) for 15 minutes or 10 µM SP600125 (SP) for 30 minutes prior to stimulation with 10 nM insulin (INS) for the indicated times. Cells were fixed and stained with antibodies for (A) phosphorylated ERK (ERK-PP) or (B) phosphorylated JNK (JNK-PP) and FITC-conjugated secondary antibodies (green). DNA was stained with DAPI (blue).

Chapter 6

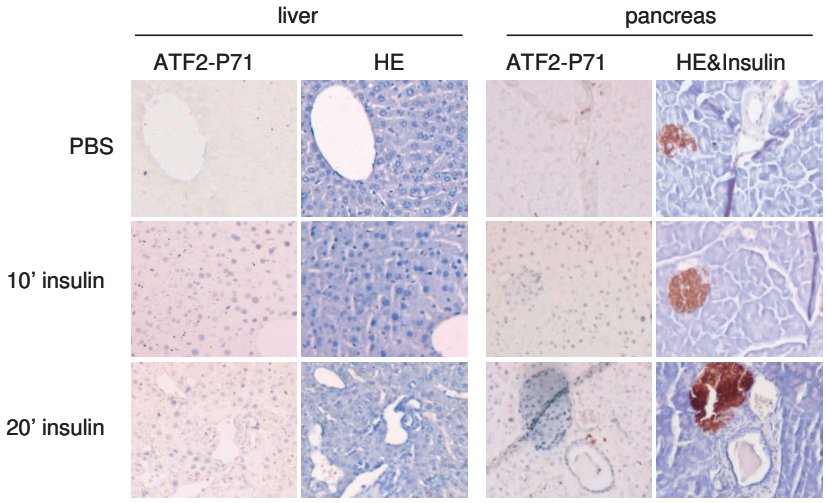

Figure 1. Immunohistochemical staining of mouse liver and pancreas tissue sections with phospho-ATF2-Thr71 antibodies (ATF2-P71), or hematoxylin (HE; blue) in combination with insulin (brown). Mice were infused with either PBS or insulin for the indicated times. Photographs are representative of 2-3 independent animals.

Appendix